UNIVERSITEIT VAN PRETORIA
UNIVERSITY OF PRETORIA
YUNIBESITHI YA PRETORIA

Fibroblast growth factor 21 and Growth and differentiation factor 15 as potential systemic biomarkers of mitochondrial toxicity and associations with disease severity and immune suppression in HIV-1 infected patients in Tshwane, South Africa

Submitted in fulfilment of the requirements for the degree of Master of Science in Medical Immunology

By

Senku Ramabula

Department of Immunology

Faculty of Health Sciences

University of Pretoria

July 2021

DECLARATION

I, Senku Ramabula, hereby declare that this work, which I submit for a Master's degree in Medical Immunology to the University of Pretoria, is my own original work and has not previously, in its entirety or in part, been submitted by me for a degree at this or any other tertiary institution. Where another person's work has been used, it has been properly acknowledged and referenced. Procedures were carried out in accordance with the ethical rules prescribed by the Faculty of Health Sciences Research Ethics Committee of the University of Pretoria.

Signature: 

Date: 8 July 2021

ACKNOWLEDGEMENTS

The writing of this dissertation has been a product of hard work, resilience and support provided by the various person/s and organizations that I would like to thank below;

1. First and foremost, my parents, Noko and Maria, who have always believed in me and like good parents have always tried to provide the means for me to achieve my dreams. I would also like to thank my siblings for all the love and support they've continuously given their "baby" sister. Lethabo, you will always be the best and only sister I have ever had and I will miss you greatly. My life is better because I knew you.
2. I am truly honoured and relieved to have been financially supported by the Poliomyelitis Research Foundation (PRF) (Grant number: PRF Ramabula 19/62), National Research Foundation (NRF) (Grant number: SFH180613345456) and the University of Pretoria postgraduate grant, who have all lightened my financial burdens and have allowed me to solely focus on the successful completion of my M.Sc. project.
3. The National Health Laboratory Services (NHLS) development grant (Reference number: PR19830) for financially supporting the research component of my M.Sc. degree, therefore, allowing my research to contribute towards the field of HIV research.
4. My supervisor Professor Helen C. Steel, Department of Immunology, University of Pretoria, for sharing her extensive knowledge in immunology with me and for being as committed (if not more) as me, in seeing the completion of this thesis through.
5. I would also like to thank my co-Supervisor Professor Theresa M. Rossouw, Department of Immunology, University of Pretoria, for her much-needed contribution and for always answering all my questions and queries promptly.
6. The senior staff members of the Department of Immunology, University of Pretoria, along with my colleagues (Divan, Charné, Louise, Mieke and Sheila) for making these past two years memorable and introducing me to new things which have allowed me to grow as an individual.
7. Lastly, all permanent staff members belonging to the NHLS diagnostic unit as well as the general staff members of the Department of Immunology, the University of Pretoria for always being kind and willing to help when needed.

EXECUTIVE SUMMARY

South Africa has the highest prevalence of human immunodeficiency virus (HIV) in the world with approximately 7.77 million people infected. The wide usage of antiretroviral therapy (ART) has been credited with making HIV a manageable chronic disease. Nucleoside reverse-transcriptase inhibitors (NRTIs) and nucleotide reverse-transcriptase inhibitors (NtRTIs) belong to a class of HIV drugs that act by preventing the conversion of viral ribonucleic acid (RNA) into a complementary deoxyribonucleic acid (cDNA) molecule which is later integrated into the host genome. Nucleoside reverse-transcriptase inhibitors provide the backbone of first-line HIV regimens, however, chronic use of this class of drug has been associated with several deleterious side-effects which manifest as conditions such as cardiomyopathy, hepatic steatosis (with or without lactic acidosis), myopathy and neurological disorders such as Alzheimer's and Parkinson's disease. A decrease in mitochondrial (mt) DNA and mtDNA-encoded proteins used for processes like oxidative phosphorylation (OXPHOS) may result in the accumulation of reactive oxygen species (ROS) which could, in turn, result in mitochondrial damage and affect cellular functions.

However, not all mitochondrial toxicity (MT) stems from the chronic use of NRTI/NtRTI-based ART. Several *in vitro* studies have shown that the interaction between HIV and the mitochondria could also contribute to mitochondrial dysfunction via inflammatory conditions which increase the expression of pro-inflammatory cytokines, including tumour necrosis factor-alpha, that inhibit mitochondrial function and promote cellular apoptosis.

The measurement of MT is complex. Currently accepted methods, which rely on measuring the mtDNA relative to nuclear (n) DNA (mtDNA/nDNA) ratio, require costly specimens that are difficult to obtain, such as muscle biopsies. While several studies have suggested that peripheral blood mononuclear cells (PBMCs) should reflect what is found in muscle biopsies, other concerns with the current approach include; 1) the possible amplification of homologues nDNA pseudogenes by mtDNA specific-primers, due to duplication of the mitochondrial genome within the nuclear genome; 2) errors caused by using repetitive and/or highly variable regions from genes such as beta-actin and 18S ribosomal (r) RNA, and; 3) the size differences between mitochondrial and

nuclear genomes contributing to a dilution bias which makes interpreting the results difficult. Recently, two biomarkers; serum fibroblast growth factor 21 (FGF-21) and serum growth and differentiation factor 15 (GDF-15), have been identified by several studies as possible alternatives to the current method of MT detection. To the best of our knowledge, these biomarkers have, however, not been assessed in the study of MT in HIV-infected individuals.

The present study investigated the possible associations between disease severity and use of combination (c) ART, and mitochondrial damage. The associations between the cluster of differentiation 4 positive (CD4+) T-cell count, viral load (VL), and the use of cART and the extent of MT before initiation of cART, 12-months post-cART, and the change over time were also assessed. In addition, the concentration of the systemic biomarkers (FGF-21 and GDF-15) was compared with the changes in mtDNA/nDNA ratio, as a measure of MT, in HIV-infected individuals.

Stored, remnant plasma and PBMC samples that had previously been collected from HIV-positive participants before initiation of NRTI-based cART and again after 12-months of treatment, were used in the present study. In addition, 15 healthy, HIV-negative volunteers were recruited as control subjects. Plasma samples and PBMCs had been stored at -80 degrees Celsius (℃) following collection. The extent of MT was determined by detecting changes in mtDNA content, measured as the mtDNA/nDNA ratio by utilizing a quantitative polymerase chain reaction (qPCR) assay. The systemic levels of FGF-21 and GDF-15 were assessed by measuring the concentrations of these biomarkers present in plasma samples using suspension bead array technology.

From the results obtained, it was found that there was a depletion in mtDNA copy number in the HIV-infected individuals following a 12-month NRTI-based cART regimen. In addition, when compared to the HIV-negative controls, the HIV-positive participants displayed lower expression of mtDNA. Furthermore, there was also evidence of a significant association between the age of the participant and the levels of mtDNA, in that older participants displayed a reduction in mtDNA levels. While not significant, tobacco use was found to influence mtDNA levels, with most of the tobacco users in the current study displaying a decrease in mtDNA expression. From these findings, it would be recommended that the influence of both age and tobacco use on

the expression of mtDNA be studied further. In contrast, no associations between the expression of mtDNA and the participants' CD4+ T-cell count (baseline and 12-months following treatment) and VL (baseline), were found.

It was also observed that GDF-15 was a more sensitive biomarker than FGF-21, which showed negligible differences in concentration in either the HIV-positive (baseline and 12-months post-cART) or the healthy, HIV-negative participants. The systemic levels of GDF-15 were higher in the HIV-infected participants, at both baseline and 12-months following cART, when compared to the HIV-uninfected participants.

Furthermore, the GDF-15 concentrations had a stronger associated with lower baseline CD4+ T-cell count and immune recovery, rather than with the viral load of the individuals. However, no correlation between the biomarkers FGF-21 and GDF-15 and the standard measure of MT, the mtDNA/nDNA ratio, was found. This would indicate that the biomarkers may not be a suitable alternative for determining changes in mtDNA in HIV-infected individuals placed on NRTI-based ART regimens. Growth and differentiation factor 15 levels may, however, be indicative of disease progression, particularly in relation to the CD4+ T-cell count.

TABLE OF CONTENTS

LIST OF ABBREVIATIONS

℃	Degrees Celsius
µg	Microgram
µL	Microlitre
µM	Micromolar
3TC	Lamivudine
8-OXOG	8-Oxoguanine
ABC	Abacavir
Acetyl-CoA	Acetyl coenzyme A
ADP	Adenosine diphosphate
AIDS	Acquired immunodeficiency syndrome
Ala	Alanine
ARV	Antiretroviral drugs
ATP	Adenosine triphosphate
ATV	Atazanavir
AZT	Azidothymidine
B2M	Beta-2-Microglobulin
bp	Base pair
Ca^{2+}	Calcium
CAT	Catalase
cART	Combination antiretroviral therapy
CCR5	C-C-chemokine receptor type 5
CD4+	Cluster of differentiation 4 positive
CD8+	Cluster of differentiation 8 positive
cDNA	Complementary deoxyribonucleic acid
CK	Creatine kinase
Cl-	Chloride
COBI	Cobicistat
CoQ10	Coenzyme Q10
COX	Cytochrome c oxidase

CSF	Cerebrospinal fluid
Ct	Cycle threshold
CXCR4	C-X-C chemokine receptor type 4
CYC1	Cytochrome c1
CYP450 3A4	Cytochrome P450 3A4
CYTB	Cytochrome b
CYTC	Cytochrome c
d4T	Stavudine
dATP	Deoxyadenosine triphosphate
DC	Dendritic cell
dCTP	Deoxycytidine triphosphate
ddC	Zalcitabine
ddI	Didanosine
ddNTP	Dideoxynucleoside
dGTP	Deoxyguanosine triphosphate
dH_20	Distilled water
DNA	Deoxyribonucleic acid
DNA pol-α, β, γ, θ, ζ	DNA polymerase alpha, beta, gamma, theta, zeta
dNTP	Deoxynucleotide triphosphates
DRV	Darunavir
DTG	Dolutegravir
dTTP	Deoxythymidine triphosphate
EDTA	Ethylenediamine tetra acetic acid
EFV	Efavirenz
EGTA	Ethylene glycol bis(2-aminoethyl) tetra acetic acid
ELISA	Enzyme-linked immunosorbent assay
ENF	Enfuvirtide
ETC	Electron transport chain
EVG	Elvitegravir
$FADH_2$	Flavin adenine dinucleotide
FAM	6-carboxyfluorescein
FDA	US Food and Drug Administration

FGF-21	Fibroblast growth factor 21
FTC	Emtricitabine
g	Gravitational force
GAPDH	Glyceraldehyde 3-phosphate dehydrogenase
GDF-15	Growth and differentiation factor 15
gp 41	Glycoprotein 41
gp 120	Glycoprotein 120
GPx	Glutathione peroxidase
GSH	Glutathione
H_2O	Water
H_2O_2	Hydrogen peroxide
HAART	Highly active antiretroviral therapy
HIV	Human immunodeficiency virus
HIV-1	Human immunodeficiency virus 1
HIV-2	Human immunodeficiency virus 2
HOCL	Hypochlorous acid
HRP	Horseradish peroxidase
Hrs	Hours
IMM	Inner mitochondrial membrane
IMS	Intermembrane space
IN	Integrase
INSTI	Integrase strand transfer inhibitor
IQR	Interquartile range
kDa	Kilodaltons
Log	Logarithm
LPV/r	Lopinavir/ritonavir
MGB	Minor groove binding
MGT	Modified Gomori trichome
Min	Minute
MIQE	The Minimum Information for Publication of Quantitative Real-Time PCR Experiments
mL	Millilitre

mM	Millimolar
MMP	Mitochondrial membrane potential
mRNA	Messenger RNA
MS	Microsoft
MT	Mitochondrial toxicity
MT-CYB	Mitochondrial cytochrome b
mtDNA	Mitochondrial DNA
MVC	Maraviroc
NADH	Nicotinamide adenine dinucleotide
NADPH	Nicotinamide adenine dinucleotide phosphate
nDNA	Nuclear DNA
NFV	Nelfinavir
ng	Nanogram
nM	Nanomolar
nm	Nanometer
NNRTI	Non-nucleoside reverse transcriptase inhibitor
NRTI	Nucleoside reverse transcriptase inhibitor
NTC	Non-template control
NtRTI	Nucleotide reverse transcriptase inhibitor
O_2^-	Superoxide anion
O_2	Molecular oxygen
OH^-	Hydroxyl ion/group
$^{\bullet}OH$	Hydroxyl radical
OIs	Opportunistic infections
OS	Oxidative stress
OXPHOS	Oxidative phosphorylation
PBMC	Peripheral blood mononuclear cell
PBS	Phosphate buffered saline
pg	Picogram
PI	Protease inhibitor
Pi	Organic phosphate
PIC	Pre-integration complex

PK	Pharmacokinetic
PR	Protease
qPCR	Quantitative polymerase chain reaction
RAL	Raltegravir
Redox	Reduction-oxidation
RNA	Ribonucleic acid
rRNA	Ribosomal RNA
ROS	Reactive oxygen species
RPM	Revolutions per minute
RT	Reverse transcriptase
RTP	Room temperature and pressure
RTV	Ritonavir
SDH	Succinate dehydrogenase
Sec	Seconds
SOD	Superoxide dismutase
SU	Surface protein
TCA	Tricarboxylic acid
TDF	Tenofovir disoproxil fumarate
TM	Transmembrane protein
TPV	Tipranavir
Tyr	Tyrosine
VL	Viral load
Vpr	Viral protein R
WHO	World Health Organization

LIST OF FIGURES

Chapter One

Chapter Four

Chapter Five

LIST OF TABLES

Chapter Two

Chapter Three

Chapter Four

Chapter Five

CHAPTER 1

LITERATURE REVIEW

1.1 The Prevalence of the Human Immunodeficiency Virus in South Africa

Since the discovery of the human immunodeficiency virus (HIV) over thirty years ago, it has been estimated that 75.7 million individuals worldwide have been infected.[1-2] It is a life-long condition, with no known cure, which impairs the immune system by primarily infecting specific immune cells called cluster of differentiation 4 positive (CD4+) T-cells, that are crucial for eliciting immune responses and fighting off foreign pathogens.[3] The final stage of HIV is known as acquired immunodeficiency syndrome (AIDS), which is characterized by an HIV-infected individual presenting with one or more AIDS-defining illnesses in the presence of a CD4+ T-cell count below 200 cells per cubic millimeter.[3] There are many mechanisms in which HIV damages the immune system, the most important being the decline in the CD4+ T-cell population, which is largely due to the virus progressively infecting and destroying these immune cells. Globally, South Africa bears the largest HIV burden with an estimated 7.77 million people living with HIV/AIDS by the end of 2019, accounting for approximately 20% of all HIV infections worldwide.[4]

Two types of HIV have been discovered, namely; HIV-1 and HIV-2, which are thought to have resulted from distinct cross-species transmission events.[5] Human immunodeficiency virus 1 is far more prevalent than HIV-2, in that it is responsible for most HIV infections globally.[6] Human immunodeficiency virus 2 infections were initially reported in only a few West African countries, however, the virus has since been found to have spread throughout Africa and Europe.[7-9] Human immunodeficiency virus 1 and HIV-2 are morphologically indistinguishable, with both sharing similar transmission routes and target cells; however, HIV-2 infections are less transmissible and virulent than HIV-1 infections. Human immunodeficiency virus 2-infected individuals have also been reported to present with lower plasma viral loads (VLs) and slower CD4+ T-cell decline, therefore resulting in less mortality.[10-11]

Both HIV-1 and HIV-2 are members of the *Retroviridae* family and belong to the genus *Lentivirus*.[12] Retroviruses are single-stranded, enveloped, ribonucleic acid (RNA) viruses that replicate via a deoxyribonucleic acid (DNA) intermediate, which later integrates into the host's genome, where it survives for the full life span of the host cell.[13] In some cells, often referred to as HIV latent reservoirs, the replication-competent HIV provirus becomes transcriptionally silenced and downregulates the expression of viral proteins, thereby preventing the infected host cell from presenting signs of infection.[13] Within the latent reservoirs, which are primarily thought to be resting CD4+ T-cells, the integrated transcriptionally inactivated HIV-1 provirus is protected against the host immune surveillance system and anti-viral effects of HIV treatment, therefore allowing the virus to persist indefinitely in the cell.[14-15] For these reasons, HIV-infected individuals must adhere to antiretroviral (ARV) treatment for life, as discontinuation could result in the reactivation of the latent virus within reservoirs. This, in turn, could re-establish the infection and eventually progress to the incapacitation of the immune system.[16]

Sexual transmission accounts for most of the HIV-1 infections worldwide, however, other routes such as percutaneous inoculation (contact with contaminated needles, blood or blood products), parenteral transmission (contact of contaminated bodily fluids with open wounds or mucous membranes), *in utero* transmission (from infected mothers to unborn children) and breastfeeding have also significantly contributed towards the HIV-1 pandemic.[3,17] With the introduction of combination antiretroviral therapy (cART), also known as highly active antiretroviral therapy (HAART), there has been a drastic decline in HIV-related morbidities and mortalities.[18] The life-long administration of ARVs has increased the survival of HIV-infected individuals by suppressing viral replication and lowering the plasma VL below detection limits, thereby enabling immune reconstitution.[19-20] South Africa currently supports the world's largest cART program, with an estimated 62% of the country's HIV-infected population being provided with services for HIV-related health care and treatment.[18]

Despite ARVs forming a key component in both the treatment and prevention of HIV, major concerns surrounding the drugs persist, such as the need for life-long adherence.[15] In addition, the use of ARVs increases an individual's risk of developing complications for example ARV-associated short-term side-effects, such as nausea and headaches, as

well as long-term side-effects, such as lipoatrophy, peripheral neuropathy and myopathy. The wide spectrum of toxicities can contribute to non-adherence to treatment and can, together with drug-drug interactions which decrease plasma levels of ARVs, lead to the development of drug resistance which further complicates treatment.[21] These complications underscore the need for the development of safer, more effective treatment regimens for HIV-infected individuals.[22-23]

1.2 How the Human Immunodeficiency Virus affects Immune Cells

Human immunodeficiency virus 1 mainly targets white blood cells, particularly activated T-cells expressing the CD4 glycoprotein, however, dendritic cells (DC), monocytes and macrophages have also been found to be susceptible HIV targets.[24-25] White blood cells play a crucial role in the immune system, in that they are responsible for protecting the host from potentially harmful diseases and infections.[3] In healthy individuals, the CD4+ T-cells are responsible for the stimulation, coordination and suppression of several cell-mediated and humoral immune responses.[26] During an infection, CD4+ T-cells become activated upon encountering foreign antigens, which are presented on the major histocompatibility complex class II molecules of antigen-presenting cells. The interaction between the two cells induces the activation and proliferation of naïve CD4+ T-cells, resulting in the release of cytokines which then facilitate the activation of other immune cells that aid in destroying the foreign pathogen.[26-27] When HIV-1 infects CD4+ T-cells, the virus 'hijacks' and uses the host's replication machinery to replicate itself, whilst evading the host's immune surveillance. The infection could eventually result in the apoptosis of not only the virally infected immune cells but also uninfected bystander cells, thereby progressively reducing the host's immune cell population.[28] There are several mechanisms in which cell death occurs as a result of an HIV infection, specifically in the cell it infects. These mechanisms include the cells viability being compromised as a result of damage inflicted on the plasma membrane from the continuous budding of new virons from the cell, an increase in cellular toxicity brought about by the build-up of un-integrated viral DNA, and also the HIV protease enzyme activating apoptotic procaspase 8, whilst simultaneously inactivating the anti-apoptotic Bcl-2, which results in the cell becoming more susceptible to mitochondrial dysfunction in response to either an internal or external death signals.[29-31]

Because HIV-1 eventually results in the death of the infected immune cells, HIV-1 infection is typically characterized by the gradual decline of CD4+ T-cells. For this reason, the amount of CD4+ T-cells, or the CD4+ T-cell count, has become a defining indicator of an individual's immune health.[25,32] Severely impaired immune systems, such as in the case of AIDS, have been associated with an increased incidence of opportunistic infections (OIs) such as *Pneumocystis jiroveci* pneumonia, *Mycobacterium tuberculosis*, *Candida albicans* (candidiasis), some cancers such as Kaposi's sarcoma, invasive cervical cancer as well as certain Hodgkin and non-Hodgkin lymphomas.[33-34] However, it has been reported that with the early administration of ARVs, infected individuals have a significantly decreased incidence of OIs, mainly due to the drugs ability to revive the host's immune system by restoring the CD4+ T-cell population.[15,22]

1.3 The Life-Cycle of the Human Immunodeficiency Virus

The HIV-1 life-cycle can be divided into two distinct phases; the early phase, which begins with the virus attaching to the host cell and ends with the integration of the provirus; and the late phase, which begins with the expression of viral proteins and ends with the assembly and release of the HIV-1 virion from the host cell.[35] The pathogenesis of HIV-1 infection begins with the initial attachment of the viral envelope proteins (surface glycoprotein 120 [SU/gp 120] and transmembrane glycoprotein 41 [TM/gp 41]) to the host cells CD4 surface receptor and co-receptors, namely C-C-chemokine receptor type 5 (CCR5) or C-X-C-chemokine receptor type 4 (CXCR4). This interaction leads to a conformational change of the two cells that result in the fusion of both host and viral cell membranes. After the membranes have fused, the viral capsid is expelled into the host's cytoplasm where reverse transcription takes place.[28]

Reverse transcription produces a complementary (c) DNA molecule by using the viral ribonucleic acid (RNA) as a template. The process is highly error-prone due to being catalysed by the viral reverse transcriptase (RT) enzyme which lacks proof-reading ability.[35] Also, the low fidelity of RT contributes to the genetic variability within the HIV-1 genome, which, when coupled with the high replication rate and non-uniform viral population, enables the virus to adapt quickly to changes within the host's environment which could result in the emergence of drug-resistant strains.[3,35] Within a structure called a pre-integration complex (PIC), the viral DNA molecule is transported to the cellular

nucleus where it integrates into the host's genome in a reaction catalysed by the viral integrase (IN) enzyme. The integrated provirus remains latent in the host's genomic DNA and subsequently replicates using the host's replication enzymes.[36] The viral transcripts are translated, assembled and released from the host cells surface as immature non-infectious particles. Once released, the viral protease (PR) enzyme becomes activated and cleaves the viral proteins, resulting in viral maturation, which then enables the viral particle to infect other susceptible cells and repeat the life-cycle. The life-cycle of HIV-1 is summarised in Figure 1.1.[36]

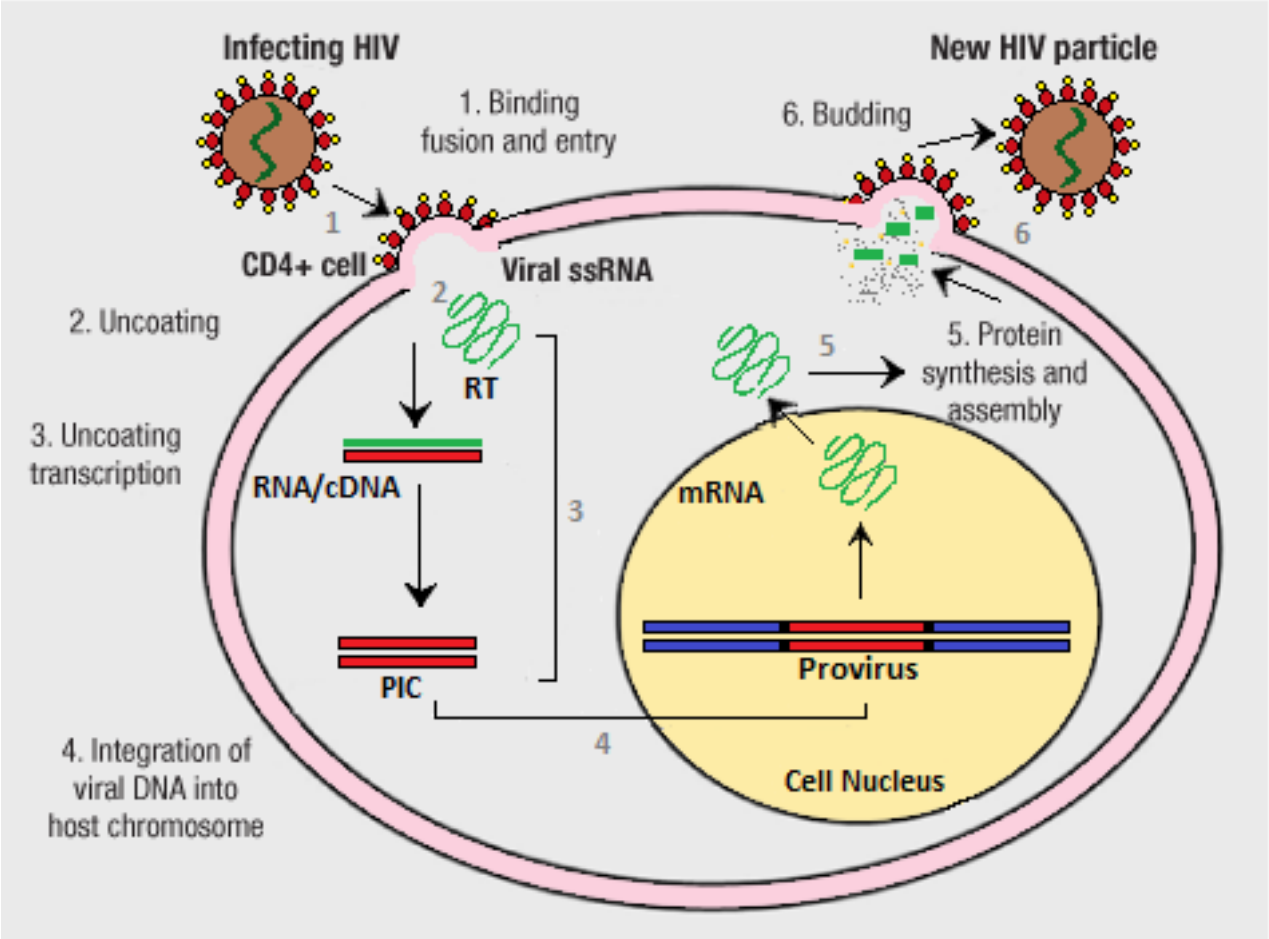

Figure 1.1: The basic life cycle of HIV-1. 1) Binding, fusion and entry are the first steps of HIV-1 infection, which involves the virus entering the target cell by the envelope proteins (gp 120 and gp 41) attaching to the CD4 receptor and co-receptors on the target cell. 2) This interaction leads to a conformational change resulting in the fusion of both cells and subsequent uncoating of the virus and expulsion of the HIV capsid, containing the viral RNA, into the cellular cytoplasm. 3) In the cellular cytoplasm, the viral RNA is used as a template to transcribe a new cDNA molecule in a reaction catalysed by the viral RT enzyme. 4) Within a PIC the viral DNA is transported into the cellular nucleus where viral IN catalyses the integration of the viral DNA into that of the host. 5) The transcription of the provirus is carried out using cellular enzymes and the newly synthesised viral RNA proteins are then assembled and released from the host cells surface. 6) Upon budding from the host cell surface, the virus matures with the assistance of viral PR and then goes on to infect new target cells. (Modified from Fanales-Belasio *et al.*, 2010 with permission for use from Annali dell Istituto Superiore di Sanità).

1.4 Classes of Antiretroviral Drugs Available

The efficacy of HIV-1 treatment has dramatically improved since the approval of zidovudine (also known as azidothymidine [AZT]), the first marketed ARV drug, over three decades ago.[37] The current management of HIV-1 involves a life-long regimen of a combination of drugs that aims to decrease the risks of disease progression.[20] There are currently over twenty-five United States Food and Drug Administration (FDA)-approved ARVs on the market, belonging to one of six mechanistic classes which include; 1) reverse transcriptase inhibitors such as nucleos(t)ide reverse transcriptase inhibitors (NRTIs/NtRTIs) and non-nucleoside reverse-transcriptase inhibitors (NNRTIs); 2) integrase strand transfer inhibitors (INSTIs); 3) entry and fusion inhibitors, such as CCR5 antagonists; 4) protease inhibitors (PIs), and; 5) pharmacokinetic (PK) enhancers.[38]

Several steps of the HIV-1 life-cycle have successfully been targeted by ARVs and these are depicted in Figure 1.2.[39] The initial drugs were designed to target enzymes exclusively expressed by the virus such as RT and PR, while a newer drug class, *viz.* INSTIs, targets the IN enzyme.[40-41] The entry point of the virus into host cells has also been recognised as a possible target for therapeutic intervention and has subsequently led to the development of several classes of ARVs such as chemokine receptor antagonists and fusion/entry inhibitors. Fusion/entry inhibitors, such as enfuvirtide (ENF) and maraviroc (MVC), inhibit viral entry by either preventing the interaction of the virus with the target CD4+ T-cell, thereby preventing the interaction between the host CCR5 co-receptors and the gp 120 protein, or inhibiting the formation of the six-helix bundles by the gp 41 protein which are used for the virus-host membrane fusion.[20] The fusion and entry of the virus into the host cell is a crucial step, as it allows the viral genome to be released into the host cell where reverse transcription will take place. Reverse transcribing the viral RNA into a cDNA molecule enables the virus to protect its genetic material and also enables it to use the vast supply of host deoxynucleotide triphosphates (dNTPs) for the synthesis of the viral cDNA.[20]

Reverse transcriptase was the first HIV-1 enzyme to be successfully targeted by NRTIs/NtRTIs and NNRTIs, and these account for nearly half of all approved anti-HIV drugs.[20] Examples of RT inhibitors include NRTIs/NtRTIs such as; abacavir (ABC), tenofovir disoproxil fumarate (TDF), emtricitabine (FTC) and lamivudine (3TC), and

NNRTIs such as efavirenz (EFV). These drugs inhibit the polymerase activity of the enzyme in one of two ways: 1) NRTIs/NtRTIs inhibit viral replication by binding to and directly inhibiting viral reverse transcriptase resulting in premature chain termination, and; 2) NNRTIs act as allosteric inhibitors of the enzyme.[15,20]

The successful completion of reverse transcription is mandatory as it provides a mechanism that enables HIV-1 to persist within the host's genome.[20] There are currently four INSTIs available on the market, which prevent the HIV-1 provirus from integrating into the host's genomic DNA, however, only two of the drugs, *viz.* raltegravir (RAL) and dolutegravir (DTG), are currently available in South Africa.[25] Integrase strand transfer inhibitors function by inhibiting IN strand transferring activity, which is needed to insert the proviral cDNA into the host DNA.[20] Because of the low rate of drug resistance associated with DTG, the World Health Organisation (WHO) recommends its use in all the new ARV regimens administered to ARV-naïve HIV-infected individuals.[42] Notably, since 2019, the preferred first-line cART regimen in South Africa comprises TDF, 3TC and DTG.[43]

Before a virus particle can successfully infect a new target cell, viral maturation is required. During viral maturation, the newly translated viral polypeptides are proteolytically cleaved by the viral PR. Protease inhibitors are a novel, potent class of ARVs that work by inhibiting the viral PR enzyme, thus preventing the final stages of viral maturation resulting in an immature defective virus.[23] The administration of PIs typically requires the concomitant use of a booster agent to enable slower drug metabolism and enhance drug levels; hence most PI-based regimens involve four-drug combinations, with the fourth agent being a boosting agent. Examples of common PIs include; ritonavir (RTV)-boosted lopinavir (LPV), atazanavir (ATV) and darunavir (DRV).[15,39]

Lastly, unlike other classes of ARVs that directly target the virus' life cycle, PK enhancers such as low-dose RTV and cobicistat (COBI) have no anti-HIV activity and merely act as boosters, augmenting the effect of other drugs. Both RTV and COBI are used as booster agents for PIs, as they are potent inhibitors of the cytochrome P450 3A4 (CYP450 3A4) enzyme system which is responsible for the metabolism of many drugs.[23] When the CYP450 3A4 system is inhibited by RTV or COBI (co-administered with other ARVs), it results in prolonged systemic exposure of the virus to the ARVs, thereby allowing for a

reduction in the number of tablets that have to be taken, which could improve drug adherence.[44]

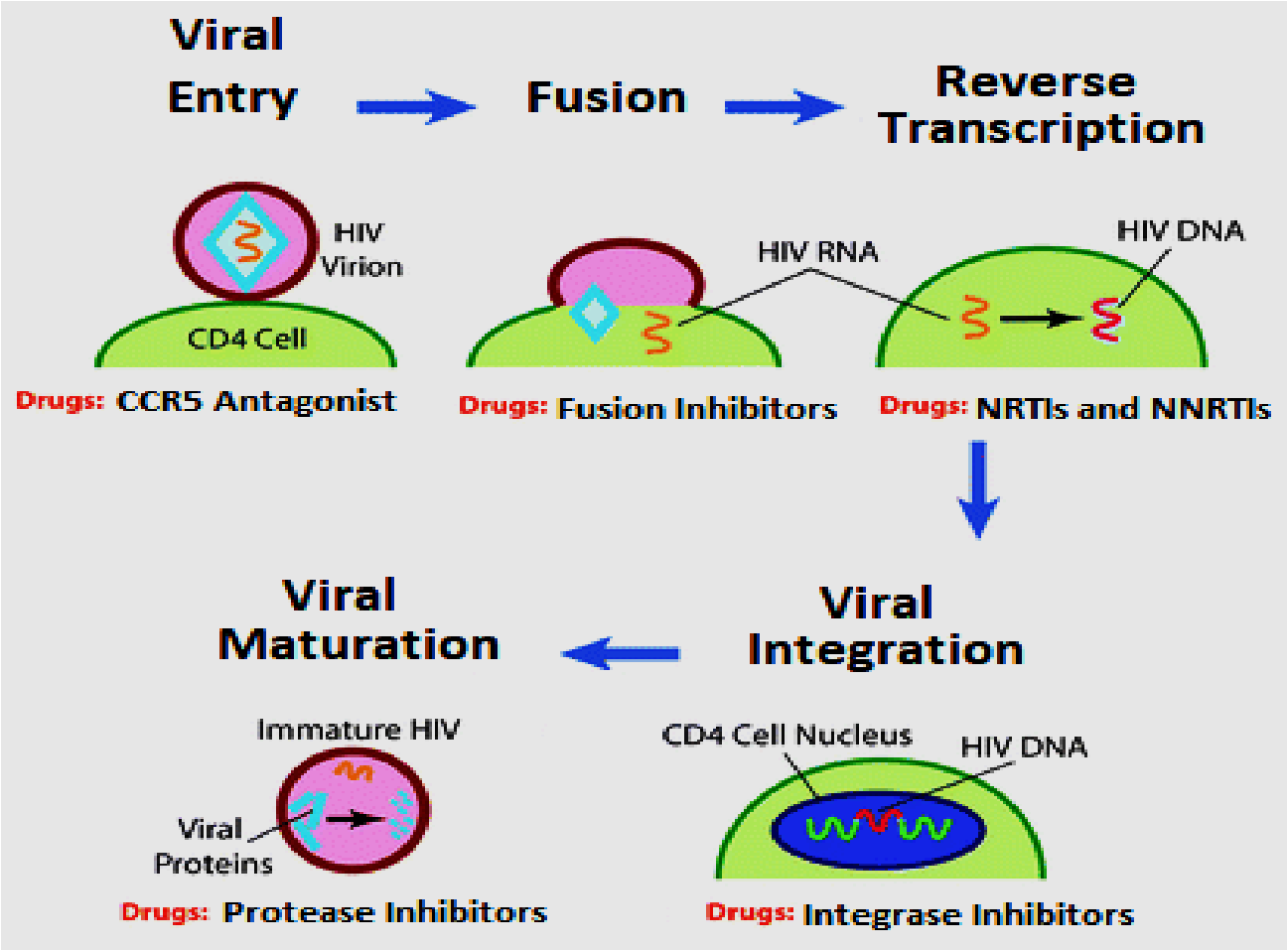

Figure 1.2: The steps targeted in the HIV-1 life-cycle and the respective antiretroviral drugs. Current ARV drugs are designed to target five crucial steps in the HIV-1 replication cycle. These steps include: inhibiting the entry and fusion of the virus into target cells; preventing reverse transcription of viral RNA into a cDNA molecule; inhibiting the integration of viral cDNA into the host genome, and; blocking the maturation of the virus particle by inhibiting the viral PR enzyme. (Modified from Romashova and Ananikov (2016) with permission for use from The Royal Society of Chemistry).

The recommended combination for cART typically consists of two NRTIs (or one NRTI with one NtRTI) in addition to a third drug from a different class, preferably an INSTI, however, an NNRTI, CCR5 antagonist, or PI with a PK enhancer can also be used.[23,37] Until recently (2019), the WHO recommended that the preferred first-line cART regimen should consist of a combination of TDF, 3TC or FTC, with EFV co-formulated in a single tablet.[42] The use of a triple combination approach is most successful in reducing complications such as drug resistance which has previously been associated with both mono- and dual-therapy approaches.[45] A major limitation of cART to date, as previously

mentioned, surrounds the issue of negative side-effects associated with prolonged use of the drugs.[46] All cART drugs have side-effects; however, the effect varies among the different drug classes. For example, common side-effects associated with NRTIs include bone marrow suppression, lactic acidosis and mitochondrial toxicity (MT) whereas NNRTIs have been associated with certain dermatological and hepatic complications.[47-48] In an attempt to reduce these side-effects, a new regimen, as mentioned above, with EFV being replaced by DTG, has been implemented in South Africa.[43]

1.4.1 Nucleoside Reverse Transcriptase Inhibitors

As described above, NRTIs form the backbone of any standard cART regimen and are perhaps the most significant drug class to have been developed for HIV treatment. Many studies have reported that, in combination with other drugs, NRTIs are highly potent, easily absorbed and have a favourable PK profile with a low risk of drug-to-drug interaction.[49] Molecularly, NRTIs are activated intracellularly when they are phosphorylated to their active diphosphate or triphosphate form. These drugs act by interfering with the viral RT enzyme by mimicking native dNTPs (dATP, dCTP, dGTP and dTTP) which are used by HIV during reverse transcription to produce a cDNA molecule. The NRTI analogues differ from native dNTPs by lacking a 3' hydroxyl (OH^-) group on the deoxyribose sugar moiety and are hence called dideoxynucleosides (ddNTPs). The 3'OH- is mandatory for forming a phosphodiester bond between two dNTPs thus allowing the DNA strand to grow. Upon being activated, NRTIs compete with native dNTPs for the viral RT binding site. Once inside the binding site, the analogues displace native dNTPs and are incorporated into the new chain instead, thus terminating DNA synthesis. This inhibition is due to the inability of ddNTPs to form new 5' to 3'-phosphodiester bonds with incoming dNTPs or ddNTPs.[50-51] Therefore, NRTIs can inhibit HIV replication by either; 1) competing with native dNTPs for the activation site in the viral RT, or; 2) prematurely terminating the newly synthesised chain when incorporated.[52]

Earlier designs of NRTIs, such as AZT, have been associated with the development of adverse and, sometimes, lethal side-effects such as cardiomyopathy, hepatic steatosis (with or without lactic acidosis), myopathy and nephrotoxicity.[23,51] It has since been postulated that a common pathway may exist for the development of the various conditions, namely NRTI-induced MT, which is thought to be a result of the drug directly

interfering with the function of the mitochondrial replication enzyme, DNA polymerase gamma (DNA pol-γ). These inferences may result in depletion of mitochondrial (mt) DNA, which could bring about an array of consequences such as energy insufficiencies and a decline in overall cellular functions. Mitochondrial toxicity is a general term referring to changes in normal mitochondrial function brought about by factors such as ageing, certain infections and medication such as ARVs (*i.e.* NRTIs). The presentation of mitochondrial disorders has been categorised into three groups: 1) individuals presenting with clearly recognised syndromes which are associated with specific mtDNA abnormalities; 2) individuals with unusual clinical presentations suggesting a possible pathological mtDNA mutation; and, 3) individuals presenting with a cluster of features suggesting possible mtDNA depletion.[53] Common symptoms may include vision and hearing impairments, recurring metabolic crises and myopathies affecting the proximal limbs or external ocular muscles.[54-55]

1.4.2 Nucleotide Reverse Transcriptase Inhibitors

Tenofovir disoproxil fumarate was the first marketed NtRTI and, similar to the NRTIs, the drugs mode of action involves direct interference with HIV-1 RT.[56] The difference, however, lies in the number and rate of intracellular phosphorylation steps required for both drugs to become activated. Unlike NRTIs which require three phosphorylation steps, NtRTIs bypass the slow initial phosphorylation stage to quickly reach the drugs active diphosphate form after only two steps.[56-57] Diphosphate nucleotide analogues are less permeable than triphosphate nucleosides, thus allowing the drug to remain in the body longer and thereby providing prolonged inhibition of viral replication.[56] Tenofovir disoproxil fumarate, administered orally, is absorbed rapidly and expelled by the kidneys, hence the need for dosage adjustment in individuals with renal failure.[58] The chronic use of TDF has since been found to contribute to a decrease in bone density and the onset of renal tubular dysfunction, with the risk of acquiring the latter being thought to increase when the drug is taken in combination with a boosted PI.[59-60] With the rising concern of cART-associated toxic effects, *in vitro* studies related to TDFs toxicity profile have suggested that the drug is far more tolerable than most NRTIs as part of a long-term regimen. Further studies, involving various cell types, have also shown NtRTIs to cause only minimal MT compared to their nucleoside counterpart.[61]

Although NRTIs and NtRTIs are primarily responsible for mitochondrial dysfunction, other classes of ARVs, specifically NNRTIs and PIs, have also been reported to interfere with mitochondria.[62] The underlying mechanisms are unclear and, unlike NRTIs and NtRTIs, do not involve inhibiting the mitochondrial DNA pol-γ enzyme or reducing the mtDNA content. In fact, studies have found that the mtDNA content in participants administered both drugs increased over time.[63] In addition, most of the findings on the MT profile for PIs and NNRTIs are confounded by the co-administration of NRTIs, making it difficult to understand the independent effect of these drug classes on MT.[62] This is discussed in more detail in section 1.8.

1.5 The Mitochondria and their Functions

Each cell contains thousands of mitochondria, which are double membrane-bound, intracellular organelles found in all mammalian cells, with the exception of red blood cells. Mitochondria are exclusively maternally inherited and are the only organelles (besides the nucleus) to have their own genomic DNA and subsequently encode their own proteins.[64] The mitochondria play many crucial roles in the cell, such as initiating and implementing cellular apoptosis, maintaining calcium (Ca^{2+}) homeostasis and regulating the immune system, however, the most important role of the mitochondria involves the production of adenosine triphosphate (ATP), the cell's energy currency, via oxidative phosphorylation (OXPHOS).[65] Oxidative phosphorylation is a metabolic pathway that takes place on the highly folded inner mitochondrial membrane (IMM) called the cristae. The pathway is comprised of two coupled reactions; a) the electron transport chain (ETC), which involves the coupling of reduction-oxidation (redox) reactions in several multi-subunit complexes, with the translocation of protons across the IMM into the intermembrane space (IMS), and; b) chemiosmosis, which involves the coupling of protons translocating down their concentration gradient, from the IMS back into the IMM, with the generation of ATP.[65-66]

The ETC occurs in a series of high energy-releasing redox reactions catalysed by protein complexes that are scattered throughout the IMM.[65] These reactions are initiated by the reducing agents, nicotinamide adenine dinucleotide (NADH) and flavin adenine dinucleotide ($FADH_2$), which is produced from beta (β)-oxidation, glycolysis and the tricarboxylic acid (TCA) cycle. Both agents act as electron donors to electron acceptors in the ETC and are shuffled through each complex until they are donated to the final electron

acceptor, molecular oxygen (O_2), which is then reduced to water (H_2O).[67] The four major complexes of the ETC are; Complex I (NADH dehydrogenase); Complex II (succinate dehydrogenase [SDH]); Complex III (cytochrome c reductase), and; Complex IV (cytochrome c oxidase [COX]). Other proteins involved include the electron carriers coenzyme Q10 (CoQ10) and the cytochrome c complex (CYTc), as well as Complex V, which is also known as ATP synthase.[68]

During chemiosmosis, the oxidation of NADH and $FADH_2$ results in two electrons being donated to Complex I or Complex II, and subsequently being passed by CoQ10 to Complex III and by CYTc to Complex IV which then reduces O_2 to H_2O.[69] The redox reaction that occurs at each ETC complex generates a large amount of energy, which is utilized to translocate protons through the IMM into the IMS, thereby establishing an electrochemical gradient. The protons are then translocated back through Complex V into the IMM and in doing so, utilize, what has been termed as the proton-motive-force, to generate enough energy to drive the phosphorylation of organic phosphate (P_i) and adenosine diphosphate (ADP) into ATP.[65] The process of OXPHOS is illustrated in Figure 1.3.[68]

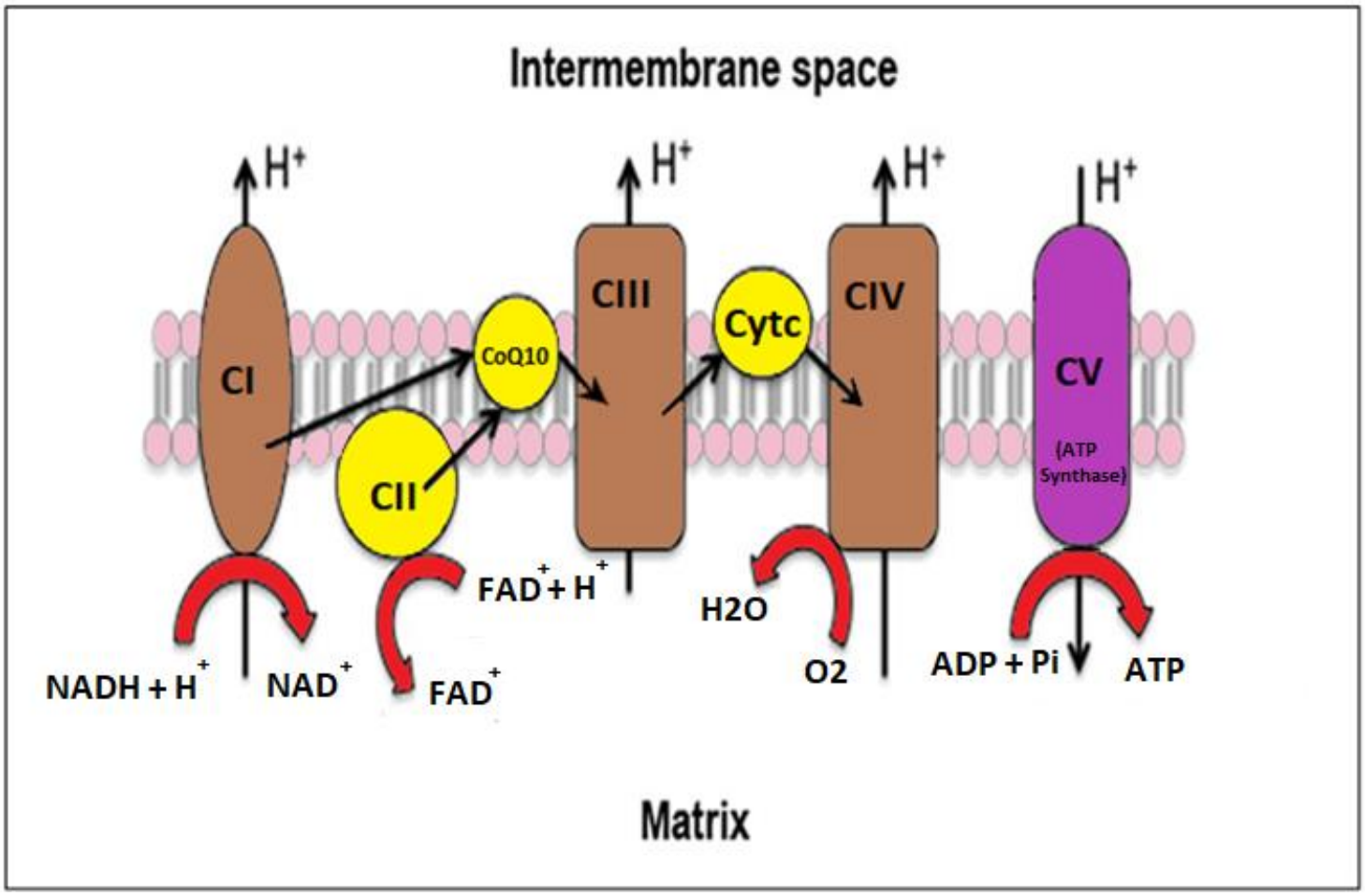

Figure 1.3: Oxidative phosphorylation system in the mitochondria. The OXPHOS process consists of five protein complexes (CI-CV) and an ATPase enzyme that is dispersed along the inner mitochondrial membrane. During ATP synthesis NADH and $FADH_2$ are oxidized by Complex I and Complex II, respectively, donating electrons that are then transported to Complex III via the CoQ10. The electrons are then transferred to the Complex IV via CYTc, which donates the electrons to molecular O_2 which is reduced to H_2O. As the electrons are transported through the complexes, protons are expelled across the IMM into the IMS, establishing an electrochemical gradient. The protons flow back into the mitochondrial matrix using Complex V ATP channels, which, in turn, drive the production of ATP from ADP and P_i. (Modified from Ho *et al*. with permission for reprint by Springer).

1.5.1 Effects of Reactive Oxygen Species

During OXPHOS, not all electrons which are transferred through the complexes reach the final acceptor molecule. Occasionally, several electrons 'leak out' of the ETC and react with oxygen to form harmful unstable molecules.[70] Oxygen is extremely susceptible to forming free radicals, due to the molecule's outer shell possessing two unpaired electrons in differing orbitals.[71] These oxidative molecules are collectively known as reactive oxygen species (ROS), and have been defined as being 'O_2 derived by-products of OXPHOS which carry additional electrons, giving them the ability to oxidize other

molecules'.[72] Within cells, ROS may be produced by phagocytic cells (*i.e.* neutrophils and macrophages), endoplasmic reticulum and peroxisomes, however, the mitochondrial ETC remains their primary generator.[73] These oxidative species are generally classified as either being; 1) free radicals (*i.e.* superoxide anions [$O_2^{\cdot-}$], hydroxyl radicals [•OH] and hypochlorous acid [HOCl]), which contain unpaired electrons, or; 2) non-radicals (*i.e.* hydrogen peroxide [H_2O_2]), which are products of free radicals sharing their unpaired electrons. In smaller quantities, ROS are valued for their role in mediating several cellular processes such as autophagy, proliferation, immune defences, cellular redox signalling and increasing CCR5 and CXCR4 expression; however, in larger quantities, they have been shown to have detrimental effects on several cellular components such as DNA, proteins and lipids, and may also affect the intracellular redox state which could, in turn, promote both apoptotic and necrotic pathways.[70,74-75]

A consequence of excessive or inadequate removal of ROS is oxidative stress (OS), which may damage cellular macromolecules and hinder several metabolic functions.[76] Oxidative stress has since been linked to the onset and progression of over a hundred pathologies including; cancers, diabetes mellitus, neurodegenerative disorders and cardiovascular disease.[77] Oxidative stress induced by ROS results from an imbalance between the cell's metabolic production of ROS and its biological ability to counteract or repair the damage, in favour of the former. In this condition, the body's natural antioxidant levels are vastly exceeded by those of the generated reactive species, thereby creating an oxidative environment that leads to essential biological components being oxidized.[71] Consequences of the prolonged OS include interferences with normal mitochondrial function, peroxidization of lipids and lipoproteins, inactivation of enzymes, modification of proteins, induction of OS-related DNA damage and in severe cases, triggering cellular apoptosis.[78-79] It has been shown that mtDNA is a major target for OS. During OS, mutations may occur in mtDNA that could interfere with the mitochondria's membrane permeability, defence systems and ability to produce energy. Once damaged, mtDNA could further amplify OS by reducing the expression of crucial ETC proteins which could then result in more ROS being produced, therefore, dysregulating the organelle potentially leading to cellular apoptosis.[80]

1.5.2 Cellular Defences against Reactive Oxygen Species

Given that the accumulation of ROS can induce OS-related cell death and has been implicated in several pathologies, the ability to neutralize them is crucial for all life forms. Cellular antioxidant defence systems comprise of small molecules and large enzymes that act to counterbalance the detrimental effects of ROS.[81] Antioxidants have been defined by Halliwell and Gutteridge as being 'any substance that is present in lower concentrations compared to an oxidizable substance, that significantly delays or inhibits the oxidation of that substance'.[82] These endogenously or exogenously acquired molecules are effective in neutralizing oxidative species via several mechanisms which include prevention, scavenging, as well as repairing of ROS damage.[71] Antioxidants can be classified, based on their biological activity, as either being enzymatic (*i.e.* superoxide dismutases [SODs], catalases [CATs] and glutathione peroxidases [GPxs]) or non-enzymatic (*i.e.* vitamins C [ascorbic acid] and -E [α-tocopherol], uric acid, β-carotene and glutathione [GSH]).[83-84] They can also be described according to their solubility profile as being either water-soluble (mainly found in the cytoplasmic matrix) or lipo-soluble (mostly present in cellular membranes).[81]

Enzymatic antioxidants are usually considered the first line of antioxidant defence against ROS.[81] They are comprised of a system of enzymes which utilize multi-step processes in the presence of co-factors, such as iron, zinc, copper and manganese, to reduce dangerous oxidative species into harmless products such as H_2O, alcohols and O_2.[81] The primary function of these antioxidants is to prevent and suppress ROS formation, with deficiencies linked to pathologies such as diabetes mellitus, Alzheimer's disease, cardiovascular disease and schizophrenia.[85] The three most important enzymatic antioxidants include; SODs, CATs and GPxs.[71]

Non-enzymatic antioxidants include low-molecular-weight substances which function by disrupting and inhibiting free radical chain reactions. These molecules act like scavengers in that they scavenge ROS by donating free electrons, thereby, making them harmless and easier to neutralize.[81] These molecules can protect against lipid peroxidation, cell apoptosis, activate and regulate several transcription factors, and revert other antioxidants to their active forms.[86]

1.6 Mitochondrial Replication

Unlike nuclear (n) DNA which is linear, mtDNA is a circular, double-stranded molecule of approximately 16.6 kilobases.[87] Each mitochondrion contains multiple copies of mtDNA, which comprises 37 genes encoding for 22 transfer ribonucleic acids (RNAs), two ribosomal (r) RNA and thirteen proteins.[88] The thirteen proteins are essential in synthesizing crucial proteins involved in OXPHOS, which include the subunit components of ETC complexes, as well as the ATPase.[88] For these reasons, proper maintenance of the genome is crucial. As mtDNA can only encode for a few proteins, as much as 99% of the organelles' total proteins are encoded for by nDNA, some of which make up the organelles maintenance and repair system.[89] Possible inadequacies in, or malfunctions of, these repair systems may result in imbalances between mitochondrial bioenergetics, biogenesis and cellular apoptosis.[90] This is evidenced by the association between the accumulation of mtDNA damage or reduction in mitochondrial copy numbers and the aetiology of several conditions affecting, among others, the brain, heart, liver and muscles.[87,91]

Mitochondrial replication is completely independent of the cell cycle and makes use of distinct nDNA-encoded replication machinery, such as mitochondrial-specific DNA pol-γ, mitochondrial single-stranded DNA-binding protein, DNA ligase, helicase TWINKLE and mitochondrial RNA polymerase.[92] Out of the four known polymerases (DNA pol-β,-theta [θ],-zeta [ζ] and PrimPol) which play a role in the mitochondria, DNA pol-γ is solely responsible for the replication and repair of mtDNA.[93-94] The DNA pol-γ holoenzyme is a heterotrimeric complex consisting of two subunits: the 140 kilodalton (kDa) catalytic subunit, DNA polymerase gamma subunit A (POLγA) and the 55 kDa dimeric accessory subunit, DNA polymerase gamma subunit (POLγB).[95] Deoxyribonucleic acid polymerase gamma subunit A is a highly accurate polymerase that belongs to the family A group of enzymes and contains a 3'-5' proofreading exonuclease activity, as well as a 5' deoxyribose phosphate lyase activity, that is used for base excision repair. Deoxyribonucleic acid polymerase gamma subunit b enhances the interaction between the holoenzyme with the template and also increases the efficiency and processivity of the POLγA subunit.[95-96] As a whole, DNA pol-γ functions in conjunction with the other nDNA-encoded mitochondrial-specific proteins to form the minimal mitochondrial replication apparatus.[87]

Interestingly, it has been reported that unlike the other polymerases, DNA pol-γ is more sensitive to inhibition by anti-HIV nucleoside analogues.[97] As previously mentioned, when pol-γ incorporates ddNTP analogues (*i.e.* AZT, stavudine [d4T], 3TC, *etc*.) it results in the inhibition of DNA pol-γ, thereby prematurely terminating processes such as mtDNA replication and repair. Disrupting these essential processes may result in mitochondrial damage, potential loss of function and mtDNA depletion which could, in turn, manifest as toxicities that closely resemble those seen in inherited mitochondrial diseases.[98] It is thought that the sensitivity of the enzymes to ddNTPs is attributed to a single tyrosine (Tyr) residue, Tyr951, within the B motif of pol-γ. The Tyr, which has since been found to be consistent in all poly-γ sequences, is essential for the recognition of the ddNTP/dNTP sugar moieties by the enzyme.[96] It has been reported that the substitution of the Tyr951 with a phenylalanine residue reduced the enzyme's sensitivity to being inhibited by ddNTP analogues by a factor of 5000, while minimally affecting the enzyme's overall function.[96]

1.7 Human Immunodeficiency Virus-Induced Mitochondrial Toxicity

As previously mentioned, a hallmark of HIV-1 infection is the progressive decline in CD4+ T-cell populations and immune dysfunction, however, the virus has also been shown to induce states of chronic inflammation, such as OS, which are known to weaken and damage biological components.[99] It has long been suggested that HIV may promote OS by inhibiting the synthesis and activity of several antioxidants (*i.e.* GSH) and dysregulating certain OS pathways, resulting in the escalation of ROS which may induce mitochondrial damage, the extent of which greatly depends on the stage of the disease.[100-101] Similar findings have been reported by others where it was demonstrated, in a small population of monocytes, that HIV-1 infected individuals generate higher levels of ROS, oxidized nucleic bases (*i.e.* 8-oxoguanine) and lipid peroxidation products compared to monocytes isolated from uninfected individuals.[102] The cellular effect of HIV-1 induced-ROS and the succeeding OS may promote disease progression by inducing HIV-1 replication and the production of pro-inflammatory cytokines such as tumour necrosis factor-alpha, through the activation of nuclear factor-kappa light chain enhancer of activated B cells (NF-κB), or through the activation of certain genes, which in turn further promote OS.[100] Consequences of such oxidative conditions include; the inhibition of several mitochondrial functions, lipid peroxidation, immune cell activation (*i.e.* lymphocytes and phagocytes), chronic inflammation and, notably, the apoptosis of CD4+ and CD8+ T-cells.[76,103-104]

It has been well documented that several complications (*i.e.* peripheral neuropathy, cardiomyopathy and nephropathy) commonly associated with HIV infection, closely resemble those brought about by NRTIs, hence the speculation that HIV-induced ROS may also result from the virus directly affecting the mitochondria.[105] One mechanism in which HIV may contribute to mitochondrial dysfunction involves the binding of the regulatory protein, viral protein R (Vpr), to the inner channel of the mitochondria permeability transition pore, which subsequently leads to imbalances in the redox state of cells and induces inflammatory conditions which favour cellular apoptosis.[106-107] HIV virulence factors, which are important for the successful replication of HIV-1 (*i.e.* transactivator of transcription protein and negative regulatory factor), have also been shown to increase mitochondrial Ca^{2+} uptake which, in turn, promotes viral transcription, ROS production and eventually cellular apoptosis.[108-109] Therefore, it could be postulated that the amount of HIV RNA present is proportional to the ROS.[110]

HIV has also been shown to have a direct effect on mtDNA, as previously noted in a study by Morse *et al.*[111] These authors found a positive correlation between the severity of HIV infection and the extent of mitochondrial damage, using a huMITOchip microarray on peripheral blood mononuclear cells (PBMCs) and adipose tissue from HIV-positive cART-naïve participants relative to HIV virally-suppressed participants. Furthermore, Miura *et al.* reported a positive correlation between the mtDNA levels in HIV-infected individuals and the CD4+ T-cell count, however, a negative correlation was found between mtDNA and HIV VL.[110,112] In addition, studies have shown that when the infection is coupled with chronic use of certain ARVs that are known to indirectly target mitochondria by inhibiting the mitochondrial adenylated kinase and adenosine nucleoside translocators, individuals taking AZT are subjected to prolonged complications and increased susceptibility to various MT-associated symptoms, examples of which include lethargy, hypotonia, movement disorders and vision and hearing impairments.[110,112-113] A study by Yu *et al.*, which investigated the mitochondrial function of HIV-infected individuals who were either cART-naïve or cART-exposed, reported increased mitochondrial mass in the CD4+ and CD8+ T-cell population of both groups, with a decline in CD4+ T-cells. An increase in ROS was also reported in the CD4+ T-cells, which the authors ascribed to the virus influencing the CD8+ T-cell mitochondrial membrane potential. However, the study found that the mitochondrial mass declined in both groups following long-term treatment with cART.[114] This has recently been extensively reviewed by Schank *et al.*[115]

1.8 Nucleoside and Nucleotide Reverse Transcriptase Inhibitor-Induced Mitochondrial Toxicity

As previously mentioned, NRTIs form the cornerstone of cART, however, prolonged administration of this class of drug has been shown to increase the incidence of side-effects, with the most prevalent being mitochondrial toxicities.[116] These toxicities are commonly associated with older NRTIs (*i.e.* AZT, d4T, didanosine [ddI], *etc.*) and may only be expressed upon reaching the specific biological threshold of mitochondrial dysfunction within each cell type.[52,117] Individuals put on chronic NRTI-based regimens have been shown to display mitochondrial defects in skeletal muscle and a consistent accumulation of NRTI-induced mtDNA somatic mutations, thereby eventually resulting in the dysregulation of the mitochondria.[117] Mitochondrial toxicity has a broad spectrum of clinical manifestations including; cardiomyopathy, skeletal myopathies, hepatic steatosis (with or without lactic acidosis) and nephrotoxicity, which can be difficult to reverse and may be life-threatening.[51,118-119] The NRTI, AZT, has been associated with the development of skeletal myopathy in HIV-infected individuals after being administered for a minimum of 6 months. The effects of this condition include fatigue and muscle loss.[120-121] In addition, AZT has also been shown to promote OS, affect the ETC, disrupt ultra-structures of cardiac mitochondria and downregulate the expression of cytochrome b (CYTB) mRNA.[122-123]

The exact pathogenesis underlying NRTI-induced MT remains vague, however, several studies have reported that during cART, NRTI ddNTPs may not only directly target viral RT, but also indirectly affect the mitochondrial replication enzyme, DNA pol-γ.[51] Inhibition of mitochondrial replication results in depletion of mtDNA which may lead to mitochondrial dysfunction and impaired OXPHOS, a condition that Lewis and Dalakas called the 'DNA pol-γ hypothesis'.[50] Evidence of reduced levels of mtDNA in various tissues of HIV-infected individuals who were on chronic NRTI-based HIV regimens have been found.[124] However, newer formulations of NRTIs such as ABC, TDF and 3TC have since been shown to be weaker inhibitors of mtDNA polymerases and contribute less to toxicities associated with mitochondrial syndromes.[125]

Several studies have demonstrated that not all NRTI drugs affect mitochondria with the same intensity.[91] It is thought that the intensity at which each NRTI affects DNA pol-γ is

dependent on the amount and class of drug being administrated; for example, certain drug combinations increase the development of MT; and certain drugs, such as d4T and ddI, have been shown to contribute to a greater extent to mitochondrial dysfunction when compared to AZT, 3TC and TDF.[52] Many studies have since shown that drugs, commonly known as D-category drugs (*i.e.* zalcitabine [ddC], d4T and ddI), have the most potent effect on the mitochondrial polymerase enzyme.[126]

As previously mentioned, other classes of ARVs, namely, NNRTIs and PIs, have been shown to also affect the mitochondria, however, via a different mechanism and to a lesser extent than both NRTIs and NtRTIs.[57,61] It has been suggested that PIs cause mitochondrial damage by affecting ROS and ATP production, mitochondrial membrane potential (MMP) and inducing apoptosis.[62] Several studies have shown PIs, such as nelfinavir (NFV), to increase ROS, resulting in a decrease in ATP and GSH.[127] Furthermore, it has also been suggested that several PIs may target the mitochondrial processing protease, which is crucial in cleaving the amino-terminal leader peptide of the matrix protein during mitochondrial importation.[128]

Similarly, the mitochondrial damage caused by NNRTIs revolves around biogenetics, ROS production and apoptosis.[62] In fact, studies have pointed to NNRTIs, such as EFV, favouring apoptosis, occurring through mitochondrial pathways and manifesting as a reduction in MMP, activation in caspase-3 and -9, and release of mitochondrial apoptogenic factors.[129-130] Moreover, when human coronary artery endothelial cells were treated with EFV there was an increase in OS (increased ROS and decreased GSH) and a decrease in MMP.[131] It has also been found that EFV-induced MT in hepatic cells is due to dysfunction of the ETC, reduced MMP and increased ROS.[130] As such, it can be postulated that the effects EFV have on the mitochondria are related to the development of hepatotoxicity and other metabolic side-effects which are commonly associated with the drug.[62]

Despite the significant effort and interest in finding a solution for NRTI-induced MT, the understanding of the exact pathophysiological events leading to the condition remains vague. However, with the discontinuation or adjustment of treatment, recovery of the mtDNA content is possible.[132]

1.9 Current Techniques used to detect Mitochondrial Toxicity

The current methods used to detect MT are complex and not standardized due to their invasive and costly nature.[133] However, due to the seriousness of the complications associated with drug-induced MT, there is a need within the field of HIV management for an alternative method of detection. Currently, several diagnostic methods, which combine clinical, laboratory, biochemical, pathological and genetic analysis are being used. These approaches have, however, been shown to have limitations and require additional confirmatory tests.[104,134]

1.9.1 Biochemical Analysis in Blood, Cerebrospinal Fluid and Urine

Most diagnostic procedures for detecting mitochondrial disorders involve assaying for selective mitochondrial biomarkers in either blood, cerebrospinal fluid (CSF) or urine. These generally comprise measurement of lactate, pyruvate, urine organic acids and amino acids.[135]

Lactic acidosis is the best recognised clinical abnormality associated with the effects of early mitochondrial dysfunction. Under normal conditions, pyruvate is converted to acetyl-CoA by the mitochondria and then shuffled into the TCA cycle to produce energy. However, when there is mitochondrial disruption, the production of pyruvate is either transaminated to alanine (Ala) or shifted to lactate, which then hinders the production of energy.[136] This results in the gradual accumulation of lactate within the blood.[121]

Elevated lactate levels may suggest the presence of a mitochondrial disorder and, as such, lactate may be a useful biomarker of mitochondrial dysfunction.[135] The ratio of lactate to pyruvate, which is denoted as L/P, is often used to distinguish disorders associated with pyruvate metabolism (*i.e*. pyruvate dehydrogenase or pyruvate carboxylase) from those of the ETC, with the sensitivity of the ratio being 31%, and specificity being 100%. Nevertheless, the ratio alone is only reliable when elevated lactate levels have also been reported.[135,137-138]

Measuring the concentration of amino acids present in the blood (plasma or serum), urine or CSF is another diagnostic method of assessing mitochondrial disorders, albeit not as common as the other biochemical methods. This method is most useful when elevated

concentrations of the non-essential amino acid, Ala, are detected in both blood and CSF, particularly when states of hyperalaninaemia are detected in fasting specimens.[32] Elevated Ala concentrations indicate an accumulation of pyruvate, which is most commonly associated with mitochondrial disease and other metabolic conditions such as urea cycle disorders and pyruvate carboxylase. The Ala concentrations are compared relative to the concentrations of the essential amino acid, lysine. A normal alanine:lysine ratio is considered to be < 3:1, with anything above indicating true hyperalaninaemia, which has been associated with mitochondrial diseases.[139] Other amino acids which have been associated with mitochondrial dysfunction include glycine, proline and sarcosine.[32,139]

Organic acids are by-products of the breakdown of macromolecules such as proteins, fats and carbohydrates. Changes in urinary organic acid levels have been reported in individuals with mitochondrial dysfunction and testing can be performed in selected clinical settings. As reported in a retrospective study, elevated levels of malate and fumarate were positively correlated with the presence of mitochondrial dysfunction in individuals with known mitochondrial disorders.[140] In another study, it was suggested that elevated concentrations of the urinary organic acid, dicarboxylic aciduria, a known by-product of mitochondrial fatty acid metabolism, were also found in individuals with mitochondrial disorders.[32]

The above-mentioned methods of determining MT are plagued with limitations and their reliability and sensitivity have yet to be established, as elevated levels have also been reported in other non-mitochondrial disorders such as hepatic dysfunction, metabolic disorders and renal failure, as well as in conditions of physical stress. There is thus a need for further investigations to identify a more reliable biomarker.[140-142]

1.9.2 Tissue Biopsy

The use of tissue biopsies (*i.e.* muscle, liver, kidney, *etc*.) has long been considered the gold standard for detecting and diagnosing mitochondrial disorders. This method relies on obtaining cryopreserved sections of tissue samples (*i.e.* skeletal muscle samples, as these samples are most often affected by mitochondrial dysfunction) to detect the presence of mitochondrial disorders, using various techniques such as histological and genetic analysis.[143-144] A major advantage of using tissue sample testing, as opposed to

biochemical testing techniques, is that tissue samples enable the detection of tissue-specific mtDNA mutations and quantification of mtDNA content (copy number).

1.9.2.1 Tissue Sample Histological Techniques

Histological analysis remains the most widely used diagnostic tool to screen for mitochondrial dysfunction in tissue samples and utilizes stains to analyze the samples under a light microscope. An example of a commonly used histological technique involves modified Gomori trichrome (MGT) stains, which enable the assessment of the muscle morphology and presence of abnormalities such as mitochondrial accumulation.[143] The stains also enable the detection of ragged-red fibres, a hallmark of mitochondrial disorders, which stain red and have a 'fibre cracking' appearance with an abnormal subsarcolemmal aggregation of mitochondria.[145]

A more sensitive method of staining involves the detection of NADH, SDH and COX activity. The pattern presented by SDH and COX stains usually indicates mitochondrial distribution within the sample and, unlike NADH stains, primarily aims to identify mitochondria.[142] Like MGT stains, SDH stains show the accumulation of mitochondria, which stain blue in muscle fibres, and are commonly termed ragged-blue fibres. Cytochrome c oxidase stains are simultaneously used with SDH stains to increase levels of detection of 'negative-COX (Complex IV) fibres' (which are easily identifiable as they stain blue compared to the brown positive-COX fibres in the preparation) whilst simultaneously measuring the activity of SDH. The presence of negative-COX fibres indicates the complex's poor activity during ETC, especially when coupled with high levels of SDH, strongly suggesting possible mitochondrial dysfunction.[32,134]

Similar to previously mentioned biochemical methods, histological techniques of detecting mitochondrial dysfunction, by way of stains, have been marred by limitations, particularly the lack of sensitivity and the need for fresh frozen tissue. In addition, the presence of the fibres have also been associated with other pathologies, such as myopathies, dystrophies and inflammatory myopathies.[146] Therefore, further evaluation of the method is recommended, so as to reduce the incidence of false positivity.[142,144,147]

1.9.2.2 The Quantification of Mitochondrial DNA within Tissue Samples

To genetically diagnose mitochondrial disorders, the simultaneous evaluation of both nDNA and mtDNA is required, followed by quantitative analysis.[148] Previously utilized techniques of mitochondrial evaluation include; Northern blotting, Southern blotting, gel electrophoresis, restriction fragment length polymorphism and temperature gradient gel electrophoresis analysis. These methods are, however, semi-quantitative, labour-intensive and require a large amount of DNA.[149-150]

These limitations have paved the way for the use of quantitative polymerase chain reaction (qPCR) approaches (*i.e.* TaqMan probe and SYBR green-based assays) to detect mitochondrial dysfunction, with the most frequent method determining the ratio between a target mtDNA gene and a reference nDNA gene, usually denoted as mtDNA/nDNA.[151] Using this method, several studies have found increased levels of mtDNA relative to nDNA to be associated with a variety of diseases which include; cancers, metabolic diseases and brain injuries, whilst decreased levels of mtDNA relative to nDNA have been associated with; ageing, Parkinson's disease and tumour development and progression.[152-154] When compared to other methods of measuring MT, qPCR is the most accepted as it allows for the mtDNA copy number to be determined without the need for additional reactions or assays which could potentially influence the results. However, like many other currently used MT detection approaches, it too has limitations such as; the measurements being affected by various pre-analytical factors, as well as differences in reproducibility between different laboratories, partly due to most published studies not describing their methods in sufficient detail.[151,155]

Despite muscle biopsies being the current standard for the diagnosis of mitochondrial dysfunction, it is an invasive method which requires special expertise and has been associated with some complications.[133] The procedure is also uncomfortable for individuals thereby making these biopsies a less attractive means of sampling. The method has also been affected by concerns about the sensitivity and specificity of each test. Therefore, less invasive sampling methods, which reduce the expense, expertise, as well as the number of specimens and techniques performed, are required.[133]

Blood is considered the preferred sample choice for measuring MT and a number of studies have attempted to evaluate the extent of mtDNA damage in PBMCs as an indicator of early MT.[133,156] Several studies have reported mtDNA depletion in PBMCs isolated from HIV-positive treatment-naïve individuals.[122] This method is, however, increasingly reported as being controversial due to the presence of mitochondria in the blood platelets possibly over-representing mtDNA levels in the PBMC samples, hence the need for a reliable systemic biomarker for detecting MT.

1.10 Fibroblast Growth Factor 21

Fibroblast growth factor 21 (FGF-21) is a hormone-like cytokine belonging to the FGF super-family, which is abundantly synthesized in the liver (and to a lesser degree in adipose tissue, the pancreas and skeletal muscles). It has been reported that FGF-21 plays an important role in the regulation of essential metabolic adaptations to maintain the homeostasis of the body.[157] An example of this being to improve energy expenditure and metabolic profiles during states of fasting and ketosis, as well as reducing inflammation.[158-159] The appearance of the FGF-21 receptor, FGFRT β-klotho complex, has been shown to determine the specific target tissue for the cytokine, with notable targets including; the liver, pancreas, adipose tissue, skeletal muscle and the central nervous system.[160-161]

It should be noted that most studies investigating the role of FGF-21 are mainly based on its role as a modulator of metabolism in health and diseases*;* however, there is limited data available regarding its role in HIV. Fibroblast growth factor 21 is capable of exerting either autocrine, endocrine, or paracrine control on specific target tissue types, in an attempt to achieve metabolic stability. In mice, FGF-21 has been reported to be primarily regulated by the peroxisome proliferator-activated receptor alpha, a key regulator of various genes involved in lipid metabolism.[158,162] This growth factor primarily promotes mechanisms such as the uptake and metabolism of glucose, storage of adipocytes, fatty acid oxidation, glucogenesis and ketogenesis and also increases energy expenditure and improves insulin sensitivity, by increasing insulin receptors in the liver and inhibiting lipolysis in adipose tissue.[158,163]

Apart from regulating the metabolism of glucose and lipids, FGF-21 has also been reported to play an important role in regulating mitochondrial activities and enhancing OXPHOS, as elevated levels have been associated with chronic inflammation and kidney disease.[164] Suomalainen, was the first to suggest that FGF-21 may be a better biomarker of inherited mitochondrial diseases compared to other previously used biomarkers, as the specificity (91.7%) and sensitivity (92.3 %) were high.[138] These authors previously found that the mitochondrial dysfunction in skeletal muscle biopsies from individuals suffering from inherited mitochondrial disorders correlated significantly with the measured serum levels of FGF-21. These findings were based on a significant percentage of cells displaying COX defects.[138] Another study by Davis *et al.* also found a positive association between muscle weakness and elevated levels of serum FGF-21 in individuals suffering from pre-existing mitochondrial disorders and further suggested that the increase may be from the skeletal muscles attempting to counteract the underlying metabolic insufficiencies of the individual. [165]

These associations have led to further studies suggesting the use of serum levels of FGF-21 as a 'first-line diagnostic test' for mitochondrial disorders, specifically those relating to muscle tissue, thereby reducing the need for a muscle biopsy.[165] Furthermore, elevated levels of FGF-21 have been associated with significant OXPHOS defects, and these same defects are a common underlying mechanism of many HIV-related conditions associated with the long-term use of NRTI-based treatment. It can, therefore, be hypothesized that mitochondrial dysfunction brought about by HIV treatments may also result in elevated levels of plasma/serum FGF-21.[51,138]

1.11 Growth and Differentiation Factor 15

Growth and differentiation factor 15 (GDF-15), also known as macrophage inhibitory cytokine-1, is a member of the transforming growth factor β superfamily.[166] Growth and differentiation factor 15 is widely expressed in the lungs, kidneys, pancreas, skeletal muscles and notably, elevated levels are often associated with stress-related conditions, leading to it being used as a biomarker of OS, mitochondrial disease, inflammation and hormonal changes.[167-168] Elevated levels of GDF-15 have also been reported in age-related conditions such as cardiovascular disease, diabetes, cancer, cognitive impairment as well as inflammation.[169-171]

As mitochondrial dysfunction has been reported to be a notable characteristic of ageing, it can be postulated that GDF-15 may also be a useful biomarker of mitochondrial dysfunction.[172] By measuring the GDF-15 concentrations in the serum or plasma of healthy individuals, as well as in individuals with non-mitochondrial and mitochondrial disorders, Yatsuga and colleagues demonstrated that GDF-15 is a sensitive and specific biomarker for diagnosing and monitoring the progression of mitochondrial disorders. These authors reported GDF-15 to have a 97.9% sensitivity and a 95.2% specificity, making it a credible diagnostic candidate.[173] Several studies have since shown that individuals possessing a thymidine kinase 2 gene mutation had significantly higher concentrations of GDF-15, particularly in serum and skeletal muscle. Importantly, significantly elevated levels of GDF-15 have also been detected in the serum of individuals with inherited mitochondrial disorders, which correlates with the previously stated findings.[168,174] A study conducted by Montero *et al*., which aimed to evaluate the use of GDF-15 as a possible biomarker for mitochondrial disease, differed from that conducted by Yatsuga *et al*. by including children below the age of 18 years as well as individuals with and without both mitochondrial and nDNA mutations.[173,175] The findings of the study showed GDF-15 to be sensitive enough to be used as a biomarker of mitochondrial dysfunction and suggested that GDF-15 be used in conjunction with another biomarker, such as FGF-21, to increase the efficiency of the results obtained.[173]

Non-invasive methods of determining MT would greatly enhance the ability to diagnose ARV-related MT early and allow for the monitoring of such conditions within an HIV-infected population. Both FGF-21 and GDF-15 have been proposed as potential candidates for MT detection. While GDF-15 has been shown to have a broader scope in detecting overall MT, FGF-21 is more specific for mitochondrial disorders manifesting in muscle tissue.[165] There is, however, still limited data on the reliability of these biomarkers, especially in the context of HIV-infected individuals. Given that infected people are treated with life-long ARVs, the risk of developing a potentially chronic condition, possibly as a result of MT, is ever increasing and the need for reliable, non-invasive testing is growing.

1.12 Rationale of the Study

The gold standard for MT detection includes the use of tissue samples (*i.e*. muscle and liver) acquired via biopsies, however, these methods are invasive and not acceptable in asymptomatic individuals.[176] In the present study, the extent of mtDNA damage was evaluated in PBMCs as an indicator of early MT.[177-178] Several recent studies have suggested that PBMCs should reflect what is found in muscle biopsies, due to NRTI-based regimens leading to depletions of most cellular mtDNA reserves.[179-180] In addition to monitoring depletions of mtDNA to screen for MT, the plasma levels of two candidates, FGF-21 and GDF-15, have been proposed as potential systemic biomarkers of MT.[181-182] Compared to biopsies, the measurement of systemic biomarkers is easier, less-invasive and more suited to the clinical setting.

The present study investigated MT in HIV-infected participants before initiation of a cART regimen consisting of a standard first-line combination of TDF, FTC and EFV, and again after 12-months of cART. Participants were recruited at a Community Health Centre in Tshwane, South Africa, as part of a large prospective study assessing treatment outcomes of individuals initiated on cART. The present study aimed to examine the possible associations between disease severity and cART with mitochondrial damage and to assess systemic biomarkers as an alternative to the mtDNA/nDNA ratio as a measure of MT in HIV-1 infected individuals. The data obtained adds valuable insight into the role of HIV itself and the effect of cART on mitochondrial dysfunction and provides support for further investigation into less invasive alternatives for MT determination in this group of individuals.

1.13 Aim and Objectives

1.13.1 Aim

The aim of this study was to investigate the possible associations between disease severity and cART, and mitochondrial damage. In addition, the association between systemic biomarkers and the mtDNA/nDNA ratio as a measure of MT in HIV-1 infected individuals was assessed.

1.13.2 Objectives

The objectives of this study were to:

1. Determine the extent of MT by detecting changes in mtDNA content, measured as the mtDNA/nDNA ratio in PBMCs before initiation of NRTI-based cART and again after 12-months of treatment by utilizing real-time qPCR.

2. Assess the association between pre-treatment and 12-month mtDNA/nDNA and each of the following: cART use, CD4+ T-cell count and HIV viral load (VL).

3. Compare the biomarkers, FGF-21 and GDF-15, measured using suspension array technology, with changes in the mtDNA/nDNA ratio as a measure of MT.

4. Assess the association between the pre-treatment and 12-month FGF-21 and GDF-15 and each of the following: cART use, CD4+ T-cell count and HIV VL.

CHAPTER 2

MATERIALS AND METHODOLOGY

2.1. Study Design

This study was a retrospective study that made use of peripheral blood mononuclear cells (PBMCs) and plasma samples that had previously been collected as part of a larger study titled: *The assessment of early warning indicators and markers of immune activation as risk factors for HIV-1 drug resistance* (ethics approval number 469/2013).

2.2. Study Population

The participants were recruited from a human immunodeficiency virus (HIV) treatment clinic at the Eersterust Community Health Centre located in the city of Tshwane, South Africa. The participants comprised combination antiretroviral therapy (cART)-naïve HIV-positive adults who were considered eligible for cART-initiation in accordance with the World Health Organisation (WHO) guidelines.[42] Informed consent was obtained from all recruited participants in the study. A total of 305 participants had been recruited in the main study. Of these, 214 participants were initiated on a standard first-line cART regimen which consisted of tenofovir disoproxil fumarate (TDF), emtricitabine (FTC) and efavirenz (EFV), and were followed-up for 12-months. Following 12 months of cART, 122 participants returned for 12-month blood tests and 98 were virally suppressed at this time point. Only participants who achieved virological suppression on the standard cART regimen were considered for the current study. Fifty-six participants had sufficient plasma samples from both time points to enable assessment of systemic levels of fibroblast growth factor 21 (FGF-21) and growth and differentiation factor 15 (GDF-15). Only 39 participants had sufficient PBMCs from both time points sampled for deoxyribonucleic acid (DNA) extraction.

The exclusion criteria for the larger study included individuals who were enrolled in a clinical trial, individuals who were part of an observational cohort for whom more follow-up efforts were made, individuals who had previously started and stopped cART at the

clinic as well as individuals transferred from another cART site and who were taking a cART regimen at the time of transfer. For the current study, an additional exclusion criterion included an incomplete set of samples (either PBMCs or plasma) collected at both baseline and 12-months post treatment.

This study evaluated two time points for each of the selected 56 participants, namely baseline (pre-treatment - month 0) and endpoint (month 12) samples. Participants were grouped according to their HIV viral load (VL) detected at baseline; Group 1, which included 30 HIV-infected individuals with high pre-treatment HIV VLs (> 100,000 copies/ millilitre [mL]); Group 2 included 13 HIV-infected individuals with low pre-treatment HIV VLs (< 10,000 copies/mL); and Group 3 included 13 HIV-infected individuals with intermediate VLs (10,000-100,000 copies/mL).

In addition, the present study included control PBMCs and plasma samples obtained from 15 healthy, HIV-negative volunteers, recruited as part of an ongoing study in the Department of Medical Immunology, University of Pretoria (Ethics approval number 116/2017). The control samples were collected at a single time point. Both the isolated PBMCs as well as the plasma samples were stored at -80 degrees Celsius (℃) until use. The inclusion criteria for the control participants in this study were that they should be certified as healthy following an assessment by a trained nurse. The recruited individuals were between 24 and 65 years of age. Individuals were excluded if they were found to be unwell upon examination by the nurse or if they had taken any medication on the day of venepuncture. All records were captured on Microsoft (MS) Excel spreadsheets that will be stored for 15 years in the Department of Medical Immunology at the University of Pretoria, with access to the information strictly limited to the researchers involved in the study.

2.3 Ethical Considerations

Ethics approval for both the previous studies was obtained from the Research Ethics Committee, Faculty of Health Sciences, University of Pretoria (UP REC reference number 469/2013 and 116/2017, respectively). Approval was granted for the collection and processing of plasma and isolation of PBMCs, as well as the analysis thereof.

In addition, the current study was granted ethical approval (UP REC reference number 489/2019) from the Research Ethics Committee, Faculty of Health Science, University of Pretoria.

Participation in both of the above-mentioned studies was completely voluntary, and participant's confidentiality was maintained by assigning unique numbers to each participant sample, to ensure anonymity.

2.4 Methodology

2.4.1 Collection, Processing and Analysis of Blood Samples

2.4.1.1 Whole Blood Collection

Whole blood samples were collected in vacutainer tubes containing ethylenediamine tetra acetic acid (EDTA) as an anticoagulant (Becton Dickinson, Franklin Lakes, NJ, USA). Two EDTA tubes (10 mL) were drawn from each participant and inverted approximately ten times to prevent the blood from clotting.

2.4.1.2 Cluster of Differentiation 4 Positive T-cell Count Determination

The cluster of differentiation 4 positive (CD4+) T-cells were quantified at baseline and again at the 12-month clinic visit. The analyzes were performed on an FC500 flow cytometer (Beckman Coulter, Brea, CA, USA) using the CD3/4/8 protocol software. The analyzes were performed by Ms Gisela van Dyk from the Department of Medical Immunology, University of Pretoria with the results being reported as cells/microlitre (µL).

2.4.1.3 Viral Load Determination

The VL for each participant was established as the amount of HIV ribonucleic acid (RNA) present in the blood. This was done using the NucliSENS® MiniMAG® extraction kits according to the manufacturer's instructions (bioMerieux Inc., Boxtel, NLD). The assay was performed by Ms Gisela van Dyk from the Department of Medical Immunology, University of Pretoria with the results being reported as copies/mL.

2.4.1.4 Isolation of Peripheral Blood Mononuclear Cells

Peripheral blood mononuclear cells for the 56 HIV-infected individuals were previously isolated from venous blood collected in EDTA blood collection tubes using Ficoll-density gradient centrifugation. The PBMCs from the 15 control samples were also isolated from blood collected in EDTA-containing collection tubes (10 mL) as follows: Fifteen millilitres of Ficoll (Histopaque 1077, Sigma Diagnostics, St. Louis, MO, USA) was added to 50 mL sterile conical tubes. Whole blood was slowly overlaid onto the Ficoll using a sterile serological pipette at a 45-degree angle where after the tube was centrifuged (Beckman Coulter, Brea, CA, USA) at 600 x gravitational force (g) for 25 minutes (mins) at room temperature (18-26°C) and pressure (RTP) with the brake OFF. After centrifugation, a sterile Pasteur pipette was used to carefully remove the top plasma layer, taking caution not to disrupt the cloudy white lymphocyte and monocyte layer (PBMC layer). The PBMC layer was then carefully collected into a clean conical tube. Phosphate buffered saline (PBS, pH 7.4) containing ethylene glycol bis (2-aminoethyl) tetra acetic acid (EGTA, 250 micromolar [µM]) was added at a ratio of 1:5 and gently mixed by inverting the tube. The solution was then centrifuged (Beckman Coulter) at 4°C for 10 mins at 300 x g with the brake ON. Following the centrifugation step, the resultant supernatant was discarded without disrupting the pellet and the pellet was resuspended in 15 mL of PBS. The sample was again centrifuged (Beckman Coulter) at 4°C for 10 mins at 300 x g. The resultant supernatant was once again discarded without disturbing the pellet followed by resuspension of the pellet in 1 mL of PBS. The cells were counted on a Microstar light microscope (Reichert-Jung, Cambridge, UK) using a haemocytometer and diluted with PBS to a final concentration of 1 x 10^7 cells/mL. The PBMCs were aliquoted in sterile tubes followed by a final centrifugation step at 4°C for 10 mins at 300 x g. The resultant pellets were then stored at -80°C (Thermo Fisher Scientific, Inc., Waltham, MA, USA) until use.

2.4.1.5 Preparation of Plasma from Whole Blood

The plasma samples were prepared within 4 hours (hrs) following collection of the whole blood. Upon receipt, the whole blood samples were centrifuged (Beckman Coulter) for 10 mins at 400 x g at RTP, with the brake OFF. The top plasma layer was then carefully aspirated (without disrupting the cell layer) into 2 mL sterile cryovial tubes and stored at

-80℃ (Thermo Fisher Scientific, Inc.) in the Department of Medical Immunology, University of Pretoria, until use.

2.4.1.6 Determination of Cotinine Levels in Stored Plasma Samples

Cotinine concentrations were measured in the stored plasma samples using the Neogen cotinine human forensic drug detection enzyme-linked immunosorbent assay (ELISA) (Neogen, Lexington, KY, USA). Plasma cotinine was used as an objective measure of tobacco use by the participants which could potentially alter pharmacokinetic and pharmacodynamic drug interactions as a result of the constituents present in cigarette smoke.[183] Tobacco products are also known to be contaminated with lipopolysaccharide which is an immunostimulant and may further result in increased levels of plasma biomarkers.[184-185] The assay was performed according to the manufacturer's instructions. The assay was a solid-phase competitive immunoassay, which utilized a 96-well plate pre-coated with cotinine capture antibodies that could bind to either the cotinine or the cotinine enzyme conjugate. Briefly, the reagents and samples were brought to RTP, followed by the addition of 20 µL of the standards, samples and controls to the respectively designated wells. One hundred microlitres of cotinine horseradish peroxidase (HRP) enzyme conjugate concentrate was then added to each well, after which, the plate contents were mixed on a plate shaker (Thomas Scientific, Swedesboro, NJ, USA) for 20 seconds (sec). The plate was incubated for 30 mins at RTP, to allow the cotinine in the samples to compete with the HRP enzyme conjugate for the antibody binding sites. Following incubation, the plate was washed three times with distilled water (dH_2O) using an automated plate washer (BioTek Instruments Ltd, Winooski, VT, USA). Substrate reagent (100 µL) was then added to each well, and the plate incubated for a further 15 mins at RTP. Following this incubation period, acid stop solution (100 µL) was added to each well, followed by a brief mixing of the plate contents on a plate shaker (Thomas Scientific). A colourimetric reaction takes place between the substrate and enzyme conjugate with an inverse relationship between colour intensity and the concentration of cotinine within the sample being observed. The optical density of the colour reaction was determined using a microplate spectrophotometer (PowerWaveX, Bio-Tek Instruments Inc., Winooski, VT, USA) set at a wavelength of 450 nanometres (nm). The results were recorded as nanograms (ng)/mL with levels $\geq$ 15 ng/mL taken as being positive for tobacco use.[186]

2.4.2 Assessment of Mitochondrial to Nuclear Deoxyribonucleic Acid Ratio in Peripheral Blood Mononuclear Cells using Real-Time Quantitative Polymerase Chain Reaction

2.4.2.1 Genomic Deoxyribonucleic Acid Extraction

Previously isolated PBMCs were used to prepare genomic DNA using the QIAamp DSP DNA Blood Mini Kit (Qiagen, Hilden, Germany). The samples were thawed, mechanically sheared with a pipette and adjusted to a volume of 200 µL by adding PBS (pH 7.4).

Before DNA extractions were performed, the work area and equipment were thoroughly decontaminated with 10% hypochlorous acid followed by 70% ethanol. All the required reagents and buffers were prepared at RTP as per the instructions of the manufacturer. Briefly, 20 µL of QIAGEN proteinase K was added to appropriately labelled clean microcentrifuge tubes, followed by the addition of 200 µL of the sample. This was followed by the addition of 200 µL AL buffer and each tube was briefly vortexed (Scientific Industries, Inc., New York, NY, USA) for approximately 15 sec to ensure lysis of the PBMCs. The tubes were then transferred to a pre-heated heating block (FMH instruments, Cape Town, South Africa) set to 56℃ and incubated for 10 mins. At the end of the incubation period, the samples were removed and briefly centrifuged (Lasec SA (Pty) Ltd., Midrand, South Africa) to remove any droplets that may have remained in the lid of the tube. Absolute ethanol (96–100%) (200 µL) was added to each tube and mixed by pulse vortexing (Scientific Industries, Inc.) after which the sample was given another brief centrifuge (Lasec SA, (Pty) Ltd) for 15 sec to remove any droplets that may have remained in the lid.

QIAamp mini spin columns were prepared for each sample in clean 2 mL collection tubes. The lysed samples were pipetted onto the columns, taking care not to wet the rim of the column, and then centrifuged (Kubota Corporations, Tokyo, Japan) at 5,000 x g for 1 min. The columns were transferred to clean 2 mL collection tubes, with both the filtrate and collection tube from the previous step being discarded. Buffer AW1 (200 µL) was carefully added onto the columns followed by centrifugation (Kubota Corporations) at 5,000 x g for 1 min. The spin columns were again transferred into clean 2 mL collection tubes, with both the filtrate and collection tubes being discarded. Buffer AW2 (500 µL)

was carefully added onto each column and the columns centrifuged (Kubota Corporations) at 10,000 x g for 3 mins. The resultant filtrate was discarded, and the columns were again centrifuged (Kubota Corporations) at 10,000 x g for 2 mins to eliminate the possibility of Buffer AW2 carry-over occurring. The filtrate and 2 mL collection tubes were discarded and the columns transferred into clean 1.5 mL microcentrifuge collection tubes. One hundred microlitres of AE buffer was added to each column followed by incubation at RTP for 5 mins. The tubes were then centrifuged (Kubota Corporations) for 1 min at 5,000 x g to elute the DNA.

2.4.2.2 Yield and Quality Assessment of Isolated Genomic Deoxyribonucleic Acid

The quantity and quality of the genomic DNA extracted from the PBMC samples were assessed immediately following extraction using a Thermo Fisher Scientific NanoDrop™ 1000 spectrophotometer (Thermo Fisher Scientific Inc., Waltham, MA, USA). The samples were analyzed by pipetting 2 µL of each sample directly onto the measurement pedestal. The results were processed using the NanoDrop™ 1000 3.8.1 software, and the DNA concentrations were expressed as ng/µL. The Beer-Lambert law was used to determine the concentration of the DNA, with an A260 reading of 1.0 being approximately 50 micrograms (µg)/mL of double-stranded DNA.[181] The purity was calculated using the standard A260/280 nm and A260/230 nm absorbance ratio. The results were captured on an MS Excel spreadsheet, which will remain stored in the Department of Medical Immunology, University of Pretoria, for 15 years (see Appendix C and D).

The isolated DNA samples were stored at -80℃ (Thermo Fisher Scientific Inc.) until further use.

2.4.2.3 Real-Time Quantitative Polymerase Chain Reaction

The Minimal Information for Publication of Quantitative real-time PCR Experiments (MIQE) guideline is a set of information pertaining to conducting qPCR experiments that must be met by researcher and authors alike to ensure that the resulting qPCR data is accurate, reliable and reproducible. The MIQE guidelines are crucial in ensuring that the integrity of the scientific literature, consistency and reproducibility between laboratories

and transparency of the experiments is maintained to increase confidence in the reliability of the results.[187-188] (See Appendix H)

For the purpose of the present study, quantitative polymerase chain reaction (qPCR) was used to determine the expression of the mitochondrial cytochrome b (*MT-CYB*) gene.

2.4.2.3.1 Selected Oligonucleotide Primers and TaqMan Probes

Quantitative PCR was used to quantify mitochondrial (mt) DNA and nuclear (n) DNA genes, from the extracted genomic DNA in the PBMC samples. The TaqMan assay was designed as a single-plex analysis and employed previously described primers and probes.[182] The mitochondrial target was a single region within the *MT-CYB* gene, which was normalised against the nuclear target or housekeeping/reference gene, which was the nuclear beta-2-microglobulin (*B2M*) gene and expected to be unaffected by the experiment or treatment.[182] The amplified mitochondrial target was 723-base pairs (bp) long and the reference nDNA gene was 96-bp long. Detection was achieved using TaqMan™ probes, which were designed with a 6-carboxyfluorescein (FAM) dye on the 5' end and a minor groove binding (MGB) non-fluorescent quencher on the 3' end (Applied Biosystems; Thermo Fisher Scientific Inc.). The primers and probes used in the qPCR assay to amplify the *MT-CYB* gene and the *B2M* gene are listed in Tables 2.1 and 2.2, respectively.

Table 2.1: Primers and probe used to amplify the mitochondrial cytochrome b (*MT-CYB*) gene.

Primer/Probe	Oligonucleotide sequence	Product size (bp)
MT-CYB Forward	5'-GCC TGC CTG ATC CTC CAA AT-3'	723
MT-CYB Reverse	5'-AAG GTA GCG GAT GAT TCA GCC-3'	
MT-CYB Probe	5'-FAM CAC CAG ACG CCT CAA CCG CCT T MGB-3'	

Table 2.2: Primers and probe used to amplify the nuclear beta-2-microglobulin (*B2M*) gene.

Primer/Probe	Oligonucleotide sequences	Product size (bp)
B2M -Forward	5'-CCA GCA GAG AAT GGA AAG TCA A-3'	96
B2M -Reverse	5'-TCT CTC TCC ATT CTT CAG TAA GTC AAC T-3'	
B2M -Probe	5'-FAM ATG TGT CTG GGT TTC ATC CAT CCG ACA MGB-3'	

The qPCR reaction mix was made-up to a final volume of 20 µL and comprised 200 nanomolar (nM) primers, 150 nM TaqMan probe (Thermo Fisher Scientific Inc.), reverse transcriptase (RT) PCR-grade water, DNA template, and TaqMan® Universal Master Mix II (Thermo Fisher Scientific Inc.). The exact quantity of each reagent used is given in Table 2.3. Amplification and detection of the product was performed using the Bio-Rad CFX96 Touch™ Real-Time System (Bio-Rad Laboratories Inc., Hercules, CA, USA) with the cycle conditions being described in Table 2.4.

Table 2.3: The qPCR reaction mix used in the assays.

Reagents	Stock	Final concentration	Volume X1 Reaction (µL)
Reaction Mix	-	X1	10
Forward primer	100 µM	200 nM	2
Reverse primer	100 µM	200 nM	2
TaqMan probe	100 µM	150 nM	2
RT PCR grade water	-	-	2
DNA template	-	<183 ng/reaction*	2
Final volume			20

* Concentration varies for each sample, however, 183 ng/µL is the highest captured concentration.

Table 2.4: The qPCR conditions used for the TaqMan assay.

Cycles	Temperature	Time	Cycle number
Activation	50℃	2 mins	1
Denaturation	95℃	10 mins	1
Amplification	95℃	15 sec	30
Final extension	60℃	1 min	

Fluorescence was detected at the end of each annealing step, with each run including a non-template control (NTC) (template DNA omitted and replaced with RT PCR-grade water) and two standards. For each assay, a melting point dissociation curve was generated, which, when examined, confirmed that only the desired target was amplified and that no primer-dimers were present.

2.4.2.3.2 Determining the Mitochondrial Deoxyribonucleic Acid Relative to Nuclear Deoxyribonucleic Acid Ratio

Following each run, a cycle threshold (Ct) value was obtained for each of the targeted genes. Gibson *et al.* defined the Ct value as being the lowest cycle number at which the fluorescence generated by the PCR, intersects with the threshold levels, which are higher than the background noise.[189] Therefore, samples having low Ct values would indicate that the fluorescence was detected quicker, thus suggesting that the sample in question had a high initial DNA concentration, and *vice versa*.

Relative quantification was used to determine the mtDNA fold change in each group. This method of quantification does not require the use of a standard curve, and instead makes use of several mathematical equations to analyze the data. The current study made use of the comparative Ct method, also known as the $2^{-\Delta\Delta Ct}$ method, as described by Livak and Schmittgen and illustrated in Table 2.5. This three step method assumes that 100% PCR efficiency was achieved and uses one internal control gene to calculate the fold change of the expression of the normalized desired gene relative to the untreated control.[190] The purpose of the internal control gene is to correct any variability which may occur during the various steps of the qPCR experiments. This may include the differences in the

integrity and amount of ribonucleic acid (RNA) added, and/or the efficiency of the synthesis. Common standard housekeeping genes such as glyceraldehyde 3-phosphate dehydrogenase (GAPDH), beta (β)-actin and ribosomal (r) RNA have proven to be useful as internal control genes.[190-191] For the purpose of this study *B2M* was chosen as the internal control gene, which has been shown to be an excellent candidate as an internal control, as per a study by Milhem *et al*.[192]

The first step requires converting the Ct value into a normalised relative quantity by using the delta (Δ)-Ct quantification model. The basic principle of this model is that a 'difference (delta) in quantification cycle value between two samples is transformed into relative quantities using the exponential function with the efficiency of the PCR reaction as its base'.[191] A value of two for the base E of the exponential function assumes 100% PCR efficiency was achieved. The ΔCt value is obtained by calculating the difference between the Ct value of the desired gene and the internal control from the same participant at the same time point. This step is then repeated for a second sample (either an untreated sample or the same sample post-treatment, as in the case of the present study) for which the expression of the desired gene in the first equation is to be related to.

Next, the two ΔCt values are subtracted from each other (former from latter), resulting in a value referred to as the ΔΔCt value, which is then used to calculate the fold change. The fold change is calculated using the Livak equation, $2^{-\Delta\Delta Ct}$, and gives the fold expression of the desired gene relative to the other chosen sample.[190]

This approach allows for any sample to be selected as a normalising gene, either an untreated sample or a sample with higher or lower expression. This is because the choice of sample does not affect the relative quantitative results. Despite the values seeming different at first, it can be assured that the true fold differences are identical.[191]

Participants with fold changes that are less than one are stated as displaying a possible reduction in mtDNA levels, which may then translate into mitochondrial toxicity (MT), whereas, fold changes that are greater than one, indicate the possible recovery of mtDNA in that particular participant. A fold change of one indicates no change in mtDNA levels over time.

Table 2.5: Equations used for calculating fold change, $2^{-\Delta\Delta Ct}$ **(**Livak and Schmittgen [2001]).[190]

Theory behind the calculation

Calculate delta Ct (ΔCt) by finding the difference between the desired and internal control gene cycle threshold values for same sample at the same time point.

Step 1:

$$\Delta Ct\ (1) = Ct\ (\text{desired gene}) - Ct\ (\text{internal control gene})$$

Step 2: Find the ΔCt of the sample that the expression of desired gene from Step 1 will be compared to (untreated sample or post-treatment). This depends on the study question.

$$\Delta Ct\ (2) = Ct\ (\text{desired gene}) - Ct\ (\text{internal control gene})$$

Step 3: Calculate the ΔΔCt value by finding the difference between the two ΔCt values.

$$\Delta\Delta Ct = \Delta Ct\ (1) - \Delta Ct\ (2)$$

Step 4: Next, the ΔΔCt is used to calculate the relative fold expression, by using the $2^{-\Delta\Delta Ct}$ equation.

$$\text{Relative fold expression} = 2^{-\Delta\Delta Ct}$$

The equations used for this study are as follows:

Equation 1: Calculating fold change between 12 months and baseline

Equation 1.1:

$$\Delta Ct = Ct\ (mtDNA) - Ct\ (nDNA)\ \text{baseline}$$

Equation 1.2:

$$\Delta Ct = Ct\ (mtDNA) - Ct\ (nDNA)\ \text{12-months}$$

Equation 1.3:

$$\Delta\Delta Ct = \Delta Ct\ (\text{baseline}) - \Delta Ct\ (\text{12-months})$$

Equation 1.4:

$$\text{Relative fold expression} = 2^{-\Delta\Delta Ct}$$

Equation 2: Calculating fold change between HIV-infected participants and controls at baseline

Equation2.1:

$$\Delta Ct = Ct\ (mtDNA) - Ct\ (nDNA)\ \text{baseline}$$

Equation 2.2:

$$\Delta Ct = Ct\ (mtDNA) - Ct\ (nDNA)\ \text{controls}$$

Equation 2.3:

$$\Delta\Delta Ct = \Delta Ct\ (\text{baseline}) - \Delta Ct\ (\text{controls})$$

Equation 2.4:

$$\text{Relative fold expression} = 2^{-\Delta\Delta Ct}$$

2.4.3 Plasma Biomarkers

2.4.3.1 Measurement of Fibroblast Growth Factor 21 and Growth and Differentiation Factor 15 Plasma Concentrations

The levels of the biomarkers, FGF-21 and GDF-15, were measured in the stored plasma samples using a custom ProcartaPlex™ Multiplex Immunoassay (Thermo Fisher Scientific, Inc.). This suspension bead array employs magnetic microsphere technology to detect multiple protein targets simultaneously.

Prior to running the assay, all reagents were brought to RTP and prepared according to the manufacturer's instructions. Briefly, the frozen samples were thawed at RTP, vortexed and centrifuged (Beckman Coulter) at 300 x g for 10 mins to remove all particulate matter. All incubation steps were carried out at RTP with gentle agitation (Thomas Scientific, Swedesboro, NJ, USA) and protected from light. To each well, 50 µL of the magnetic bead solution was added after which the plate was washed twice using an automated magnetic plate washer (Bio-Rad Laboratories Inc., Hercules, CA, USA). Universal assay buffer (25 µL) was added to each well, followed by the addition of 25 µL of prepared standards, samples and a blank to the appropriately assigned wells. The plate was then sealed and incubated for 2 hrs as described above. This step allowed for the antigen-specific antibody-coupled bead to react with targeted antigens in the samples and standards. Following incubation, the assay plate was washed twice using an automated magnetic plate washer (Bio-Rad Laboratories, Inc.) to remove any unbound protein. Detection antibodies (25 µL) were then added to each well, the plate was again sealed and incubated for an additional 30 mins at RTP, protected from light. After this incubation period, the plate was washed again as described above followed by the addition of 25 µL of streptavidin R-phycoerythrin conjugate to each well. The plate was sealed and incubated for 30 mins where after it was washed a final two times followed by the addition of 120 µL of reading buffer to each well. The plate was then sealed and shaken vigorously for two mins using a microplate shaker (BioTek Instruments, Inc., Winooski, VT, USA) to ensure that the beads were resuspended. The biomarkers were then assayed for on a Bio-Rad Luminex® 200™ Suspension Array System (Bio-Rad Laboratories Inc.). Bio-Plex Manager Software 6.0 was used for bead acquisition and analysis of median fluorescence intensity. The results were recorded as picograms (pg)/mL.

2.5 Data and Statistical Analysis

All statistical analyzes were conducted in consultation with Ms Tanita Cronje, Department of Statistics, Internal Statistical Consultation Service, University of Pretoria.

For the analyzes of the mtDNA levels obtained using qPCR, the experimental data were captured on an MS Excel spreadsheet and exported to the R Core Team (2020) (R: A language and environment for statistical computing. [R Foundation for Statistical Computing, Vienna, Austria]) software for processing. The analysis consisted of descriptive statistics such as frequencies and proportions, and made use of tables to organize the data.

For the analysis of the plasma biomarkers, the experimental data were captured on an MS Excel spreadsheet, cleaned and exported to Stata/IC 16.1 for Mac and R (Stata Corp. LLC, College Station, TX, USA). Firstly, descriptive statistics were used to describe the data using median and interquartile range (IQR) since the data had a non-normal distribution. Graphical representations were used to assist in visualizing aspects of the data. The statistical procedures used to assess the relevant associations and changes over time (at a 5% level of significance) included non-parametric tests such as the Mann-Whitney U test, Kruskal-Wallis H test, as well as the Wilcoxon signed-rank tests. Outliers, defined as values outside two SDs above or below the mean, were excluded.

For continuous variables, such as age, CD4+ T-cell count and VL, categories were constructed by grouping participants according to the median (in the case of age), and according to two and three categories as defined in the literature.[193-194] The groups for the CD4+ T-cell count (at both the pre-treatment and 12-month time points) and two categories for VL (only at pre-treatment) are shown in Tables 2.6, 2.7, 2.8 and 2.9, respectively.

Table 2.6: The two categories used to analyze the pre-treatment and 12-month post-cART CD4+ T-cell count.

Category	Immunological state of participant
Pre-treatment CD4+ T-cell count	
Category 1: < 200 cells/µL	Severe immunodeficiency
Category 0: ≥ 200 cells/µL	Moderate immunodeficiency
12-month post-cART CD4+ T-cell count	
Category 1: < 500 cells/µL	Moderate to severe immunodeficiency
Category 0: ≥ 500 cells/µL	No immunodeficiency

Table 2.7: The three categories used to analyze the pre-treatment and 12-month post-cART CD4+ T-cell count.

Category	Immunological state of participant
Pre-treatment CD4+ T-cell count	
Category 1: < 100 cells/µL	Very severe immunodeficiency
Category 2: ≥ 100 but < 200 cells/µL	Severe immunodeficiency
Category 3: ≥ 200 cells/µL	Moderate immunodeficiency
12-month post-cART CD4+ T-cell count	
Category 1: < 350 cells/µL	Severe immunodeficiency
Category 2: ≥ 350 but < 500 cells/µL	Moderate immunodeficiency
Category 3: ≥ 500 cells/µL	No immunodeficiency

Table 2.8: The two categories used to analyze the pre-treatment VLs.

Category	Immunological state of participant
Pre-treatment VL	
Category 0: < 100,000 copies/mL	Low VL
Category 1: ≥ 100,000 copies/mL	High VL

Table 2.9: The three categories used to analyze the pre-treatment VLs.

Category	Immunological state of participant
Pre-treatment VL	
Category 1: < 10,000 copies/mL	Low VL
Category 2: ≥ 10,000 but < 100,000 copies/mL	Moderate VL
Category 3: ≥ 100,000 copies/mL	High VL

CHAPTER 3

ASSESSING MITOCHONDRIAL DAMAGE BY DETERMINING THE MITOCHONDRIAL TO NUCLEAR DEOXYRIBONUCLEIC ACID RATIO

3.1 Introduction

Mitochondrial toxicity (MT) has been associated with the long-term use of antiretroviral (ARV) medication, particularly those belonging to the nucleoside reverse transcriptase inhibitor (NRTI) class. Mitochondrial toxicity can manifest as a variety of symptoms which include; nerve, heart and muscle disorders.[23,121] Studies have shown that the human immunodeficiency virus 1 (HIV-1) *per se* affects the mitochondria by inhibiting mitochondrial function and promoting cellular apoptosis.[80] As discussed in Chapter 1, MT is often measured using muscle biopsy specimens and relies on quantifying the mitochondrial deoxyribonucleic acid (mtDNA) to nuclear (n) DNA ratio, represented as mtDNA/nDNA.[151] Several studies have suggested that peripheral blood mononuclear cells (PBMCs) should reflect what is found in muscle biopsies, due to NRTI-based regimens leading to depletion of most cellular mtDNA reserves.[180,195]

The study presented in this chapter, investigated the extent of mitochondrial damage observed in HIV-infected participants treated with NRTI-based combination antiretroviral therapy (cART) by determining the mtDNA/nDNA ratio in PBMCs using real-time quantitative polymerase chain reaction (qPCR) before treatment initiation and following 12-months of cART. The associations between the extent of mitochondrial damage and the severity of the HIV disease, as measured by cluster of differentiation 4 positive (CD4+) T-cell count and HIV viral load (VL) in blood, and the use of cART were also determined.

3.2 Study Design

As stated in Chapter 2, section 2.1, the present study was a retrospective study which made use of samples that had been collected as part of a larger study titled: *The assessment of early warning indicators and markers of immune activation as risk factors for HIV-1 drug resistance*. In addition, PBMC samples from 15 healthy, HIV-negative volunteer donors were included as controls.

3.3 Study Population

Participants who had achieved virological suppression on the standard cART regimen, consisting of two NRTIs (tenofovir disoproxil fumarate [TDF] and emtricitabine [FTC]), and one non-nucleoside reverse transcriptase inhibitor (NNRTI) (efavirenz [EFV]) were considered for the current study. Samples from 39 out of the 56 participants were analyzed due to the exclusion of 17 participants as a result of insufficient PBMCs being available for DNA extraction at both time points. The samples from HIV-infected, treatment-naïve participants were characterized into 3 groups, based on their pre-treatment viral loads (VLs): less than 10,000 copies/millilitre (mL), 10,000 to 100,000 copies/mL and more than 100,000 copies/mL.

In addition, PBMCs collected from 15 healthy, HIV-negative participants, who had been recruited as part of an on-going study in the Department of Medical Immunology, University of Pretoria, were included as controls for this study. For these participants, blood was collected at a single time point and PBMCs were isolated and stored at -80 degrees Celsius (℃) until use.

3.4 Ethical Considerations

As mentioned in Chapter 2, section 2.3, informed consent was obtained from all recruited participants, and the above-mentioned studies were both granted ethical approval from the Research Ethics Committee, Faculty of Health Sciences, University of Pretoria (UP REC reference number 469/2013 and 116/2017, respectively). In addition, the current study was also granted ethical approval (UP REC reference number 489/2019). Participation in either of the above-mentioned studies was completely voluntary, with the inclusion and exclusion criteria for participants being described in detail in Chapter 2, section 2.2. All

records were captured anonymously in Microsoft (MS) Excel spreadsheets that will be stored for 15 years in the Department of Medical Immunology at the University of Pretoria, with access to the information strictly limited to the researchers involved in the study.

3.5 Materials and Methods

3.5.1 Whole Blood Collection

Whole blood samples were collected in vacutainer tubes containing ethylenediamine tetra acetic acid (EDTA) as an anticoagulant (Becton Dickinson, Franklin Lakes, NJ, USA) (see Chapter 2, Section 2.4.1.1).

3.5.2 Cluster of Differentiation 4 Positive T-cell Count Determination

The CD4+ T-cell surface markers were previously determined at baseline and again following the 12-month clinic visit on an FC500 flow cytometer (Beckman Coulter, Brea, CA, USA) using the CD3/4/8 protocol software with the results being reported as cells/microlitre (µL) (see Chapter 2, section 2.4.1.2). The baseline CD4+ T-cell counts were only available for 37 participants, while the 12-month post-cART CD4+ T-cell count was only recorded for 38 of the participants. This may be due to the relevant participants missing their follow-up appointments or insufficient blood being drawn at the time of the clinic visit.

3.5.3 Viral Load Determination

The VL for each participant was established as the amount of HIV ribonucleic acid (RNA) present in the blood using the NucliSENS® MiniMAG® extraction kit according to the manufacturer's instructions (bioMerieux Inc., Boxtel, NLD) and reported as copies/mL (see Chapter 2, section 2.4.1.3).

3.5.4 Determination of Cotinine Levels in Stored Plasma Samples

Cotinine concentrations, as an objective determination of tobacco use, were measured in the stored plasma samples using the Neogen cotinine human forensic drug detection enzyme-linked immunosorbent assay (ELISA) (Neogen, Lexington, KY, USA). The assay

was performed according to the manufacturer's instructions, as described in Chapter 2, section 2.4.1.6. The results are reported as nanograms (ng)/mL.

3.5.5 Isolation of Peripheral Blood Mononuclear Cells

Peripheral blood mononuclear cells were isolated from the venous blood collected in EDTA-containing blood collection tubes using Ficoll-density gradient centrifugation. The isolation of PBMCs was performed as described in Chapter 2, section 2.4.1.4. The isolated PBMCs were stored at -80℃ (Thermo Fisher Scientific Inc., Waltham, MA, USA) until use.

3.5.6 Genomic Deoxyribonucleic Acid Extraction and Preparation

The isolated PBMCs were used to prepare genomic DNA using the QIAamp DSP DNA Blood Mini Kit (Qiagen, Hilden, Germany) as described in Chapter 2, section 2.4.2.1. The eluted DNA was stored at -80℃ (Thermo Fisher Scientific, Inc.) until use.

3.5.7 Yield and Quality Assessment of isolated Genomic Deoxyribonucleic Acid

The quantity and quality of the genomic DNA extracted from the PBMC samples was assessed immediately following extraction using the Thermo Scientific NanoDrop™ 1000 Spectrophotometer (Thermo Fisher Scientific Inc.) and processed using the NanoDrop™ 1000 3.8.1 software as described in Chapter 2, section 2.4.2.2. The DNA concentrations were expressed as ng/µL (see Appendix E).

3.6 Real-Time Quantitative Polymerase Chain Reaction

3.6.1 Selected Oligonucleotide Primers and TaqMan Probes

Quantitative PCR (qPCR) was used to quantify mtDNA and nDNA genes from the extracted genomic DNA as described in Chapter 2, section 2.4.2.3.1.[182] The TaqMan assay was designed as a single-plex analysis and employed previously described primers and probes which adhered to the Minimum Information for Publication of Quantitative Real-Time PCR Experiments (MIQE) guidelines, as described in Chapter 2, section 2.4.2.3.[187] (see Appendix H)

3.6.2 Determining the Mitochondrial Deoxyribonucleic Acid relative to Nuclear Deoxyribonucleic Acid Ratio

The mtDNA/nDNA ratio between the different sample groups was calculated as described in Chapter 2, section 2.4.2.3.2, Table 2.5.[190] Participants with a fold change less than one were considered to be displaying a reduction in mtDNA levels, which may, in turn, translate into MT, whereas, fold changes that were greater than one indicated the possible recovery of mtDNA in a particular participant. A fold change of one was indicative of no change in mtDNA levels over time and was grouped together with the latter category.

3.7 Data and Statistical Analysis

All statistical analyzes were conducted in consultation with Ms Tanita Cronje, Department of Statistics, Internal Statistical Consultation Service, University of Pretoria, and are described in detail in Chapter 2, section 2.5.

3.8 Results

3.8.1 Demographic Information

Thirty-nine out of the 56 recruited HIV-positive participants, as well as all 15 healthy, HIV-negative participants had sufficient PBMCs for DNA extraction. Participants were grouped into two categories, namely; an HIV-positive group (n=39), which consisted of samples obtained at two time points (month 0 and 12-months) and an HIV-negative group, which consisted of 15 healthy, HIV-negative donor samples collected at a single time point. Following DNA amplification, one of the 15 healthy, HIV-negative participants was excluded from this study due to the participant displaying a very high cycle threshold (Ct) value which could not be explained. The corresponding demographic data of the 39 HIV-positive participants and remaining 14 healthy, HIV-negative individuals are presented in Table 3.1.

The median age of the HIV-positive and HIV-negative groups were not significantly different (HIV-positive: 38 years [Interquartile range [IQR]: 32-45 years] and HIV-negative: 42 years [IQR: 35-50 years], respectively; p=0.441). The gender proportion of each group was also similar with females making-up approximately 65% of the groups (HIV-positive: 26 out of 39 [66.67%] and HIV-negative: 9 out of 14 [64.29%],

respectively; p=0.747). In addition, albeit not significant, the proportion of tobacco users in the HIV-negative group was slightly higher than that of the HIV-positive participants (HIV-positive: 6 out of 34 [17.65%] and HIV-negative: 3 out of 14 [21.42%], respectively; p=0.405). Due to there being a limitation in the number of assays available for cotinine determination, 34 HIV-positive participants were chosen at random to act as a representative for the cohort. In addition, the tobacco use status of the HIV-negative participants was collected on recruitment of the participants into the study. The analysis also showed there to be no association between the use of tobacco with age (p=0.412), gender (p=0.735), CD4+ T-cell count at baseline (p=0.248), CD4+ T-cell count at 12-months post-cART (p=0.389) and VL (p=0.792) (results not shown).

All HIV-positive participants were prescribed a standard first-line cART regimen consisting of TDF, FTC and EFV. A significant increase in the CD4+ T-cell count of the HIV-positive participants was observed over the 12-month study period, from a median of 202 (IQR: 119 - 343) cells/µL (CD4+ T-cell percentage of 13.30% [9.00 – 20.00]) at baseline to 463 (IQR: 358 - 621) cells/µL (CD4+ T-cell percentage of 26.78% [18.00 – 33.00]) after 12-months on treatment. Furthermore, the VL for all participants was found to decrease from a median of 114,000 (IQR: 9,800 - 560,000) copies/mL to a fully suppressed HIV VL of below 50 copies/mL after 12-months on treatment. In addition, it was found that the pre-treatment CD4+ T-cell count and VL had a significant negative correlation, as expected (p=0.025).

Table 3.1: Demographic characteristics of the study population together with comparisons between HIV-positive and HIV-negative participants.

Categories	Statistical measure	HIV-positive n=39	HIV-negative n=14	*p*-value
Age (Years)	Median (IQR)	38 (32-45)	42 (35-50)	0.441
Gender	n (%)			
Male		13 (33.33)	5 (35.71)	0.747
Female		26 (66.67)	9 (64.29)	
Tobacco users ┼	n (%)	6 (17.65)	3 (21.42)	0.405
CD4+ T-cell count at baseline (cells/µL) *	Median (IQR)	202 (119 - 343)	N/A	N/A
CD4+ T-cell count at 12-months (cells/µL) **	Median (IQR)	463 (358 - 621)	N/A	N/A
CD4+ T-cell percentage (%) at baseline *	Median (IQR)	13.30 (9.00 – 20.00)	N/A	N/A
CD4+ T-cell percentage (%) at 12-month **	Median (IQR)	26.78 (18.00 – 33.00)	N/A	N/A
HIV viral load at baseline (copies/mL)	Median (IQR)	114,000 (9,800 - 560,000)	N/A	N/A
HIV viral load at 12-months (copies/mL)	Median (IQR)	Non-detectable (0 - < 50)	N/A	N/A

* Data available for 37 participants

** Data available for 38 participants

┼ Data available for 34 participants

3.8.2 Assessment of Mitochondrial to Nuclear Deoxyribonucleic Acid Ratio in Peripheral Blood Mononuclear Cells using Real-Time Quantitative Polymerase Chain Reaction

3.8.2.1 Validation of Primers and Probes

The TaqMan assay was designed as a single-plex analysis and employed previously described primers and probes (see Chapter 2, section 2.4.2.3.1).[182] However, the specificity of the primers and probes was further assessed independently using the primer and probe design tools from the Integrated DNA Technologies website in order to evaluate if the prescribed primer and probe designs followed the recommended MIQE guidelines.[196]

3.8.2.2 Efficiency of Quantitative Polymerase Chain Reaction Assay

The efficiency of the assay for both the nDNA and mtDNA genes in both the HIV-positive participants and healthy, HIV-negative individuals was measured using standard curves which were generated by serially diluting a sample of known concentration (determined using a NanoDrop™ 1000 spectrophotometer [Thermo Fisher Scientific Inc.]) (ng/µL) from the healthy volunteer group. The dilution range was generated with a five-point series, ranging from 1.84×10^{2} to 1.84×10^{-5} ng/mL for the mitochondrial cytochrome b (*MT-CYB*) gene and 1.84×10^{2} to 5.88×10^{-2} ng/mL for the nuclear beta-2-microglobulin (*B2M*) gene. Furthermore, each sample was run in duplicate. The resulting Ct values from these runs were plotted against the logarithm (Log) of their concentrations and used to test the efficiency. The efficiency was recorded as 100.60% for the *B2M* gene and 99.1% for the *MT-CYB* gene, indicating that the quantification of both targets was highly accurate (see Appendix E).

3.8.3 The Mitochondrial Deoxyribonucleic Acid Fold Change in the Study Population

The captured baseline, 12-month post-cART and healthy control delta (Δ) Ct values from the HIV-positive (n=39) and HIV-negative (n=14) participants, were used to determine the mtDNA fold change relative to another sample, using the $2^{-\Delta\Delta}$ CT method, as described in Chapter 2, section 2.4.2.3.2, Table 2.5 (see Appendices F and G). The expression of mtDNA was interpreted as the fold change at one point relative to another; as follows: a) the HIV-positive baseline expression of mtDNA relative to the 12-months post-cART expression, b) the HIV-positive baseline expression of mtDNA relative to the expression of the gene in the healthy, HIV-negative participants, and c) the HIV-positive 12-months

post-cART expression of mtDNA relative to the expression in the healthy, HIV-negative individuals. The fold changes within these categories are shown in Table 3.2.

Table 3.2: Mitochondrial DNA fold change determined for the study population using the $2^{-\Delta\Delta Ct}$ method.

Participant groups	Fold change
HIV-positive at baseline relative to the 12-months post-cART	0.804 (0.526 - 1.643)
HIV-positive at baseline relative to the healthy, HIV-negative participants	0.331 (0.217 - 0.474)
HIV-positive at 12-months post-cART relative to the healthy, HIV-negative participants	0.319 (0.247 - 0.529)

From the results obtained, it was observed that HIV-positive participants, regardless of treatment stage, had lower mtDNA levels than HIV-negative participants, with the most significant difference observed between the 12-month post-cART expression of mtDNA relative to that of the healthy, HIV-negative individuals. It was also evident that a reduction, albeit a slight one, in mtDNA occurred in participants following cART administration over 12-months, as seen by the downregulation of the gene from baseline to 12-months post-cART.

3.8.3.1 Determining the Mitochondrial Deoxyribonucleic Acid Fold Change over Time

Based on the calculated mtDNA fold change over 12-months on treatment, the HIV-positive (n=39) participants were categorised into two groups which consisted of the participant displaying a fold change of less than one (n=17), suggesting a reduction of mtDNA, therefore possibly indicating MT; or, greater than or equal to one (n=22), suggesting a possible recovery in mtDNA in those participants. Of note is that no participant had a fold change equal to one.

3.8.3.2 Demographic Information of the Human Immunodeficiency Virus-Positive Participants According to their Mitochondrial Deoxyribonucleic Acid Fold Change over 12-Months of Combination Antiretroviral Therapy

The demographic data for each group that the HIV-positive participants were assigned to according to the differences in their mtDNA fold change at 12-months post-cART compared to that at baseline are shown in Table 3.3.

Table 3.3: The demographic characteristics of the HIV-positive participants according to the expression of mtDNA following 12-months of cART.

Categories	Statistical measure	mtDNA depletion: < 1 n=22	mtDNA recovery: ≥ 1 n=17	*p*-value
				Fisher's exact test
Gender **Male** **Female**	n (%)	14 (63.64%) 8 (36.36%)	12 (70.59%) 5 (29.41%)	0.704
Tobacco users†	n (%)	5 (22.73%)	1 (0.06%)	0.226
				Kruskal-Wallis H test
Age (Years)	Median (IQR)	42 (35-52)	35 (31 - 38)	**0.010** ††
CD4+ T-cell count at baseline (cells/µL) *	Median (IQR)	216 (103 - 306) #	182 (125-366) ##	0.679
CD4+ T-cell count at 12-months (cells/µL) **	Median (IQR)	456 (370 -583)	489 (368 - 620) ##	0.768
HIV viral load at baseline (copies/mL)	Median (IQR)	77000 (11400 - 240000)	240000 (26000 - 720000)	0.240

* Data available for 37 participants
** Data available for 38 participants
# Data available for 21 participants
Data available for 16 participants
† Data available for 34 participants
†† Values in bold indicate significance

From the data recorded, it was observed that more than half (22 out of 39 [56.4%]) of the HIV-positive participants presented with signs of a possible reduction in mtDNA levels following 12-months of cART. A significant association between the median age of the participants in either group (42 [IQR 35 – 52] years and 35 [IQR 31 – 38] years, respectively) and the expression of mtDNA over time was found (p=0.010), with older participants more likely to display signs of mtDNA depletion. This finding was further substantiated when the age of the participants was further dichotomized according to the median age as well as according to the Joint United Nations Programme on HIV/acquired immunodeficiency syndrome (AIDS) (UNAIDS) cut-off of 50 years, into two additional subgroups.[197] The first grouping entailed categorising participants as either having an age that was less than or equal to 38 years, or greater than 38 years; the second grouping consisted of categorising participants as having an age that was less than or equal to 50 years, or greater than 50 years. These results are shown in Tables 3.4 and 3.5

Table 3.4: The associations between two age-defined subgroups and changes in mtDNA following 12-months of cART.

Categories	Statistical measure	mtDNA depletion: < 1 n=22	mtDNA recovery: ≥ 1 n=17	Chi-square test	*p*-value
Age (Years) (n=39)					
≤ 38 (n=20)	n	8	12	4.496	**0.034***
> 38 (n=19)	n	14	5		

* Values in bold indicate significance

Table 3.5: The associations between two age-defined subgroups and changes in mtDNA following 12-months of cART.

Categories	Statistical measure	mtDNA depletion: < 1 n=22	mtDNA recovery: ≥ 1 n=17	*p*-value
Age (Years) (n=39)				
≤ 50 (n=20)	n	3	17	**0.012***
> 50 (n=19)	n	19	0	

* Values in bold indicate significance

When analysing the results from both subgroups, a significant difference in the levels of mtDNA between the two age groups was found (p=0.034 and 0.012, respectively). Furthermore, from the results presented in both tables (Tables 3.4 and 3.5) it was evident that participants who were older experienced mtDNA depletion to a greater extent than the younger participants in this study. Interestingly, it was also found that no participants over the age of 50 years experienced any sign of mtDNA recovery.

No association was found between gender and use of tobacco products with changes in the level of mtDNA over time (p=0.704 and 0.226, respectively) (Table 3.3). It is interesting to note, however, that out of the 6 tobacco users, 5 had depletion of mtDNA while only 1 showed recovery of mtDNA levels. The small sample size is likely to have precluded the detection of statistically significant differences. Furthermore, analysis using the Kruskal-Wallis test revealed that there was no association between the mtDNA fold change of the 6 tobacco users and the non-tobacco users (p=0.3424) (results not shown).

In addition, the median baseline CD4+ T-cell count of participants who displayed reduced levels of mtDNA, was slightly higher than those of the participants who showed increased levels of mtDNA following the 12-month cART administration period (216 [IQR: 103 - 306] cells/µL and 182 [IQR: 125 - 366] cells/µL, respectively); nonetheless, no association with MT was found (p=0.679). Furthermore, no association between the 12-month CD4+

T-cell count and changes in mtDNA levels between the different groups was found. Similarly, while higher baseline VLs were found in participants who displayed mtDNA recovery than in participants with reduced mtDNA levels (240,000 [IQR: 26,000 - 720,000] copies/mL and 77,000 [IQR: 11,400 - 220,000] copies/mL, respectively; p=0.240), no significant association was found (Table 3.3).

3.8.3.3 The Association between Two Cluster of Differentiation 4 Positive T-Cell Count Subgroups and the Baseline Delta Cycle Threshold Values

Given the interest of exploring the impact of HIV itself on MT, the CD4+ T-cell counts were characterized into clinically relevant categories. The associations between the two CD4+ T-cell count categories (baseline [CD_0] [results available for 37 participants] and 12-months post-cART [CD_12] [results available for 38 participants]), with the baseline ΔCt values were evaluated.

At baseline (CD4_0), the participants (n=37) were grouped as either having a CD4+ T-cell count below 200 cells/µL (n=19), or greater than or equal to 200 cells/µL (n=18). Post-cART (CD4_12), the participants (n=38) were grouped according to either having a CD4+ T-cell count below 500 cells/µL (n=23), or greater than or equal to 500 cells/µL (n=15). These results are shown in Tables 3.6 and 3.7, respectively.

Table 3.6: The association between two baseline CD4+ T-cell count subgroups with the baseline ΔCt values.

Categories	Statistical measure	Baseline delta Ct values	*p*-value
CD4+ T-cell count at baseline (CD4_0) (cells/µL) (n=37) *			
< 200 (n=19)	Median (IQR)	1.257 (0.524 - 2.316)	0.331
≥ 200 (n=18)	Median (IQR)	0.684 (0.538 - 1.073)	

* Based on the determined CD4+ T-cell count obtained at baseline from 37 participants

Table 3.7: The association between two CD4+ T-cell count subgroups, 12-months post-cART treatment, with the baseline ΔCt values.

Categories	Statistical measure	Baseline delta Ct values	*p*-value
CD4+ T-cell count at 12-months (CD_12) (cells/µL) (n=38) *			
< 500 (n=23)	Median (IQR)	0.804 (0.538 - 1.364)	0.823
≥ 500 (n=15)	Median (IQR)	0.774 (0.476 - 1.995)	

* Based on the determined CD4+ T-cell count obtained at 12-month post-cART from 38 participants

From analysis of the results, no association was found between the two CD4+ T-cell subgroups from either time point with the baseline ΔCt values (p=0.331 and 0.823, respectively)

3.8.3.4 The Association between Three Cluster of Differentiation 4 Positive T-Cell Count Subgroups and the Baseline Delta Cycle Threshold Values

The CD4+ T-cell count was subsequently separated into three defined subgroups (baseline [CD_0] [results available for 37 participants] and 12-months post-cART [CD_12] [results available for 38 participants]), in which their association with the baseline Δ Ct values were assessed.

At baseline (CD4_0), the participants (n=37) were grouped as either having a CD4+ T-cell count below 100 cells/µL (n=7), greater than or equal to 100 but less than 200 cells/µL (n=12), or greater than or equal to 200 cells/µL (n=18). Post-cART (CD4_12), the participants (n=38) were grouped according to either having a CD4+ T-cell count below 350 cells/µL (n=9), greater than or equal to 350 but less than 500 cells/µL (n=14), or greater than or equal to 500 (n=15). These results are presented in Tables 3.8 and 3.9, respectively.

Table 3.8: The association between three baseline CD4+ T-cell count subgroups with the baseline ΔCt values.

Categories	Statistical measure	Baseline delta Ct values	*p*-value
CD4+ T-cell count at baseline (CD4_0) (cells/μL) (n=37) *			
< 100 (n=7)	Median (IQR)	0.534 (0.369 - 4.653)	0.235
≥ 100 but < 200 (n=12)	Median (IQR)	1.348 (0.693 - 2.096)	
≥ 200 (n=18)	Median (IQR)	0.684 (0.578 - 1.073)	

* Based on the determined CD4+ T-cell count obtained at baseline from 37 participants

Table 3.9: The association between three CD4+ T-cell count subgroups, 12-months post-cART treatment, with the baseline ΔCt values.

Categories	Statistical measure	Baseline delta Ct values	*p*-value
CD4+ T-cell count at 12-months (CD_12) (cells/μL) (n=38) *			
< 350 (n=9)	Median (IQR)	0.774 (0.470 - 2.316)	0.960
≥ 350 but < 500 (n=14)	Median (IQR)	0.791 (0.524 - 1.876)	
≥ 500 (n=15)	Median (IQR)	0.804 (0.538 - 1.364)	

* Based on the determined CD4+ T-cell count obtained at baseline from 38 participants

The findings from the present study show no association between the recorded baseline ΔCt values with any of the three CD4+ T-cell count subgroups at either of the two-time points investigated (p=0.235 and 0.960).

3.8.3.5 The Association between Two Viral Load Subgroups and the Baseline Delta Cycle Threshold Values

The HIV-infected participants were then characterized into two defined subgroups according to their recorded baseline VLs (VL_0). The participants were grouped as either having a baseline VL below 100,000 (n=18) copies/mL or a VL that was equal to or greater than 100,000 (n=21) copies/mL. These results are shown in Table 3.10.

Table 3.10: The association between two baseline viral load (VL) subgroups, with the baseline ΔCt values.

Categories	Statistical measure	Baseline delta Ct values	*p*-value
Viral load at baseline (VL_0) (copies/mL) (n=39)			
< 100,000 (n=18)	Median (IQR)	0.602 (0.476 - 1.073)	0.059
≥ 100,000 (n=21)	Median (IQR)	1.257 (0.655 - 1.995)	

The association between the baseline ΔCt and the baseline VL categories just missed statistical significance (p=0.059). Indeed, when observing the median values between the two VL groups, it was found that the ΔCt values were higher for participants in the higher VL subgroup but, once again, the small sample size could account for the absence of the differences reaching significance.

3.8.3.6 The Association between Three Viral Load Subgroups and the Baseline Delta Cycle Threshold Values

The participants recorded baseline VLs (VL_0) were also characterized into three defined subgroups. The participants were categorised as either having a VL of less than 10,000 copies/mL (n=9), great than or equal to 10,000 copies/mL but less than 100,000 copies/mL (n=9), or greater than or equal to 100,000 copies/mL (n=20). The results are presented in Table 3.11.

Table 3.11: The association between three baseline viral load (VL) subgroups, with the baseline ΔCt values.

Categories	Statistical measure	Baseline delta Ct values	*p*-value
Viral load at baseline (VL_0) (copies/mL) (n=39)			
< 10,000 (n=9)	Median (IQR)	0.804 (0.578 - 1.876)	
≥ 10,000 but < 100,000 (n=9)	Median (IQR)	0.538 (0.470 - 0.621)	**0.031***
≥ 100,000 (n=21)	Median (IQR)	1.320 (0.606 - 2.155)	

* Values in bold indicate significance

In contrast to what was observed when the baseline VL was divided into two subgroups, the differences between the three groups now reached statistical significance (p=0.031), with participants with the highest baseline VL being found to have the highest baseline ΔCt values, when compared to those with lower recorded baseline VLs.

3.8.3.7 The Association between Two Defined Cluster of Differentiation 4 Positive T-Cell Count Subgroups and the Mitochondrial Deoxyribonucleic Acid Fold Change Following 12-Months of Combination Antiretroviral Treatment

The effect of a 12-month cART regimen on the expression of mtDNA was assessed using the mtDNA fold change measured at 12-months post-cART compared to that determined at baseline.

The associations between the two CD4+ T-cell count subgroups at each time point (baseline [CD_0] [n=37] and 12-months post-cART [CD_12] [n=38]), and the mtDNA fold change 12-months after treatment are shown in Table 3.12 and Table 3.13. The participants were categorised into two defined subgroups according to their CD4+ T-cell count measured at baseline and 12-months post-cART, as well as whether the individuals

displayed a depletion or recovery in mtDNA following 12-months of cART. These groups are described in detail in Chapter 3, section 3.8.3.3.

Table 3.12: The associations between two baseline CD4+ T-cell count subgroups and changes in mtDNA following 12-months of cART.

Categories	Statistical measure	mtDNA depletion: < 1 n=21	mtDNA recovery: ≥ 1 n=16	Chi-square test	*p*-value
CD4+ T-cell count at baseline (CD4_0) (cells/µL) (n=37) *					
< 200 (n=19)	n	9	10	1.403	0.236
≥ 200 (n=18)	n	12	6		

* Based on the determined CD4+ T-cell count obtained at baseline from 37 participants

Table 3.13: The association between two 12-month post-cART CD4+ T-cell count categories and the effect of a 12-month cART regimen on the expression of mtDNA.

Categories	Statistical measure	mtDNA depletion: < 1 n=22	mtDNA recovery: ≥ 1 n=16	Chi-square test	*p*-value
CD4+ T-cell count at 12-months (CD_12) (cells/µL) (n=38) *					
< 500 (n=23)	n	14	9	0.212	0.646
≥ 500 (n=15)	n	8	7		

* Based on the determined CD4+ T-cell count obtained at 12-month post-cART from 38 participants

No association between the two CD4+ T-cell count subgroups from either of the two-time points with changes in mtDNA over time was found following analysis of the results using the Pearson's Chi-square test (p=0.236 and 0.646, respectively).

3.8.3.8 The Association between Three Defined Cluster of Differentiation 4 Positive T-Cell Count Subgroups and the Mitochondrial Deoxyribonucleic Acid Fold Change Following 12-Months of Combination Antiretroviral Treatment

The associations between the three CD4+ T-cell count categories, at baseline (CD_0) (n=37) and 12-months post-cART (CD_12) (n=38), and the mtDNA fold change 12-months after treatment were assessed and the results are shown in Table 3.14 and Table 3.15. The participants were characterized into three defined subgroups according to their CD4+ T-cell count measured at baseline and 12-months post-cART. These groups are described in detail in Chapter 3, section 3.8.3.4.

Table 3.14: The associations between three baseline CD4+ T-cell count subgroups and changes in mtDNA following 12-months of cART.

Categories	Statistical measure	mtDNA depletion: < 1 n=21	mtDNA recovery: ≥ 1 n=16	Fisher's exact test	*p*-value
CD4+ T-cell count at baseline (CD4_0) (cells/µL) (n=37) *					
< 100 (n=7)	n	5	2	4.017	0.208
≥ 100 but < 200 (n=12)	n	4	8		
≥ 200 (n=18)	n	12	6		

* Based on the determined CD4+ T-cell count obtained at baseline from 37 participants

An analysis of the data revealed there to be no association between the three baseline CD4+ T-cell count subgroups and changes in mtDNA expression as determined by Fisher's exact test (p=0.208 and 4.017, respectively), as shown in Table 3.14. However, more than half (12 out of 21 [57.14%]) of the participants who showed a decrease in mtDNA levels had a baseline CD4+ T-cell count greater than or equal to 200 cells/µL, with the remaining participants in the group falling into the other two baseline CD4+ T-cell subgroups (CD4+ T-cell greater than or equal to 100 but less than 200 cells/µL: 4 out of 21 [19.05%] and CD4+ T-cell count less than 100 cells/µL: 5 out of 21 [23.81%]).

Table 3.15: The association between three 12-month post-cART CD4+ T-cell count categories and the effect of a 12-month cART regimen on the expression of mtDNA.

Categories	**Statistical measure**	**mtDNA depletion: < 1 n=22**	**mtDNA recovery: ≥ 1 n=16**	**Chi-square test**	***p*-value**
CD4+ T-cell count at 12-months (CD_12) (cells/µL) (n=38) *					
< 350 (n=9)	n	5	4		
≥ 350 but < 500 (n=14)	n	9	5	0.383	0.826
≥ 500 (n=15)	n	8	7		

* Based on the determined CD4+ T-cell count obtained at 12-month post-cART from 38 participants

Similarly, the association between the 12-month post-cART CD4+ T-cell count subgroups and changes in mtDNA, as determined using the Pearson's Chi-square test, revealed no association between the three 12-month post-cART CD4+ T-cell count subgroups with changes in the expression of mtDNA over time (p=0.826), as shown in Table 3.15.

3.8.3.9 The Association between Two Defined Viral Load Subgroups and the Mitochondrial Deoxyribonucleic Acid Expression following 12-Months of Combination Antiretroviral Treatment

The associations between the two VL subgroups at baseline (VL_0) (n=39), with changes in mtDNA expression over 12-months are shown in Table 3.16.

The HIV-infected participants were characterized into two defined subgroups according to their baseline VLs (VL_0). The participants were grouped as described in detail in Chapter 3, section 3.8.3.4.

Table 3.16: The association between two defined viral load subgroups and changes in mtDNA following 12-months of ARV treatment.

Categories	Statistical measure	mtDNA depletion: < 1 n=22	mtDNA recovery: ≥ 1 n=17	Chi-square test	*p*-value
Viral load at baseline (VL_0) (copies/mL) (n=39)					
< 100,000 (n=18)	n	13	5	3.400	0.065
≥100,000 (n=21)	n	9	12		

The association between the baseline VL subgroups and changes in mtDNA over time just missed statistical significance (p=0.065), as shown in Table 3.16. Most of the HIV-infected participants who displayed depletion of mtDNA (13 out of 22 [59.09%]) were in the lower baseline VL subgroup (less than 100,000 copies/mL). In contrast, most of the participants who displayed mtDNA recovery (12 out of 17 [70.59%]) were in the higher VL subgroup (equal or greater than 100,000 copies/mL).

3.8.3.10 The Association between Three Defined Viral Load Subgroups and the Mitochondrial Deoxyribonucleic Acid Expression following 12-Months of Combination Antiretroviral Treatment

The HIV-infected participants were characterized into three defined subgroups according to their baseline VLs (VL_0). The participants were grouped as described in detail in Chapter 3, section 3.8.3.5. The results are shown in Table 3.17.

Table 3.17: The association between three defined viral load subgroups and changes in mtDNA following 12-months of ARV treatment.

Categories	Statistical measure	mtDNA depletion: < 1 n=22	mtDNA recovery: ≥ 1 n=17	Fisher's exact value	*p*-value
Viral load at baseline (VL_0) (copies/mL) (n=39)					
< 10,000 (n=9)	n	5	4		
≥10,000 but < 100,000 (n=9)	n	8	1	4.931	0.066
≥ 100,000 (n=20)	n	9	12		

The analysis of the results showed there to be no association between the three baseline VL subgroups and the expression of mtDNA following 12-months of cART, as determined by a Pearson's Chi-square test (p=0.085).

3.8.4 Relationship between the Logarithmically Transformed Variables and the Mitochondrial Deoxyribonucleic Acid Fold Change

To reduce the skewness of the original data, certain continuous variables were logarithmically transformed by replacing the variable (x) with the Log (x). The transformed variables include; 1) the CD4+ T-cell count (baseline and 12-months post-cART); 2) the baseline VL, and; 3) the mtDNA fold change. The relationships between these transformed values and the mtDNA fold change were then determined.

3.8.4.1 Correlation between the Transformed Cluster of Differentiation 4 Positive T-Cell Count (Baseline and 12-Months Post-Combination Antiretroviral Treatment) and Baseline Viral Load with the Mitochondrial Deoxyribonucleic Acid Fold Change over Time

In order to determine whether there was a significant association between the mtDNA fold change and either of the transformed variables (CD4+ T-cell count [baseline and 12-months post-cART] and baseline VL) a Pearson's correlation test was performed. The results are presented in Tables 3.18, 3.19 and 3.20, respectively.

Table 3.18: Pearson's correlation matrix for the Log of the mtDNA fold change and the Log of the CD4+ T-cell count at baseline.

Categories		Log mtDNA fold change	Log CD_0
Log mtDNA fold change:	Pearson's correlation (r)	1.000	
	p-value	-	
	n	37	
Log CD_0:	Pearson's correlation (r)	-0.046	1.000
	p-value	0.789	-
	n	37	37

* Based on the determined CD4+ T-cell count obtained at baseline from 37 participants

Table 3.19: Pearson's correlation matrix for the Log of the mtDNA fold change and the Log of the CD4+ T-cell count at 12-months post-cART.

Categories		Log mtDNA fold change	Log CD_12
Log mtDNA fold change:	Pearson's correlation (r)	1.000	
	p-value	-	
	n	38	
Log CD_12:	Pearson's correlation (r)	0.123	1.000
	p-value	0.461	-
	n	38	38

* Based on the determined CD4+ T-cell count obtained at 12-month post-cART from 38 participants

Following a Pearson's correlation test, no relationship between either of the Log CD4+ T-cell count time points and Log mtDNA fold change (p=0.789 and 0.461, respectively) was found.

In addition, no association was found between the baseline VL and the mtDNA fold change after logarithmic transformation (p=0.448).

Table 3.20: Pearson's correlation matrix for the Log of the mtDNA fold change and the Log of the VL at baseline.

Categories		Log mtDNA fold change	Log VL_0
Log mtDNA fold change:	Pearson's correlation (r)	1.000	
	p-value	-	
	n	39	
Log VL_0:	Pearson's correlation (r)	0.122	1.000
	p-value	0.448	-
	n	39	39

3.8.4.2 Linear Regression Analysis between the Mitochondrial Deoxyribonucleic Acid Fold Change and the Transformed Cluster of Differentiation 4 Positive T-Cell Count (Baseline and 12-Months Post-Combination Antiretroviral Treatment) and Baseline Viral Load

A linear regression analysis was performed in order to determine whether a linear relationship between transformed variables (CD4 + T-cell count at baseline and 12-months post-cART and baseline VL) with changes in the mtDNA fold change over time existed. The results are shown in Tables 3.21, 3.22 and 3.23, respectively.

Table 3.21: The linear regression analysis for the Log of the mtDNA fold change over time and the Log of the CD4+ T-cell count at baseline.

Log mtDNA fold change	Coeff.	Std. Err.	t	P > ltl	95% Conf. Interval)		*F* (1, 35)	Prob > F	R-Squared
Log CD4+ T-cell count at baseline	-0.047	0.175	-0.270	0.789	-0.402	0.307	0.070	0.789	0.002
Constant	0.202	0.918	0.220	0.828	-1.663	2.066			

* Based on the determined CD4+ T-cell count obtained at baseline from 37 participants

Abbreviations: Coeff=Coefficient; **Std. Err**=Standard error of the regression; **t**=t-value; **95% Conf. Interval**=95% Confidence interval; ***F***=F-value

Table 3.22: The linear regression for the Log of the mtDNA fold change over time and the Log of the CD4+ T-cell count at 12-months post-cART.

Log mtDNA fold change	Coeff.	Std. Err.	t	P > ltl	95% Conf. Interval)		*F* (1, 36)	Prob > F	R-Squared
Log CD4+ T-cell count at 12-months post-cART	0.131	0.176	0.750	0.460	-0.225	0.487	0.560	0.461	0.015
Constant	-0.846	1.071	-0.790	0.435	-3.019	1.326			

* Based on the determined CD4+ T-cell count obtained at baseline from 38 participants

Abbreviations: Coeff=Coefficient; **Std. Err**=Standard error of the regression; **t**=t-value; **95% Conf. Interval**=95% Confidence interval; ***F***=F-value

The linear regression established that the transformed CD4+ T-cell count at baseline and at 12-months post-cART could not statistically predict the mtDNA fold change (*F* [1.35] and *F* [1,36] =0.070 and 0.560, *p*=0.789 and 0.461; respectively). Furthermore, the analysis pointed to the Log CD4+ T-cell count at either time point, accounting for 0.20% (baseline) and 1.50% (12-months post-cART) of the variability in the fold change. The regression equations were as follows: mtDNA fold change=0.202 - 0.047x, where x=Log CD4+ T-cell count at baseline, and mtDNA fold change=-0.846 + 0.131x, where x=Log CD4+ T-cell count at 12-months post-cART.

Table 3.23: The linear regression analysis for the Log of the mtDNA fold change and the Log of the VL at baseline.

Log mtDNA fold change	Coeff.	Std. Err.	t	P > ltl	95% Conf. Interval		*F* (1, 39)	Prob > F	R-Squared
Log VL_0 at baseline	0.032	0.041	0.770	0.448	-0.052	0.115	0.590	0.440	0.016
Constant	-0.393	0.471	-0.830	0.409	-1.348	0.562			

Abbreviations: Coeff=Coefficient; **Std. Err**=Standard error of the regression; **t**=t-value; **95% Conf. Interval**=95% Confidence interval; ***F***=F-value

From the results obtained, it was established that the transformed baseline VL could not predict the fold change in mtDNA [*F* (1, 39) =0.590, *p*=0.448]. Furthermore, the variability of the fold changes was accounted for by 1.56% of the Log of the VL at baseline. The regression equation used was as follows: mtDNA fold change=-0.393 + 0.032x, where x=Log baseline VL.

3.9 Discussion

Antiretroviral drugs, particularly those of the NRTI class, have been associated with adverse effects in cART-treated individuals.[22,116] It has been well documented that HIV-infected individuals commonly develop at least one drug-related toxicity, with the most complicated being MT, which is induced by depleted mtDNA levels which consequently progress to mitochondrial dysfunction and deregulation of cellular metabolism.[22,198] Many studies encourage the use of PBMCs, instead of tissue samples, for the diagnosis and monitoring of MT since they are less invasive and easier to obtain. However, using PBMCs as surrogates for tissue is still controversial with many studies producing contradictory results. Whether these reported results are a consequence of using PBMCs is yet to be established.[122,180,199] In the present study, the mtDNA/nDNA ratios in the DNA isolated from PBMCs of HIV-positive individuals at two time points and healthy, HIV-negative individuals at one time point, were determined.

A longitudinal analysis of the mtDNA/nDNA ratios for samples, extracted from PBMCs from peripheral venous blood, collected from the HIV-infected individuals at baseline and 12-months post-cART, showed a slight downregulation in the mtDNA levels observed at 12-months post-treatment. This would suggest that the long-term, chronic use of the cART regimen, consisting of TDF, FTC and EFV, prescribed to the participants of this study negatively affected mtDNA levels. These findings are similar to those observed in other studies which also found an association between the use of NRTIs with mitochondrial damage and mtDNA depletion, albeit with older regimens containing stavudine (d4T) or azidothymidine (AZT).[66,195] Furthermore, when comparing the expression of mtDNA in the HIV-infected groups with the healthy, HIV-negative participants, the HIV-infected individuals showed significantly lower levels of mtDNA, with the greatest difference observed after 12 months of cART.

These findings coincide with those reported by Côté *et al*, who found that HIV-positive individuals had significantly lower mtDNA/nDNA ratios than their HIV-negative counterparts.[122] Similarly, another study that explored the effect of cART and HIV on placental mitochondria using qPCR, also found significantly reduced mtDNA/nDNA ratios in the placenta of cART-treated HIV-infected women, when compared to HIV-negative participants.[200] This study is especially important since participants were using a wide range

of NRTIs, including TDF. Furthermore, studies found that cART regimens, which included AZT, not only induced mtDNA depletion but also increased oxidative stress (OS), secondary mitochondrial dysfunction and cellular apoptosis.[200-201] It has been postulated in the 'DNA pol-γ hypothesis' that, due to the inhibitory action of NRTIs on the mitochondrial polymerase enzyme, depletion of mtDNA, increased production of reactive oxygen species (ROS) and, therefore, energy dysfunction would be expected.[66]

The use of TDF is believed to have less of an effect on the mitochondria, compared to the older NRTI drugs. However, there has recently been a renewed interest in TDF-associated MT, specifically its role in the development of kidney dysfunction.[202] Future studies should consider looking at tissue-specific effects of different NRTIs. This is also true of EFV, especially its role in neurological and lipid side-effects. This mechanism could potentially be via depletion of ribonucleotide and deoxyribonucleotide pools.[203-204] This is in contrast to the protease inhibitors, which have been shown to inhibit mitochondrial-mediated apoptosis and could contribute to recovery of mtDNA.[205]

In contrast to the current study's findings and those from the above-mentioned studies, Morse *et al*. found that, while the adipose tissue mtDNA/nDNA was decreased in participants receiving cART, no such difference could be detected in PBMCs of HIV-negative individuals and HIV-positive individuals who were untreated or administrated NRTI-based cART regimens.[111] These findings may suggest that the use of the mtDNA/nDNA ratio from DNA isolated from PBMCs may not be as reliable a marker of HIV- and NRTI-induced MT as that determined using tissue biopsies, which are still considered to be the gold standard. It could, however, also be that the differences found may be as a result of variations in the study populations, cART regimens and duration of treatment.[198] In another study by Montaner *et al*., a decrease in mtDNA in HIV-infected individuals was found when compared to that of HIV-negative individuals, however, the HIV-infected individuals were cART-naïve. The mtDNA depletion was, therefore, attributed to the HIV infection and not the use of NRTIs.[195]

The present study's results, together with previous findings, point to the virus itself having a direct effect on the mitochondria. In fact, Morse *et al.* suggested that this damage to the mitochondria may result from HIV-associated inflammation and chronic immune cell activation.[111] High cell turnover, which is a trademark of ARV-naïve HIV-infected

individuals, is thought to interfere with mtDNA replication; however, replication is restored when the HIV-infected individuals are administered cART, possibly due to the cell turnover declining. Despite cART alleviating problems associated with mtDNA replication, the risk of developing MT increases with the wide use of drugs such as stavudine (d4T) and didanosine (ddI), and possibly even with the well tolerated NRTI, 3TC/FTC, and the newer nucleotide reverse transcriptase inhibitors (NtRTI), TDF.[198]

It has been reported that with a decline in mtDNA, there is also a coupled over-production of ROS, which is associated with OS and may lead to cellular damage and the further decline in the cellular levels of mtDNA. A study by Lee *et al*., found that exposing human cells to sublethal concentrations of hydrogen peroxide (H_2O_2) not only leads to senescent-like growth arrest of the cells, but interestingly, also increased the number of cells with functional mitochondria and mtDNA.[206-207] Furthermore, these authors found that OS induced by the decline of glutathione induced increases in mtDNA levels. In another experiment by Suzuki *et al.*, OS was induced in human fibroblast cells that were stained with nonyl-acridine orange dye, which is commonly used to monitor mitochondrial mass. The cells were then exposed to antimycin A, which inhibits cellular respiration and disrupts the electron transport chain. Antimycin A was shown to induce an increase in the mitochondrial genes, cytochrome c1 (*CYC1*) and *MT-CYB*, as was observed by an increase in intensity of the dye in the treated cells, following 72 hours of exposure to the inhibitor.[208] Most notably, just three hours before the expression of the two mitochondrial genes could be detected, the intracellular levels of H_2O_2 were found to increase, indicating that OS not only inhibits cellular growth, but also leads to increases in mitochondria and mtDNA content.[207]

Interestingly, when the influence of age, gender and tobacco use on the mtDNA fold change was assessed, it was found that age had a significant influence on the mitochondrial copy number. In fact, several studies have linked mtDNA heteroplasmy[§] and copy number with aging.[209-210] The process of aging itself, is associated with a loss in physiological integrity and increase in DNA damage over time.[211] Mitochondrial DNA is thought to be a major target of the aging process as it is prone to accumulating mutations, possibly due to increased chances of oxidative damage and it having a lower replication fidelity when compared to nDNA.[212] Studies have also linked lower mtDNA copy number with older

[§] Heteroplasmy: The co-existence of two or more variants of mitochondria DNA within the same cell.

individuals. Ding *et al*., suggested that older individuals displayed increased trends in heteroplasmy and reduced mtDNA expression, however, the study had several limitations and was unable to prove if the influence of aging on mtDNA mutations and copy number were independent from each other.[213] Furthermore, a study by Zhang *et al*., showed that when investigating the PBMCs of female participants, the degree of heteroplasmy increased by almost 58.5% in participants over the age of 70 years. In addition, the study reported that mtDNA decreased at a rate of 0.4 copies/year and that age had an independent effect on the decrease in mtDNA copy number and the increase of heteroplasmy.[214]

It is further noteworthy that in the present study, five out of six tobacco users had signs of mtDNA copy number depletion. While this finding narrowly missed statistical significance, probably due to the very small number of tobacco users in the present study, further investigation is warranted. Mitochondrial enzymes are sensitive to environmental toxicants and the individual components found in tobacco and cigarette smoke. These toxicants, which include a mixture of free radicals and chemical compounds, target the mitochondria either through the inactivation of mitochondrial enzymes or the accumulation of a compound in the organelle.[215-216] Interestingly, smoke-induced electron transport chain (ETC) impairment in lymphocytes has been associated with increases in oxidative damage.[217-218] The resulting oxidative damage has been shown to not only interfere with oxidative phosphorylation (OXPHOS) in platelets, but also increase the production of reactive species, potentially resulting in OS.[219] In addition, several *in vivo* studies have shown that exposure to components found in tobacco smoke directly target the mitochondria and lead to decreases in mtDNA copy number, which coincide with what was observed in the current study, despite this finding not being statistically significant.[220]

In order to determine whether the decreased copy number of mtDNA observed in the HIV-infected participants in the present study could be attributed to HIV either directly or indirectly decreasing the mtDNA content in PBMCs, the association between mtDNA/nDNA ratio and the baseline VL and CD4+ T-cell count at baseline and 12-months following treatment was investigated.

No association between the expression of mtDNA and the CD4+ T-cell count in HIV-infected individuals before and after treatment was found. These findings are not unique to this study, as similar results have also been reported in other studies.[122] In fact, Côté *et*

al. reported no correlation between CD4+ T-cell count and the mtDNA/nDNA ratio in treated and untreated HIV-infected individuals.[122] Importantly, however, a larger proportion of participants with the highest documented CD4+ T-cell count at baseline and at 12-months also had lower mtDNA/nDNA ratios. Interestingly, these findings are in contrast to what was reported by Miura *et al.* who found that the mtDNA levels in the PBMCs of HIV-infected participants correlated with the CD4+ T-cell count, in that the higher the mtDNA/nDNA ratio, the higher the CD4+ T-cell count.[110]

Despite no association being found between MT and the CD4+ T-cell count, Maagard *et al.* observed decreased levels of mtDNA in the CD8+ T-cells of untreated HIV-infected individuals, and a decrease in the levels of mtDNA in both CD8+ and CD4+ T-cells in HIV-infected individuals receiving NRTI-based cART regimens. From their findings, the authors suggested that using T-cells, rather than PBMCs, for the quantification of mtDNA, could possibly better reflect NRTI-induced MT in future investigations.[198]

Pertaining to the association between the VL and the expression of mtDNA, it was found that participants with higher VL had higher baseline delta Ct values and better mtDNA recovery. A higher Ct value implies that the initial amount of the starting material (mtDNA) was small, therefore these findings suggest that pre-cART, the virus may have been responsible for the downregulation in mtDNA, particularly in participants with severe infection. These results coincide with the findings of Morse *et al*. who reported that in cART-naïve HIV-infected individuals, several mitochondrial genes were downregulated in the PBMCs and adipose tissue, when compared to HIV-infected individuals receiving cART.[111] Furthermore, it has also been shown that HIV *per se*, in the absence of cART, may also contribute towards mitochondrial dysfunctions.[221] However, it should be noted that data obtained from studies using heterogenous HIV-infected population have been unreliable, as increases and decreases in mtDNA have also been linked to other pathogenic conditions, and that there is no standard in defining what would be considered an abnormal mtDNA quantity.[122,222] The increase in mtDNA observed following 12-months of treatment could be a compensation for the limited-ATP production from the ETC brought about by the decrease in mtDNA. This has been reported to be the case when observing aging skeletal muscle which has been shown to upregulate the mtDNA content to compensate for the reduced ETC functions.[223]

3.10 Conclusion

In conclusion, the results suggest that there is a reduction in mtDNA copy number in HIV-infected individuals following a 12-month NRTI-based cART regimen. HIV-infected participants, overall, had significantly lower mtDNA levels than HIV-uninfected individuals. The findings of this study coincide with those reported by other authors who found that NRTI-based cART and HIV *per se* both contribute to the development of MT, leading to depletion of mtDNA and, in turn, resulting in mitochondrial dysfunction.[15,22] Furthermore, the VL had more of an effect on the mtDNA levels than the CD4+ T-cell count, therefore, suggesting that the extent of viral replication, rather than the degree of CD4+ T-cell depletion, may have a direct effect on the mitochondria prior to cART-treatment.

Notably, the use of combined regimens of ART to treat HIV-infected individuals makes it impossible to study the effect of individual ARV drugs on MT. A suitable method to monitor the early onset and changes in HIV- and ARV-induced toxicities is therefore required. The findings from the current study indicate that the use of PBMCs for measuring MT as a result of HIV infection and the use of ARV over 12-months, do indeed make for an easier, more accessible sample when compared to the gold standard of muscle biopsies.

Future studies could possibly look at isolating DNA from T-cells, as suggested by others, to monitor MT.[110] A study comparing the effect of EFV-based ARV regimens with the newly introduced dolutegravir (DTG)-based regimens (2019) on mtDNA levels may add further to the understanding of the effect of NRTIs on MT.

3.10.1 Strengths and Limitations

There are several advantages to using the qPCR assay including that the method requires no post-PCR analysis, thereby using fewer resources and time, as well as analysing the quantification of the DNA in 'real-time' instead of at the 'end-point', which is often seen in the conventional PCR method.[224] The technique has successfully been utilized in other studies that have also detected mtDNA damage in PBMCs resulting from NRTI-based HIV regimens, which further supports the use of these cells for assessing mtDNA depletion.[122,180,225]

Limitations may include differences in the time taken between the drawing of blood and the separation of cells for each participant, the presence of PCR inhibitors and the chosen quantification method. In the present study, these factors were standardised as far as possible in order for the accurate comparison of the different tests performed.[155]

Deoxyribonucleic acid was isolated from PBMCs which are reported to potentially be contaminated with platelets. Platelets contain approximately 1.6 molecules of mtDNA while having no nDNA, therefore mtDNA measurements may be overestimated.[149,226] Furthermore, in spite of our findings, the use of PBMCs has not been published as a validated alternative method of detecting MT and many of the reports are conflicting. These inconsistencies may be due to poor recovery of live PBMCs brought about by inappropriate storage, thereby potentially leading to DNA damage.

Another limitation includes the current methodology making use of the mtDNA content as a determinant of mitochondrial depletion, which some view as problematic due to: 1) duplication of the mitochondrial genome in the nuclear genome; 2) use of regions from genes such as beta-actin and 18S ribosomal (r) RNA which are repetitive and/or highly variable for qPCR of the nuclear genome leading to errors; and 3) size differences between mitochondrial and nuclear genomes causing a dilution bias when template DNA is diluted.[151]

Despite the limitations surrounding the quantification of mtDNA in PBMCs as a biomarker of MT, the current study, like many other studies, still found the method to be sensitive and quantitative. Furthermore, the findings of the current study highlight the need for additional studies aimed at understanding the role of mtDNA in systemic pathologies.

CHAPTER 4

FIBROBLAST GROWTH FACTOR 21 AND GROWTH AND DIFFERENTIATION FACTOR 15 AS POTENTIAL BIOMARKERS OF MITOCHONDRIAL TOXICITY

4.1 Introduction

The gold standard for mitochondrial toxicity (MT) detection includes the use of tissue samples (*i.e.* muscle and liver) acquired via biopsies; however, these methods are invasive and not acceptable in asymptomatic individuals. The diagnosis usually requires confirmatory genetic analysis or the measurement of respiratory chain complex activity which has proven to be difficult to perform and is not always readily available. Furthermore, these methods may generate false-positive results if tissue samples are poorly preserved.[227] With the difficulty of quantifying mitochondrial deoxyribonucleic acid (mtDNA) and conventional blood tests, such as plasma lactate, pyruvate and creatine kinase (CK), being considered of little value due to their lack of sensitivity and specificity, alternative biomarkers have been suggested. Fibroblast growth factor 21 (FGF-21) and growth and differentiation factor 15 (GDF-15) are two potential candidates being explored to measure MT in the serum or plasma of affected individuals.[87,104,173]

Fibroblast growth factor 21 and GDF-15 have previously been reported to be useful biomarkers for detecting mitochondrial disorders.[87,173] Fibroblast growth factor 21 is a cytokine that is involved in the intermediary metabolism of carbohydrates and lipids.[157] Fibroblast growth factor 21 concentrations measured in serum have also been useful in identifying primary muscle-manifesting respiratory chain deficiencies and has been suggested as a ‘first-line diagnostic test’ for these disorders, thereby reducing the need for acquiring muscle biopsies.[87]

Growth and differentiation factor 15 expression is induced in response to conditions associated with cellular stress.[169,175] Elevated levels of this growth factor have been found in the serum of individuals with cardiovascular disease, diabetes, cancer and cognitive

impairment and have been proposed to be a predictor of disease progression in a number of these conditions, most of which are relevant in the human immunodeficiency virus 1 (HIV-1) setting as well.[23,117] With most HIV-infected individuals being treated with antiretroviral (ARV) medication, the risk of developing a potentially chronic condition (such as heart and muscle dysfunctions) due to long-term use of ARV regimens and the need for readily available, non-invasive markers, is ever increasing.[66] However, there is still limited data on how reliable these biomarkers are in detecting MT.

The present study assessed the use of systemic biomarkers *viz.*; FGF-21 and GDF-15, as an alternative to the mtDNA/nuclear (n) DNA ratio as an indicator of MT in HIV-infected individuals receiving combination antiretroviral therapy (cART).

4.2 Study Design

As described in Chapter 2, section 2.1, the present study is a retrospective study which utilised plasma samples that had been collected as part of a larger study titled: *The assessment of early warning indicators and markers of immune activation as risk factors for HIV-1 drug resistance*. In addition, plasma samples from 15 healthy, HIV-negative volunteer donors were included in order to determine a normal range of values for the test biomarkers included in this study.

4.3 Study Population

Systemic FGF-21 and GDF-15 concentrations were determined in the plasma samples of 56 HIV-infected participants collected at two-time points (0 months [baseline] and 12-months). Samples were characterized into 3 groups, based on their pre-treatment HIV viral loads (VLs): less than 10,000 copies/millilitre (mL), 10,000-100,000 copies/mL and more than 100,000 copies/mL.

In addition, plasma samples from 15 healthy, HIV-negative individuals, who were recruited as part of an ongoing study in the Department of Medical Immunology, University of Pretoria, were analyzed in order to determine a normal range of values for FGF-21 and GDF-15 for this study. These samples were collected at a single time point. Participation in either of the above-mentioned studies was completely voluntary. The inclusion and exclusion criteria for participants are described in detail in Chapter 2, section 2.2. All data were captured in Microsoft (MS) Excel spreadsheets that will be stored for 15 years in the Department of Medical Immunology's database at the University of Pretoria, with access to the information strictly limited to the investigators involved in the study.

4.4 Ethical Considerations

As mentioned in Chapter 2, section 2.3, informed consent was obtained from all recruited participants, and the above-mentioned studies, as well as the present study, were granted ethical approval from the Research Ethics Committee, Faculty of Health Sciences, University of Pretoria (UP REC reference numbers: 469/2013, 116/2017 and 489/2019,

respectively). Approval was obtained for collecting, processing and analyzing blood samples.

4.5 Materials and Methods

4.5.1 Collection, Processing and Analysis of Blood Samples

4.5.1.1 Whole Blood Collection

Whole blood samples were collected in vacutainer tubes containing ethylenediamine tetra acetic acid (EDTA) as an anticoagulant (Becton Dickinson, Franklin Lakes, NJ, USA) as described in Chapter 2, section 2.4.1.1.

4.5.1.2 Cluster of Differentiation 4 Positive T-Cell Count

As described in Chapter 2, section 2.4.1.2, Cluster of differentiation 4 positive (CD4+) T-cell count were determined at baseline and again following the 12-month clinic visit using an FC500 flow cytometer (Beckman Coulter, Brea, CA, USA) following the CD3/4/8 protocol software with the results being reported as cells/microlitre (µL).

4.5.1.3 Viral Load Determination

The VL for each participant was established as the amount of HIV ribonucleic acid (RNA) present in the blood. This was done using the NucliSENS® MiniMAG® extraction kit (bioMerieux Inc., Boxtel, NLD) with the results being reported as copies/mL (see Chapter 2, section 2.4.1.3).

4.5.2 Preparation of Blood Plasma

Plasma samples were processed within 4 hours (hrs) of collection of the whole blood as described in Chapter 2, section 2.4.1.5 and stored at -80 degrees Celsius (℃) (Thermo Fisher Scientific Inc., Waltham, MA, USA) in the Department of Medical Immunology, University of Pretoria, until use.

4.5.2.1 Determination of Cotinine Levels in Plasma Samples

Cotinine concentrations were measured in the stored plasma samples of 38 HIV-positive participants using the Neogen cotinine human forensic drug detection enzyme-linked immunosorbent assay (ELISA) (Neogen, Lexington, KY, USA) as an objective determination of tobacco use by the study participants. The assay was performed as described in Chapter 2, section 2.4.1.6. The results are reported as nanograms (ng)/mL.

4.5.3 Analysis of Plasma Biomarkers

4.5.2.2 Measurement of Fibroblast Growth Factor 21 and Growth and Differentiation Factor 15 Plasma Concentrations

The levels of the biomarkers, FGF-21 and GDF-15, were measured in the stored plasma samples using a custom ProcartaPlex™ Multiplex Immunoassay (Thermo Fisher Scientific Inc.). The assay was performed according to the manufacturer's instructions, as described in Chapter 2, section 2.4.3.1. The results are reported as picograms (pg)/mL.

4.6 Data and Statistical Analysis

The data from the plasma biomarker measurements were captured on a MS Excel spreadsheet, cleaned and exported to Stata/IC 16.1 for Mac and R (Stata Corp. LLC, College Station, TX, USA).

The data obtained for the biomarkers present in the plasma samples had a skewed, non-normal distribution, therefore, non-parametric testing was performed. Descriptive statistics were used to describe the data using median and interquartile ranges (IQR). Graphical representations were used to assist in visualizing aspects of the data. The statistical procedures used to assess the relevant associations and changes over time (at a 5% level of significance) included; the Mann-Whitney U test, Kruskal-Wallis H test, as well as the Wilcoxon signed-rank and Friedman's tests.

4.7 Results

4.7.1 Demographic Information

The demographic and clinical information for the 56 HIV-infected individuals and 15 healthy, HIV-negative participants are shown in Table 4.1.

The median age of the healthy, HIV-negative group was slightly higher (41 [IQR: 28-50] years), albeit not significantly so, compared to that of the HIV-positive group (38 [IQR: 32 - 44] years) (p=0.833). The gender proportions in both groups were similar, with females accounting for approximately 60% of each group (HIV-positive: 58.93%, HIV-negative: 60.00%; p=0.940). As previously described in Chapter 3, section 3.8.1, the number of assays available for cotinine analysis were limited, therefore the assay was only conducted on 34 HIV-positive participants as a sample of tobacco use in the cohort. The tobacco use status of the HIV-negative participants was recorded on recruitment into the study. The proportion of tobacco users in each group was approximately 20% (HIV-positive: 6 out of 34 [17.64%] and HIV-negative: 3 out of 15 [20.00%], respectively; p=0.410). Furthermore, no association was found between tobacco use with FGF-21 concentrations at baseline (p=0.810) and at 12-months post-cART (p=0.346), or GDF-15 concentrations at baseline (p=0.863) and 12-months post-cART (p=0.873) (results not shown). Laboratory evaluations (CD4+ T-cell count and VL) were performed for all recruited HIV-infected participants at enrolment (baseline) and again at the endpoint (12-months following initiation of treatment). These parameters were not determined for the healthy, HIV-negative participants.

All HIV-positive participants successfully adhered to a prescribed standard first-line cART regimen consisting of two nucleoside reverse transcriptase inhibitors (NRTIs) (tenofovir disoproxil fumarate [TDF] and emtricitabine [FTC]), and one non-nucleoside reverse-transcriptase inhibitor (NNRTI) (efavirenz [EFV]). The CD4+ T-cell counts of the HIV-positive participants were found to increase significantly over the 12-month study period, from a median of 183.5 (IQR: 110 - 315.5) cells/µL (CD4+ T-cell percentage of 12.05% [8.27 – 19.89]) at baseline to 460.5 (IQR: 323 - 609) cells/µL (CD4+ T-cell percentage of 24.74% [17.33 - 31.87]) at 12-months post-cART. The CD4+ T-cell count data was available for 54 participants at baseline and 55 participants after 12-months of

ARV treatment. Furthermore, the VL determined for the participants was found to decrease from a median of 120,000 (IQR: 16,000 - 480,000) copies/mL to a fully suppressed HIV VL of below 50 copies/mL following 12-months of cART.

Table 4.1: Demographic characteristics and clinical data of the study population.

Categories	Statistical measure	HIV-positive n=56	HIV-negative n=15	*p*-value
Age (Years)	Median (IQR)	38 (32 - 44)	41 (28 - 50)	0.833
Gender Male Female	n (%)	23 (41.07%) 33 (58.93%)	6 (40.00%) 9 (60.00%)	0.940
Tobacco user┼	n (%)	6 (17.64%)	3 (20.00%)	0.410
CD4+ T-cell count at baseline (cells/µL) *	Median (IQR)	183.5 (110 - 315.5)	N/A	N/A
CD4+ T-cell count at 12-months (cells/µL) **	Median (IQR)	460.5 (323 - 609)	N/A	N/A
CD4+ T-cell percentage (%) at baseline*	Median (IQR)	12.05 (8.27 - 19.89)	N/A	N/A
CD4+ T-cell percentage (%) at 12-month**	Median (IQR)	24.47 (17.33 – 31.87)	N/A	N/A
HIV viral load at baseline (copies/mL)	Median (IQR)	120,000 (16,000 - 480,000)	N/A	N/A
HIV viral load at 12-months (copies/mL)	Median (IQR)	Non-detectable (0 - < 50)	N/A	N/A

* Data available for 54 participants
** Data available for 55 participants
┼ Data available for 34 participants

4.7.2 Plasma Biomarker Concentrations in Human Immunodeficiency Virus-Positive and -Negative Participants at Baseline and 12- Months Post-Combination Antiretroviral Therapy

The GDF-15 concentrations observed in the plasma samples of the HIV-positive group (n=56) at baseline, were found to be almost 5-fold higher than those of the HIV-negative group (n=15), (1,335.58 [IQR: 1,028.14 - 2,193.24] pg/mL vs. 279.24 [IQR: 121.24 - 329.88] pg/mL, respectively; p=0.0001), and 6-fold higher at 12-months post-cART (1,675.80 [IQR: 1,313.86 - 2,160.60] pg/mL vs. 279.24 [IQR: 121.24 - 329.88] pg/mL, respectively; p=0.0001). These results are presented in Table 4.2. Furthermore, GDF-15 concentrations were found to increase modestly in the HIV-infected individuals following 12-months of cART (1,675.80 [IQR: 1,313.86 - 2,160.60 pg/mL), when compared to the baseline sample levels of GDF-15 (1,335.58 [IQR: 1,028.14 - 2,193.24] pg/mL). A Wilcoxon signed-rank test was performed to evaluate these changes in GDF-15 concentrations between the two time points and it was ascertained that there were no statistically significant differences in GDF-15 levels between these two-time points (z=-2.01, p=0.4440).

In contrast, the FGF-21 concentrations remained unchanged between the HIV-positive individuals, at baseline and 12-months post-cART, and the HIV-negative group, as shown in Table 4.2. A value of 8.64 pg/mL (which is the lowest value assigned for the test) was assigned for all participants with levels below the level of detection. Furthermore, a Wilcoxon signed-rank test was performed to evaluate if there were any changes in FGF-21 concentrations over the 12-months following cART initiation. This test confirmed that no significant differences between the FGF-21 levels were detected (z=1.22, p=0.2220).

Table 4.2: Fibroblast growth factor 21 and GDF-15 concentrations at baseline and 12-months post-cART, in HIV-positive and -negative participants.

Categories	Statistical measure	HIV-positive n=56	HIV-negative n=15	HIV-positive vs. HIV-negative participants: *p*-value	Baseline vs 12-months post-cART: Wilcoxon test	
					Prob>|Z|	Z
FGF-21 concentrations at baseline (pg/mL)	Median (IQR)	8.64* (8.64 - 8.64)	8.64* (8.64 - 8.64)	0.3980	0.2220	1.22
FGF-21 concentrations at 12- months post-cART (pg/mL)	Median (IQR)	8.64* (8.64 - 8.64)	8.64* (8.64 - 8.64)	0.9150		
GDF-15 concentrations at baseline (pg/mL)	Median (IQR)	1,335.58 (1,028.14 – 2,193.24)	279.24 (121.24 - 392.88)	**0.0001****	0.4440	-2.01
GDF-15 at 12-months post-cART (pg/mL)	Median (IQR)	1,675.80 (1,313.86 – 2,160.60)	279.24 (121.24 - 392.88)	**0.0001****		

* Values remain unchanged for the 25th, 50th and 75th percentiles

** Values in bold indicate significance

For most of the HIV-positive and -negative participants in the study, the measured FGF-21 concentrations fell below the detection range of the test (assigned a value of 8.64 pg/mL) at either time point. To further explore the distribution of the FGF-21 concentrations, the dataset was divided into four equal quartiles, with the lowest (≤ 25%) and highest (≥ 75%) quartile being the only two in which the participants values were distributed into. These values are shown in Tables 4.3 and 4.4.

Table 4.3: Distribution of HIV-positive and HIV-negative participants in quartiles of FGF-21 concentration at baseline.

Categories	Statistical measure	HIV-positive participants (n=56)	HIV-negative participants (n=15)	Fisher's exact test	*p*-value
FGF-21 concentrations at baseline (pg/mL)					
Quartile 1st	n	44	15	3.868	**0.049***
Quartile 4th	n	12	0		

* Values in bold indicate significance

Table 4.4: Distribution of HIV-positive in quartiles of FGF-21 concentration at 12-months post-cART.

Categories	Statistical measure	HIV-positive participants (n=56)	Fisher's exact test	*p*-value
FGF-21 concentrations at 12-months post-cART (pg/mL)				
Quartile 1st	n	52	1.135	0.287
Quartile 4th	n	4		

Similar to the findings above, both Tables 4.3 and 4.4 show that the distribution of most of the HIV-positive population fell within the first quartile of the FGF-21 concentration range. There was a significant difference in the number of HIV-positive participants assigned to each quartile for the baseline FGF-21 concentrations (p=0.049). This may be due to 12 out of 56 (21.42%) HIV-positive participants displaying baseline FGF-21 concentrations which did not fall below the detection range, but rather exhibited very high concentrations. However, no such significance was found with the 12-month post-cART

FGF-21 concentrations, with only 4 out of 56 (7.14%) HIV-positive participants displaying higher FGF-21 concentrations. The distribution of participants in the two FGF-21 concentrations quartiles from both time points are shown in Figure 4.1.

A)

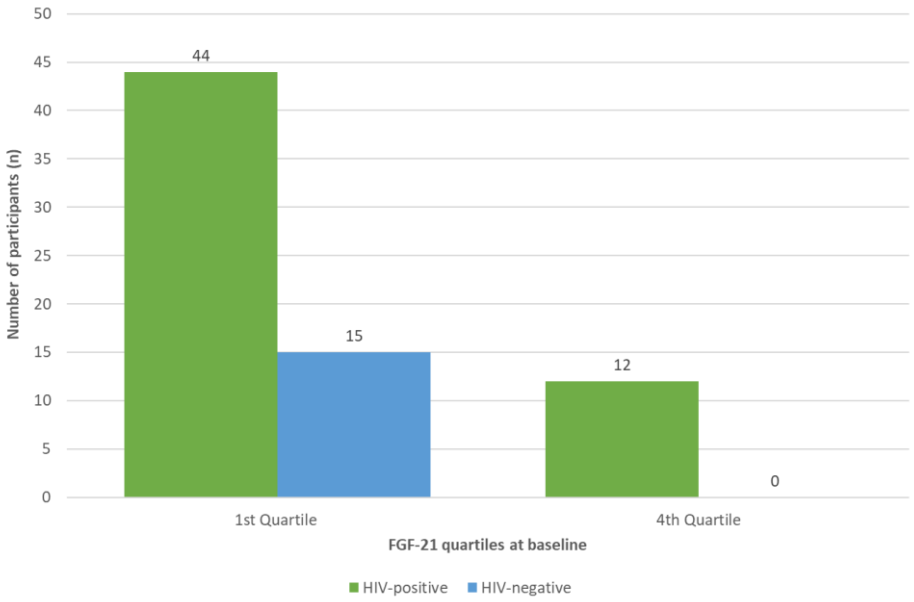

B)

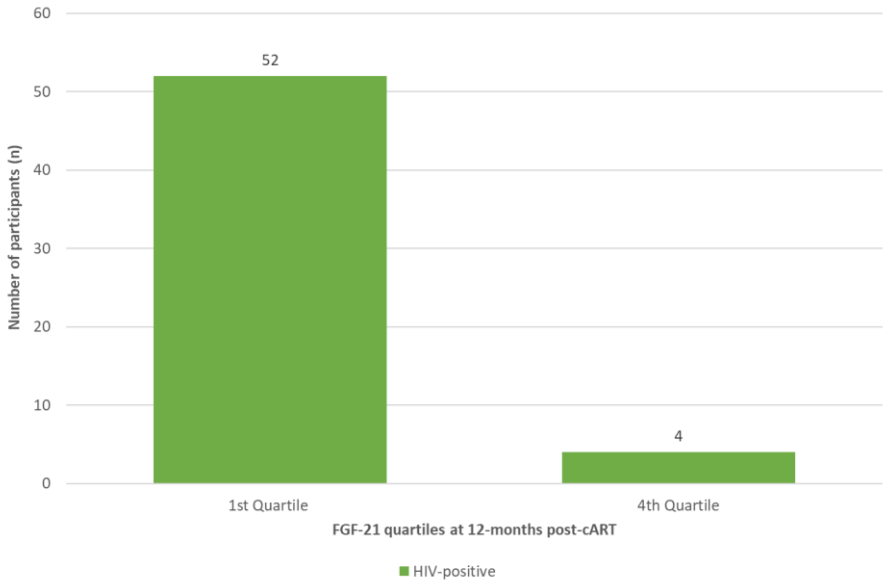

Figure 4.1: The distribution of HIV-positive and HIV-negative participants within the 1st and 4th quartile of FGF-21 concentrations at (A) baseline, and (B) 12-months post-cART. At baseline, within the first quartile all of the HIV-negative (15 out of 15 [100%]) and 44 HIV-positive (44 out of 56 [78.57%]) participants displayed FGF-21 concentrations which fell below the detection range, hence all displaying the same value. However, the remaining 12 HIV-positive (12 out of 56 [21.43%]) participants exhibited higher FGF-21 concentrations which fell within the 4th quartile range. For the HIV-positive participants, the FGF-21 quartiles at 12-months post-cART revealed that 52 participants (52 out of 56 [92.86%]) fell within the 1st quartile, with the remaining 4 (4 out of 56 [7.14%]) having higher levels.

To rule out confounding variables that may influence the concentrations of either biomarker of interest over the 12-month study period, further analyzes were performed and it was found that no demographic characteristics affected the observed levels of either FGF-21 or GDF-15 (see Appendix I).

4.7.3 The Association between Growth and Differentiation Factor 15 and Two Age Subgroups

As the FGF-21 concentrations showed negligible differences between the participants, the association between the study populations' age and the median GDF-15 concentrations at each time point was evaluated and is presented in Table 4.5. For the analysis, the ages of both HIV-positive and -negative participants were dichotomised according to the median value into two groups, namely those with an age below or equal to 38 years, and those above 38 years of age.

Table 4.5: The association between two age subgroups and the median GDF-15 concentrations at each time point.

Category	Statistical measure	GDF-15 concentrations at baseline (pg/mL) (n=71)	*p*-value	GDF-15 concentrations at 12-months post-cART (pg/mL) (n=71)	*p*-value
Age (Years) (n=71)					
≤ 38 (n=35)	Median	1555.22	**0.029***	1516.66	0.783
> 38 (n=36)	Median	1591.34		1604.71	

* Values in bold indicate significance

A statistically significant difference was observed between the median GDF-15 concentration at baseline and the two age subgroups (p=0.029). No association was found between age and median GDF-15 concentrations post-treatment (p=0.783).

4.7.4 Association between Cluster of Differentiation 4 Positive T-Cell Count and the Median Value of Fibroblast Growth Factor 21 and Growth and Differentiation Factor 15 Concentrations as per each Time Point

The HIV-infected participants (n=56) were characterized into two defined subgroups per time point according to their CD4+ T-cell count. At baseline (CD4_0), data were available for 54 individuals, with the participants being grouped as either having a CD4+ T-cell count below 200 cells/µL (n=29) or greater than or equal to 200 cells/µL (n=25). Similarly, at 12-months post-cART (CD4_12), data were only available for 55 individuals, with the participants (n=55) being grouped as either having a CD4+ T-cell count below 500 cells/µL (n=32), or greater than or equal to 500 cells/µL (n=23). These results are shown in Table 4.6.

Table 4.6: Associations between two defined CD4+ T-cell count subgroups with the median value of GDF-15 and FGF-21 concentrations at baseline and 12-months post-cART.

Categories	Statistical measure	FGF-21 concentrations (pg/mL)	*p*-value	GDF-15 concentrations (pg/mL)	*p*-value
CD4+ T-cell count at baseline (CD4_0) (cells/µL) (n=54) *					
< 200 (n=29)	Median (IQR)	8.64† (8.64 - 8.64)	0.075	1,536.47 (1,155.36 - 2,601.43)	**0.011**††
≥ 200 (n=25)	Median (IQR)	8.64† (8.64 - 8.64)		1,152.96 (806.22 - 1,616.60)	
CD4+ T-cell count at 12-months (CD_12) (cells/µL) (n=55) **					
< 500 (n=32)	Median (IQR)	8.64† (8.64 - 8.64)	0.720	1,605.95 (1,389.98 - 2,084.03)	0.891
≥ 500 (n=23)	Median (IQR)	8.64† (8.64 - 8.64)		1,791.89 (1,253.49 - 2,363.87)	

* Data available for 54 participants
** Data available for 55 participants
† Values remain unchanged for the 25th, 50th and 75th percentiles
†† Values in bold indicate significance

A significant difference in the GDF-15 concentrations were observed for the two baseline CD4+ T-cell count subgroups, as shown in Figure 4.2. The results indicate that at baseline, HIV-infected individuals with a CD4+ T-cell count < 200 cells/µL (n=29) had significantly higher concentrations of GDF-15 when compared to those individuals with a higher CD4+ T-cell count (≥ 200 cells/µL, n=25) (1,152.96 pg/mL [IQR: 806.22 - 1,616.60] vs. 1,536.47 [IQR: 1,155.36 - 2,601.43] pg/mL, respectively; p=0.011). In contrast, the levels of GDF-15 found in the 12-months post-cART CD4+ T-cell subgroups,

albeit higher than the baseline GDF-15 concentration, showed no significant differences between participants with CD4 counts ≥ 500 and < 500 cells/ µL (p=0.891).

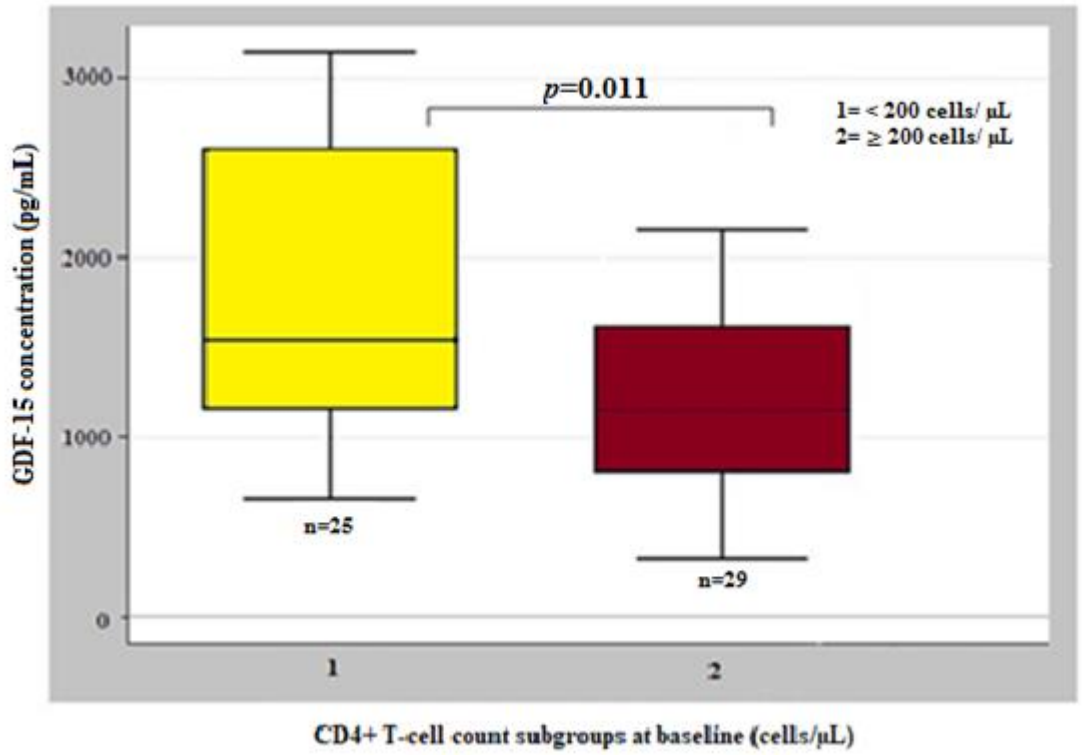

Figure 4.2: The association between two defined CD4+ T-cell count subgroups and GDF-15 concentrations at baseline. The 54 participants for whom the baseline CD4+ T-cell count data was available, were grouped into two subgroups according to their documented baseline CD4+ T-cell count: (1) < 200 cells/µL (n=29), or; (2) ≥ 200 cells/µL (n=25). Significant differences in GDF-15 concentrations were found between the two subgroups (p=0.011), with individuals in subgroup 2 displaying significantly lower baseline GDF-15 concentrations compared to those with a lower CD4+ T-cell count in subgroup 1.

In the case of FGF-21, no associations between plasma FGF-21 concentrations and CD4+ T-cell counts were observed in either of the two CD4+ T-cell count subgroups at baseline or 12-months post-cART. Therefore, the distribution of the participants from the two CD4+ T-cell count subgroups within quartiles of the FGF-21 concentrations was further evaluated. Again, the dataset was divided into four equal quartiles, with the first and fourth being analyzed. These values are presented in Tables 4.7 and 4.8.

Table 4.7: Distribution of participants from two CD4+ T-cell count subgroups in quartiles of FGF-21 concentration at baseline.

Categories	Statistical measure	FGF-21 quartiles at baseline		Fisher's exact test
		Quartile 1	Quartile 4	
CD4+ T-cell count at baseline (CD4_0) (cells/µL) (n=54) *				
< 200 (n=29)	n	19	10	**0.007****
≥ 200 (n=25)	n	24	1	

* Based on the determined CD4+ T-cell count obtained at baseline from 54 participants

** Values in bold indicate significance

Table 4.8: Distribution of participants from two CD4+ T-cell count subgroups in quartiles of FGF-21 concentration at 12-months post-cART.

Categories	Statistical measure	FGF-21 concentration quartiles at 12-months post-cART		Fisher's exact test
		Quartile 1	Quartile 4	
CD4+ T-cell count at 12-months (CD_12) (cells/µL) (n=55) *				
< 500 (n=32)	n	30	2	1.000
≥ 500 (n=23)	n	21	2	

* Based on the determined CD4+ T-cell count obtained at 12-months post-cART from 55 participants

From the analysis of the results, it is evident that at baseline, most participants from either CD4+ T-cell group fell within the first quartile (43 out of 54 [79.63%]), therefore,

exhibiting low FGF-21 concentrations at baseline. There is, however, a significant difference in the number of participants who fell into the fourth quartile, with 10 participants in the low CD4+ T-cell count subgroup (less than 200 cells/µL) and only one participant in the high CD4+ T-cell count group having levels in the fourth quartile (p=0.007). Post-cART, no significant difference was found regarding the distribution of participants into each of the two subgroups. However, similar to the results obtained for the baseline FGF-21 concentrations, the majority of participants from either subgroup fell within the first quartile range of FGF-21, with only four individuals showing higher concentrations.

4.7.4.1 Association between the Three Defined Cluster of Differentiation 4 Positive T-Cell Count Subgroups and the Median Value of Fibroblast Growth Factor 21 and Growth and Differentiation Factor 15 for each Time Point

In order to further explore whether any associations exist with CD4+ T-cell count, participants were characterized into three defined subgroups per time point according to their CD4+ T-cell count and the samples analyzed accordingly. At baseline (CD4_0), the participants (n=54) were grouped as either having a CD4+ T-cell count below 100 cells/µL (n=12), greater than or equal to 100 cells/µL but less than 200 cells/µL (n=17), or greater than or equal to 200 cells/µL (n=25). Post-cART (CD4_12), the participants (n=55) were grouped according to either having a CD4+ T-cell count below 350 cells/µL (n=15), greater than or equal to 350 cells/µL but less than 500 cells/µL (n=17), or greater than or equal to 500 cells/µL (n=23). These results are shown in Table 4.9.

Table 4.9: Associations between three defined CD4+ T-cell count subgroups and the median value of each biomarker concentrations at baseline and 12-months post-cART.

Categories	Statistical measure	FGF-21 concentrations (pg/mL)	*p*-value	GDF-15 concentrations (pg/mL)	*p*-value
CD4+ T-cell count at baseline (CD4_0) (cells/µL) (n=54) *					
< 100 (n=12)	Median (IQR)	15.87 (8.64 - 33.71)		2,642.02 (1,718.81 - 3,021.53)	
≥ 100 but < 200 (n=17)	Median (IQR)	8.64┼ (8.64 - 8.64)	0.0510	1,278.65 (1,072.85 - 1,451.13)	**0.0003**┼┼
≥200 (n=25)	Median (IQR)	8.64┼ (8.64 - 8.64)		1,152.96 (806.22 - 1,616.60)	
CD4+ T-cell count at 12-months (CD_12) (cells/µL) (n=55) **					
< 350 (n=15)	Median (IQR)	8.64┼ (8.64 - 8.64)		1,545.83 (1,360.11 - 2,118.37)	
≥ 350 but < 500 (n=17)	Median (IQR)	8.64┼ (8.64 - 8.64)	0.7730	1,607.87 (1,488.68 - 1,977.69)	0.9870
≥ 500 (n=23)	Median (IQR)	8.64┼ (8.64 - 8.64)		1,791.89 (1,253.49 - 2,363.87)	

* Data available for 54 participants

** Data available for 54 participants

┼ Values remain unchanged for the 25th, 50th and 75th percentiles

┼┼ Values in bold indicate significance

Due to the FGF-21 concentrations measured at each time point for the three CD4+ T-cell count subgroups remaining unchanged, the distribution of the participants FGF-21 concentrations were further evaluated by analyzing each quartile by dividing the dataset into four equal quartiles, with results from the first and fourth being shown in Tables 4.10 and 4.11.

Table 4.10: Distribution of participants from three CD4+ T-cell count subgroups in quartiles of FGF-21 concentration at baseline.

Categories	Statistical measure	FGF-21 concentration quartiles at baseline		Fisher's exact test
		Quartile 1	Quartile 4	
CD4+ T-cell count at baseline (CD4_0) (cells/µL) (n=54) *				
< 100 (n=12)	n	5	7	
≥ 100 but < 200 (n=17)	n	14	3	**0.001****
≥ 200 (n=25)	n	24	1	

* Based on the determined CD4+ T-cell count obtained at baseline from 54 participants

** Values in bold indicate significance

Table 4.11: Distribution of participants from three CD4+ T-cell count subgroups in quartiles of FGF-21 concentration at 12-months post-cART.

Categories	Statistical measure	FGF-21 concentration quartiles at 12-months post-cART		Fisher's exact test
		Quartile 1	Quartile 4	
CD4+ T-cell count at 12-months (CD_12) (cells/µL) (n=55) *				
< 350 (n=15)	n	13	2	0.364
≥ 350 but < 500 (n=17)	n	17	0	
≥ 500 (n=23)	n	21	2	

* Based on the determined CD4+ T-cell count obtained at baseline from 55 participants

Analysis of the results revealed there to be a significant difference in the distribution of participants between the three baseline CD4+ T-cell count subgroups, which fell in to either of the two FGF-21 concentration quartiles (p=0.001). Furthermore, most of the participants with the lowest baseline CD4+ T-cell count displayed high FGF-21 concentrations [7 out 13 (53.85%)]. Despite only a few participants having high FGF-21 concentrations, at either of the two-time points, the majority of the participants had concentrations that fell below the detection range, therefore falling in the first quartile.

An analysis of the results using the Kruskal-Wallis H test showed significant differences in GDF-15 concentrations between the three CD4+ T-cell count subgroups at baseline (p=0.0003), as presented in Figure 4.3. The HIV-infected individuals with the lowest baseline CD4+ T-cell count (< 100 cells/µL) were found to have a higher median plasma GDF-15 concentration (2,642.02 [IQR: 1,718.81 - 3,021.53] pg/mL) relative to the other two subgroups, which only showed modest differences between the different groups (1,278.65 [IQR: 1,072.85 - 1,451.13] pg/mL and 1,152.96 [IQR: 806.22 - 1,616.60] pg/mL, respectively).

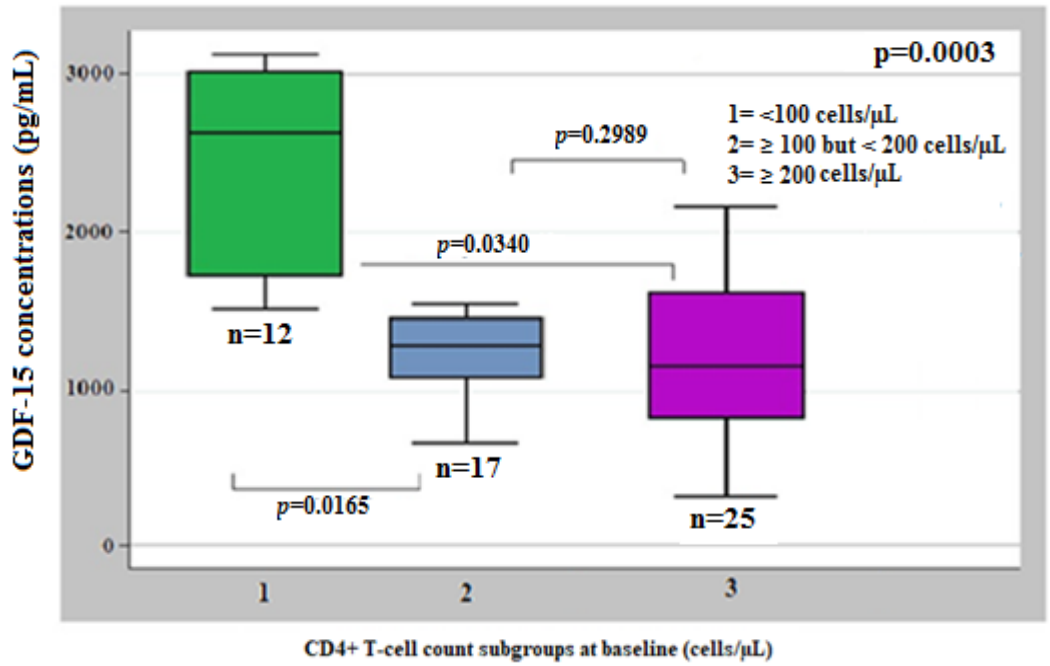

Figure 4.3: The association between three defined CD4+ T-cell count subgroups and GDF-15 concentrations at baseline. The participants (n=54), for whom the baseline CD4+ T-cell count data were available, were grouped into three subgroups according to their documented baseline CD4+ T-cell count: (1) below 100 cells/µL (n=12); (2) ≥ 100 but < 200 cells/µL (n=17); and (3) ≥ 200 cells/µL (n=25). Significant differences in GDF-15 concentrations were observed between the subgroup with the lowest CD4+ T-cell count (1) compared to the other two subgroups (p=0.0165 and p=0.0340, respectively).

In addition, in order to analyze whether there were significant differences in GDF-15 concentrations in each subgroup relative to the two other subgroups, a post-hoc Dunn's pairwise comparison test was performed. This test revealed that there were significant differences between participants with the lowest baseline CD4+ T-cell count (< 100 cells/µL) when compared to either of the other two subgroups (p=0.0165 and p=0.0340, respectively), as shown in Figure 4.3 and Table 4.12. Furthermore, the Dunn's test confirmed that there were no significant differences between the two higher baseline CD4+ T-cell count subgroups (p=0.2989).

Table 4.12: Dunn's pairwise comparison test to determine whether there were significant changes in FGF-21 and GDF-15 concentrations between the three CD4+ T-cell count subgroups at baseline and 12-months post-cART.

Categories	FGF-21 concentrations			GDF-15 concentrations		
	1 vs. 2	1 vs. 3	2 vs. 3	1 vs. 2	1 vs. 3	2 vs. 3
CD4+ T-cell count at baseline (CD4_0) (cells/µL) (n=54) *						
1) < 100 (n=12)						
2) ≥ 100 but < 200 (n=17)	**0.017**†		0.182	**0.016**†		0.298
3) ≥ 200 (n=25)		**0.001**†			**0.034**†	
CD4+ T-cell count at 12-months (CD_12) (cells/µL) (n=55) **						
1) < 350 (n=15)						
2) ≥ 350 but < 500 (n=17)	0.125		0.487	0.467		0.436
3) ≥ 500 (n=23)		0.115			0.473	

* Data available for 54 participants

** Data available for 55 participants

† Values in bold indicate significance

An analysis of the results for the GDF-15 concentrations at 12-months post-cART using the Kruskal-Wallis H test, revealed no significant differences between the three 12-month post-cART CD4+ T-cell count subgroups (p=0.987). In contrast to what was observed at baseline, the highest GDF-15 concentrations were detected in HIV-infected individuals with the highest 12-month post-cART CD4+ T-cell count subgroup (≥ 500 cells/µL) (1,791.89 [IQR: 1,253.49 - 2,363.87] pg/mL), with HIV-infected individuals with the lowest CD4+ T-cell count (< 350 cells/µL) showing the lowest GDF-15 concentration (1,545.83 [IQR: 1,360.11 - 2,118.37] pg/mL). These differences were, however, inconsequential since the Dunn's pairwise comparison test indicated that there were no

significant differences when comparing GDF-15 concentrations from each of the subgroups to one another (CD4+ T-cell count < 350 cells/µL and ≥ 350 but < 500 cells/µL, [*p*=0.467]; CD4+ T-cell count < 350 cells/µL and ≥ 500 cells/µL, [*p*=0.473]; and CD4+ T-cell count ≥ 350 but < 500 cells/µL and ≥ 500 cells/µL, [*p*=0.436]).

Analysis of the FGF-21 results using the Kruskal-Wallis H test revealed that differences in FGF-21 levels between the three CD4+ T-cell count subgroups at baseline just missed significance (*p*=0.051), as shown in Table 4.8. HIV-infected individuals with the lowest CD4+ T-cell count (< 100 cells/µL) were found to have the highest FGF-21 concentrations at baseline (15.87 [IQR: 8.64 - 33.71] pg/mL), when compared to the other two subgroups (8.64 [8.64 - 8.64] pg/mL in both instances).

A follow-up Dunn's pairwise comparison test which is presented in Table 4.12, indicated that there were significant differences between participants with the lowest CD4+ T-cell count (< 100 cells/µL, n=12) and those in either of the subgroups with higher baseline CD4+ T-cell counts (≥ 100 but < 200 cells/µL, *p*=0.017; and ≥ 200 cells/µL, *p*=0.001). The FGF-21 concentrations in the two subgroups with the highest baseline CD4+ T-cell count did not differ from one another (*p*=0.182).

Similarly, at 12-months post-cART, no significant differences were found between the FGF-21 concentrations and the three post-cART CD4+ T-cell count subgroups (*p*=0.773), as the values remained unchanged (8.64 [IQR: 8.64 - 8.64] pg/mL). This was confirmed with a Dunn's pairwise comparison test (Table 4.12).

4.7.5 Association between Viral Load Subgroups and Median Value of Fibroblast Growth Factor 21 and Growth and Differentiation Factor 15 Concentrations, as per each Time Point

The association between the median VLs and changes in biomarker concentrations at either time point are shown in Tables 4.13 and 4.16. The analysis was based on biomarker concentrations in two (Table 4.13) and three (Table 4.16) subgroups of participants, which were grouped according to their documented baseline VL. Furthermore, the distribution of the participants from the VL subgroups within the quartiles of FGF-21 concentrations

for either time point, were analyzed with the result being presented in Tables 4.14 and 4.15.

Analysis of the results using the Kruskal-Wallis H test revealed no association between the two HIV VL subgroups and their respective GDF-15 concentrations at baseline and 12-months post-cART (p=0.097 and 0.717, respectively). Individuals with the lowest VL (VL < 100,000 copies/mL; n=26) were found to display lower baseline GDF-15 concentrations compared to individuals with a high VL (VL ≥ 100,000 copies/mL; n=30) (1,214.05 [IQR: 877.34 - 1,690.75] pg/mL and 1,437.02 [IQR: 1,103.81 - 2,801.41] pg/mL, respectively) but this difference just missed statistical significance (p=0.097). However, post-cART, the plasma GDF-15 concentrations of the participants increased significantly from those observed at baseline, while the other subgroup only showed a modest increase in GDF-15 concentration (1,774.67 [IQR: 1,257.12 - 2,363.87] pg/mL and 1,575.45 [IQR: 1,357.69 - 2,049.68] pg/mL, respectively). The difference between the groups at 12 months was not significant (p=0.717).

The FGF-21 concentrations observed between the two subgroups showed no significant differences at baseline and 12-months post-cART (p=0.947 and 0.805). In contrast to GDF-15, the FGF-21 concentrations in both the VL subgroups at both time points remained unchanged (8.64 [IQR: 8.64 - 8.64] pg/mL).

Table 4.13: Associations between two viral load subgroups and changes in biomarker concentrations at baseline.

Categories	Statistical measure	FGF-21 concentrations at baseline (pg/mL)	*p*-value	FGF-21 concentrations at 12-months (pg/mL)	*p*-value	GDF-15 concentrations at baseline (pg/mL)	*p*-value	GDF-15 concentrations at 12-months (pg/mL)	*p*-value
Viral load at baseline (VL_0) (copies/mL) (n=56)									
< 100,000 (n=26)	Median (IQR)	8.64* (8.64 - 8.64)	0.947	8.64* (8.64 - 8.64)	0.805	1,214.05 (877.34 - 1,690.75)	0.097	1,774.67 (1,257.12 - 2,363.87)	0.717
> 100,000 (n=30)	Median (IQR)	8.64* (8.64 - 8.64)		8.64* (8.64 - 8.64)		1,437.02 (1,103.81 - 2,801.41)		1,575.45 (1,357.69 - 2,049.68)	

* Values remain unchanged for the 25th, 50th and 75th percentiles

Due to the measured FGF-21 concentrations showing little variation in values, the results were divided into 4 quartiles in which the distribution of participants from the two VL subgroups would be analyzed, as shown in Tables 4.14 and 4.15.

Table 4.14: Distribution of participants from two viral load subgroups in quartiles of FGF-21 concentration at baseline.

Categories	Statistical measure	FGF-21 concentration quartiles at baseline		Fisher's exact test
		Quartile 1	Quartile 4	
Viral load at baseline (VL_0) (copies/mL) (n=56)				
< 100,000 (n=26)	n	20	6	1.000
> 100,000 (n=30)	n	24	6	

Table 4.15: Distribution of participants from two viral load subgroups in quartiles of FGF-21 concentration at 12-months post-cART.

Categories	Statistical measure	FGF-21 concentration quartiles at 12-months post-cART		Fisher's exact test
		Quartile 1	Quartile 4	
Viral load at baseline (VL_0) (copies/mL) (n=56)				
< 100,000 (n=26)	n	23	3	0.328
> 100,000 (n=30)	n	29	1	

From the results, it was evident that no significant differences in the distribution of the participants from the two VL subgroups and the FGF-21 quartiles at either time point were found. Similar to what was observed with the CD4+ T-cell count, the majority of the participants from the VL subgroups at the two-time points were distributed in the first quartile (44 out of 56 [78.57%] and 52 out of 56 [92.86%], respectively), with the remaining few exhibiting higher concentrations of the biomarker.

The participants (n=56) were further characterized into three defined subgroups per time point according to their baseline VL. The participants were grouped as either having a VL below 10,000 copies/mL (n=10), greater than or equal to 10,000 but less than 100,000 copies/mL (n=16), or greater than 100,000 copies/mL (n=30). These results are shown in Table 4.16.

The analysis of the plasma GDF-15 concentrations using the Kruskal-Wallis H test, revealed no significant differences between the three VL subgroups at baseline and 12-months post-cART (p=0.173 and p=0.165, respectively). However, GDF-15 baseline concentrations were found to be highest in those individuals with high VLs (> 100,000 copies/mL) (1,437.02 [IQR: 1,103.81 - 2,801.41] pg/mL) and lowest in HIV-infected individuals with low VLs (< 10,000 copies/mL) (1,085.03 [IQR: 761.43 - 1,690.75] pg/mL). A Dunn's pairwise comparison test revealed the only significant difference in GDF-15 concentrations to be between HIV-infected subjects in the two subgroups with the highest (> 100,000 copies/mL) and lowest (< 10,000 copies/mL) VLs (p=0.035), as shown in Table 4.17.

In contrast, at 12-months post-cART, the GDF-15 concentrations in individuals with the lower VLs were higher than those with higher VLs, with the highest concentration being in HIV-infected individuals with a VL of ≥ 10,000 but < 100,000 copies/mL (1,917.31 [IQR: 1,451.07 - 2,545.02] pg/mL). A Dunn's pairwise comparison test revealed the only significant difference in plasma GDF-15 concentrations to be between participants in the subgroup with the lowest (< 10,000 copies/mL) VLs and those with a VL of ≥ 10,000 but < 100,000 copies/mL (p=0.031). The comparisons between the other subgroups were found to be not significant (< 10,000 copies/mL and > 100,000 copies/mL, p=0.158; and ≥ 10,000 but < 100,000 copies/mL and > 100,000 copies/mL, p=0.106).

The FGF-21 concentrations at baseline and 12-months post-cART remained unchanged in all three VL subgroups. Furthermore, a Dunn's pairwise test for the baseline plasma FGF-21 concentrations revealed no significant differences between the groups at baseline and 12-months post-cART.

Table 4.16: Associations between three defined viral loads subgroups and changes in biomarker concentrations at baseline.

Categories	Statistical measure	FGF-21 concentrations at baseline (pg/mL)	*p*-value	FGF-21 concentrations at 12-months (pg/mL)	*p*-value	GDF-15 concentrations at baseline (pg/mL)	*p*-value	GDF-15 concentrations at 12-months (pg/mL)	*p*-value
Viral load at baseline (VL_0) (copies/mL) (n=56)									
< 10,000 (n=10)	Median (IQR)	8.64* (8.64 - 8.64)		8.64* (8.64 - 8.64)		1,085.03 (761.43 - 1,690.75)		1,577.11 (810.16 - 977.69)	
≥ 10,000 but < 100,000 (n=16)	Median (IQR)	8.64* (8.64 - 15.87)	0.729	8.64* (8.64 - 15.87)	0.963	1,378.74 (888.99 - 1,753.21)	0.173	1,917.31 (1,451.07 - 2,545.02)	0.165
> 100,000 (n=30)	Median (IQR)	8.64* (8.64 - 8.64)		8.64* (8.64 - 8.64)		1,422.91 (1,103.81 - 2,482.62)		1,566.95 (1,357.69 - 2,049.68)	

* Values remain unchanged for the 25th, 50th and 75th percentiles

Table 4.17: Dunn's pairwise comparison test to determine whether there were significant changes in FGF-21 and GDF-15 concentrations between the three viral load subgroups at baseline.

Categories	FGF-21 concentrations at baseline			FGF-21 concentrations at 12-months			GDF-15 concentrations at baseline			GDF-15 concentrations at 12-months		
	1 vs. 2	1 vs. 3	2 vs. 3	1 vs. 2	1 vs. 3	1 vs. 2	1 vs. 2	1 vs. 3	2 vs. 3	1 vs. 2	1 vs. 3	2 vs. 3
Viral load at baseline (VL_0) (copies/mL) (n=56)												
1) < 10,000 (n=10)												
2) ≥ 10,000 but < 100,000 (n=16)	0.159		0.259	0.312		0.362	0.1923		0.158	**0.031***		0.106
3) > 100,000 (n=30)		0.292			0.405			**0.035***			0.158	

* Values in bold indicate significance

4.8 Discussion

It is well documented that progressive HIV infection is characterized by chronic inflammation, accompanied by severe immunological depletion (the most notable of these being apoptosis of CD4+ T-cell populations) and high VLs. These immunological effects include significantly higher levels of reactive oxygen species (ROS), decreased mtDNA levels and antioxidant capacities.[198] The elevated ROS levels are thought to be a result of HIV polypeptides and replication, which have been shown to harm the mitochondria, thereby contributing to mitochondrial complications such as mitochondrial dysfunction, energy depletion and deregulation of cellular metabolism.[102]

The introduction of a strict, life-long regimen of cART has resulted in delayed disease progression and recovery of immune function.[228] However, as is the case with the virus itself, the chronic use of ARV drugs, particularly NRTIs, have been shown to impair mitochondrial function by indirectly inhibiting mitochondrial replication, which may, in turn, result in oxidative stress (OS), elevated levels of ROS and MT which plays a role in the manifestation of many conditions such as cardiomyopathy, skeletal myopathies and hepatic steatosis.[51,113,228]

Both FGF-21 and GDF-15 have been recognised as potential biomarkers of mitochondrial disease, which include, but is not limited to, mtDNA depletion and deletion syndromes.[175] Furthermore, previous studies have also associated elevated concentrations of FGF-21 with metabolic disturbances (*i.e.* diabetes, obesity and congenital lipodystrophy) in HIV-negative individuals, as well as OS and inherited skeletal muscle-related mitochondrial disorders; particularly those resulting from impaired oxidative phosphorylation (OXPHOS) systems. A consequence of such impairments includes deficiencies in energy production, which may, in turn, lead to increased levels of ROS and consequent OS.[138,229] These findings were also reported by Tyynismaa *et al*., who found a positive association between FGF-21 concentrations and the presence of cytochrome c oxidase (COX)-negative fibres in the skeletal muscle of mice with mitochondrial myopathies.[162] However, in humans, no correlation has been found between elevated FGF-21 and COX-negative fibres in cART-treated HIV-infected individuals.[230]

Similarly, GDF-15 has also been recognised as an anti-inflammatory, stress-responsive cytokine, with elevated concentrations associated with HIV-related mortality, inflammation, myocardial ischemia, OS and most notably, cancer.[231-232] Several studies have investigated the effect of cART on OS, MT and adipogenesis; however, none have investigated the effect of cART, the HIV VL and CD4+ T-cell count, on the concentrations of FGF-21 and GDF-15 at baseline and 12-months post-cART.[233-235] The present study investigated the plasma concentrations of FGF-21 and GDF-15, as potential biomarkers of MT, by comparing the levels of these biomarkers in a population of 56 HIV-infected individuals with 15 healthy, HIV-negative volunteers. In addition, this study explored the association between the FGF-21 and GDF-15 concentrations and HIV disease markers (CD4+ T-cell count and VL), in the 56 HIV-positive individuals at baseline and 12-months post-cART.

The results of the current study show that systemic levels of GDF-15 were as much as five times higher in the HIV-infected group, at baseline and six times higher after 12-months of cART treatment, than in the HIV-negative group. Furthermore, when comparing the concentrations of GDF-15 in the HIV-infected participants at each time point, the levels detected at baseline were marginally lower than those observed at 12-months post-cART. To the best of our knowledge, GDF-15 has not been well studied in an HIV-positive cohort; however, a study by Secemsky *et al.* found evidence of an association between pulmonary hypertension and elevated GDF-15, which is associated with cardiac dysfunction, a well-recognised complication of HIV infection.[236]

Pertaining to the mitochondria, Yatsuga *et al.* showed that when compared to FGF-21, alternative biomarkers such as the lactate to pyruvate (L/P) ratio, lactate, pyruvate, CK and GDF-15 proved to be more sensitive in diagnosing and monitoring the severity of mitochondrial disorders in adults and children.[173] These authors showed that individuals suffering from mitochondrial disorders exhibited 6-fold higher GDF-15 concentrations when compared to individuals with non-mitochondrial disorders and healthy controls.[173] It may be postulated that with the chronic use of ARVs, the damage inflicted upon the mitochondria increases proportionally with ARV use as these agents are known to cause damage to the mitochondria, potentially leading to mtDNA damage, mitochondrial loss and elevated levels of ROS. Although not significant, the higher concentrations of plasma

GDF-15 observed at 12-months post-cART in the HIV-positive individuals in the current study could tentatively support this hypothesis.

The median FGF-21 concentrations observed in all of the HIV-negative participants in the present study, remained unchanged suggesting that the measured concentrations fell below the levels of detection for the test. Similarly, most of the HIV-positive participants also presented with undetectable FGF-21 concentrations, however, when the results were divided into four quartiles, a few individuals had concentrations which fell into the upper quartile range. It is interesting to note that none of the HIV-negative participants fell within the fourth quartile at either time point. These results correspond with the findings by Yatsuga *et al.* who reported different values for FGF-21 concentrations between individuals with diagnosed mitochondrial disorders and those in the healthy control group. Although previous studies have found elevated levels of FGF-21 expressed in the skeletal muscle of HIV-infected individuals as a result of metabolic alterations, other investigators have failed to identify any association between cART treatment and elevated systemic concentrations of FGF-21 in HIV-infected individuals, despite OS, a known side-effect of certain cART drugs, inducing FGF-21 production.[173] Moure *et al.* reported that the most likely ARV drug classes to cause elevated levels of FGF-21 were protease inhibitors (PIs), NNRTIs (EFV alone) and integrase strand transfer inhibitors (INSTIs) (elvitegravir [EVG] alone). The authors found that with regimens which include NRTIs, the concentrations of FGF-21 remained 'neutral'.[237] All the participants of the present study were on a standard first-line cART regimen which consisted of the NtRTIs, TDF and FTC as well as the NNRTI, EFV.

Most studies exploring FGF-21 concentrations in HIV-infected cohorts typically associated elevated FGF-21 levels with conditions brought about by HIV-induced metabolic disturbances such as; HIV-associated insulin resistance, lipoatrophy and lipid abnormalities. In contrast, it has been suggested that reduced FGF-21 concentrations have been associated with lifestyle interventions and metabolic homeostasis.[238]

A positive association was found between GDF-15 and CD4+ T-cell count in the HIV-positive participants of this study. The results suggest that the pre-treatment levels of GDF-15 were low for participants with higher CD4+ T-cell count and that after treatment, the levels increased as immune function was restored. To the best of our knowledge, no previous studies have

explored the association between these two variables; however, the findings were not unexpected, as with the chronic use of ARVs, the immune cell population recovers as the immune system reconstitutes itself, however, the disadvantage of the chronic use of cART is that prolonged use of the drugs coincide with prolonged exposure of the mitochondria to drugs, therefore, increasing the chances of mitochondrial damage through mutation or inhibition of mitochondrial replication proteins.[239]

No association between FGF-21 plasma concentrations and CD4+ T-cell count in HIV-infected individuals was observed. However, significance was just missed when the association between the baseline CD4+ T-cell count and FGF-21 concentration was evaluated. The lack of significance could be a due to a small sample size (n=56) being used in the current study. These findings showed that an inverse relationship existed between the participants with the lowest baseline CD4+ T-cell count and the highest measured FGF-21 concentrations. These results contrast with what was reported by Payne *et al.*, who suggested that although FGF-21 was a poor predictor of mitochondrial dysfunction in cART-treated HIV-participants, they found the strongest predictor to be the total CD4+ T-cell count gain.[230] The authors of this study reported that cART-treated HIV-infected individuals, with lower CD4+ T-cell counts, experience metabolic changes brought about by immune restoration and the return to normal health.[230] However, this association requires further investigation.

In the present study, systemic GDF-15 levels increased moderately from baseline to those observed at 12-months post-cART. In order to examine the impact of the pre-treatment VL on the test biomarker levels over time, VLs were grouped into two and three different subgroups. Interestingly, the results did show a positive association between VL and baseline GDF-15 concentrations, as HIV-infected individuals with advanced HIV (presenting with a VL ≥ 100,000 copies/mL) displayed significantly higher concentrations of GDF-15 at baseline than those with lower VLs (< 10,000 copies/mL). In addition, the 12-month levels of the biomarkers also pointed to a significant difference in GDF-15 concentrations between HIV-infected individuals in these two groups. This trend could be attributed to HIV-induced inflammatory conditions, which may also inhibit mitochondrial function and induce ROS production, therefore, suggesting a positive association between VL and inflammation, which may have led to the increased GDF-15 concentrations observed in this study.

Morse *et al.* suggested that HIV-infection *per se* has a direct effect on mitochondria, which is thought to be propelled by immune activation and inflammation.[111] Furthermore, a study conducted by Cossarizza also demonstrated a positive association between plasma mtDNA levels and the HIV VL, suggesting the increase of viraemia may play a role in eliciting damage to the mitochondria, resulting in the release of mtDNA and inflammation.[240]

No association between the plasma FGF-21 levels and HIV VL was found. To our knowledge, there is limited knowledge on the effect of HIV VL on systemic concentrations of FGF-21. However, in the present study, the systemic levels of FGF-21 remained equivalent to those of the HIV-negative individuals. Previous studies have reported that individuals with latent HIV infection displayed upregulations of genes that regulate cellular apoptosis, activation and inflammatory chemokine and cytokine production in the muscle, adipose tissue and peripheral blood mononuclear cells (PBMCs) of these individuals. In contrast, when evaluating the same genes in virally suppressed cART-exposed HIV-infected individuals, the genes were shown to be downregulated in both the PBMCs and adipose tissue, therefore, suggesting that HIV may play a major role in influencing inflammation, immune cell activation and mitochondrial dysfunction.[241-242] This has recently been extensively reviewed by Schank *et al*.[115]

The results from the current study correspond with those of Davis *et al*., who also found that GDF-15 was a better indicator of mitochondrial disease than FGF-21.[165] These authors suggest that GDF-15 is an indicator of inherited mitochondrial disease. Fibroblast growth factor 21, on the other hand, appears to be a superior indicator of mitochondrial disease when muscle manifestations are present.[165]

4.9 Conclusion

The systemic levels of GDF-15 were found to be elevated in HIV-infected participants, both at baseline and 12-months following cART, when compared to the HIV-uninfected individuals. This may have been as a result of HIV pathogenesis and immune depletion, which is commonly associated with OS and ROS production. In addition, high plasma concentrations of GDF-15 were associated with the lowest baseline CD4+ T-cell count, therefore, GDF-15 plasma concentrations may be induced by immune dysfunction. From the results of the current study, it is evident that the association between the concentration of GDF-15 and HIV VL was far less significant than that of the CD4+ T-cell count and systemic GDF-15 levels. The results from

this study imply that infection with HIV, together with the chronic administration of ARV agents, specifically NRTI-based regimens, in this case, may have an effect on the plasma levels of GDF-15. The results from this study correspond to those reported by others, in that monitoring systemic levels of GDF-15 is potentially a valuable, easily accessible biomarker for assessing MT.[155] In this setting, however, FGF-21 added no additional value as a biomarker for MT.

4.9.1 Strengths and Limitations

The strengths of this study, which investigated the potential use of the biomarkers, FGF-21 and GDF-15, to determine MT include the assessment of the biomarkers at two-time points in HIV-infected individuals. This allowed for the exploration of the effect of NRTI-based cART on the plasma concentrations of FGF-21 and GDF-15 over a 12-month period. Furthermore, this study also investigated the effects that HIV-related variables (VL and CD4+ T-cell count) may have on the concentrations of FGF-21 and GDF-15, therefore, setting the groundwork for future studies investigating these biomarkers as potential markers for monitoring MT in HIV-infected individuals.

Potential limitations of this study include; that all participants were recruited as part of a parental study with pre-set inclusion criteria, therefore, limiting the available sample size and also that the study lacked a positive control group consisting of participants with established mitochondrial disorders (*i.e.* MT). Furthermore, the inability to compare the concentrations of FGF-21 and GDF-15 found in plasma with those found in tissue that is known to express the biomarkers may have also underestimated the levels of these biomarkers in HIV-infected individuals.

.

CHAPTER 5

THE ASSOCIATION BETWEEN THE PLASMA BIOMAKERS AND MITOCHONDRIAL DEOXYRIBONUCLEIC ACID RELATIVE TO THE NUCLEAR DEOXYRIBONUCLEIC ACID RATIO IN DETERMINING MITOCHONDRIAL TOXICITY

5.1 Introduction

The current gold standard for the diagnosis of mitochondrial disorders relies on obtaining tissue samples (*i.e.* liver or muscle), on which biochemical and/or molecular tests are performed in order to diagnose and detect mitochondrial abnormalities. Molecular methods typically involve determining the mitochondrial content (mitochondrial deoxyribonucleic acid [mtDNA]) relative to the nuclear (n) DNA in a particular tissue in order to determine the mtDNA/nDNA ratio.[142] However, this method is not without challenges, as it is invasive and not practical for routine screening and monitoring. Most notably, the method has also been plagued with concerns over its sensitivity and specificity, hence the need for better diagnostic procedures.[104] Despite these limitations, the use of quantitative polymerase chain reaction (qPCR) remains the most accurate and reliable method of quantifying mtDNA in many samples, to monitor the pathophysiology of various mitochondrial diseases.

Elevated serum and/or plasma concentrations of fibroblast growth factor 21 (FGF-21) and growth and differentiation factor 15 (GDF-15) have both been associated with mitochondrial disorders and provide an easier method of sampling for both the participants and clinical staff.[173] However, the use of these biomarkers has yet to be validated and correlated to currently-used methods of diagnosis, which, as mentioned above, rely on determining the mtDNA/nDNA ratio.

In the present study, the possible associations between the concentrations of the systemic biomarkers, FGF-21 and GDF-15 (as described in Chapter 4), and the ratios obtained from the relative quantification of genomic DNA obtained from peripheral blood mononuclear cells (PBMCs) (as described in Chapter 3) were investigated. The evaluation was based on the results obtained at baseline and 12-months post-combination antiretroviral therapy (cART) for the 39 human immunodeficiency virus (HIV)-positive participants, as well as a single time point for the remaining 14 HIV-negative healthy participants. One heathy control was excluded due to presenting with exceptionally high GDF-15 and FGF-21 concentrations.

5.2 Results

5.2.1 Correlation between Logarithmically Transformed Variables (Fibroblast Growth Factor 21 and Growth and Differentiation Factor 15 Concentrations) and the Logarithmically Transformed Mitochondrial Deoxyribonucleic Acid Levels from the Same Time Point

A Pearson's correlation test was performed to measure the strength of the linear association between the logarithmically (Log) transformed mtDNA levels and transformed GDF-15 concentrations from corresponding time points, in the HIV-positive participants. However, since the differences in the FGF-21 concentrations over time remained negligible, the test was only performed for the GDF-15 concentrations at both time points. Furthermore, a correlation test was also performed for the transformed mtDNA levels and GDF-15 concentrations, for all participants (HIV-positive and HIV-negative), at baseline only. The correlation coefficients (r) and *p*-values are shown as a matrix represented in Tables 5.1, 5.2 and 5.3.

Table 5.1: Pearson's correlation between the Log of the mtDNA levels and the Log of the GDF-15 concentrations at baseline in HIV-positive participants.

Categories		Log GDF-15 concentrations at baseline	Log mtDNA
Log GDF-15 concentrations at baseline:	Pearson's correlation (r)	1.000	
	p-value	-	
	n	39	
Log mtDNA:	Pearson's correlation (r)	-0.143	1.000
	p-value	0.384	-
	n	39	39

* Based on the qPCR data and the corresponding GDF-15 concentrations obtained from 39 HIV-positive participants

Table 5.2: Pearson's correlation between the Log of the mtDNA levels and the Log of the GDF-15 concentrations at 12-months post-cART in HIV-positive participants.

Categories		Log GDF-15 concentrations at 12-months post-cART	Log mtDNA
Log GDF-15 concentrations at 12-months post-cART:	Pearson's correlation (r)	1.000	
	p-value	-	
	n	39	
Log mtDNA:	Pearson's correlation (r)	0.117	1.000
	p-value	0.479	-
	n	39	39

* Based on the qPCR data and the corresponding GDF-15 concentrations obtained from 39 HIV-positive participant

The Pearson's correlation test determined that there was no relationship between the Logarithm (Log) of the GDF-15 concentrations and the Log of the mtDNA levels, from the same time point (p=0.384 and 0.479, respectively), in HIV-positive participants. In contrast, when the entire group (HIV-positive and HIV-negative participants), at baseline, was considered (Table 5.3), the correlation test revealed that there was a significant, albeit weak, correlation between the two variables at baseline, (r=0.296; p=0.031), as also depicted in the scatter graph in Figure 5.1.

Table 5.3: Pearson's correlation between the Log of the GDF-15 concentrations and the Log of the mtDNA levels at baseline for the HIV-positive and HIV-negative participants combined.

Categories		GDF-15 concentrations	Log mtDNA
Log GDF-15 concentrations:	Pearson's correlation (r)	1.000	
	p-value	-	
	n	39	
Log mtDNA:	Pearson's correlation (r)	0.296	1.000
	p-value	**0.031****	-
	n	39	39

* Based on the qPCR data and the corresponding GDF-15 concentrations obtained from 14 HIV-negative participants and39 HIV-positive participants

** Values in bold indicate significance

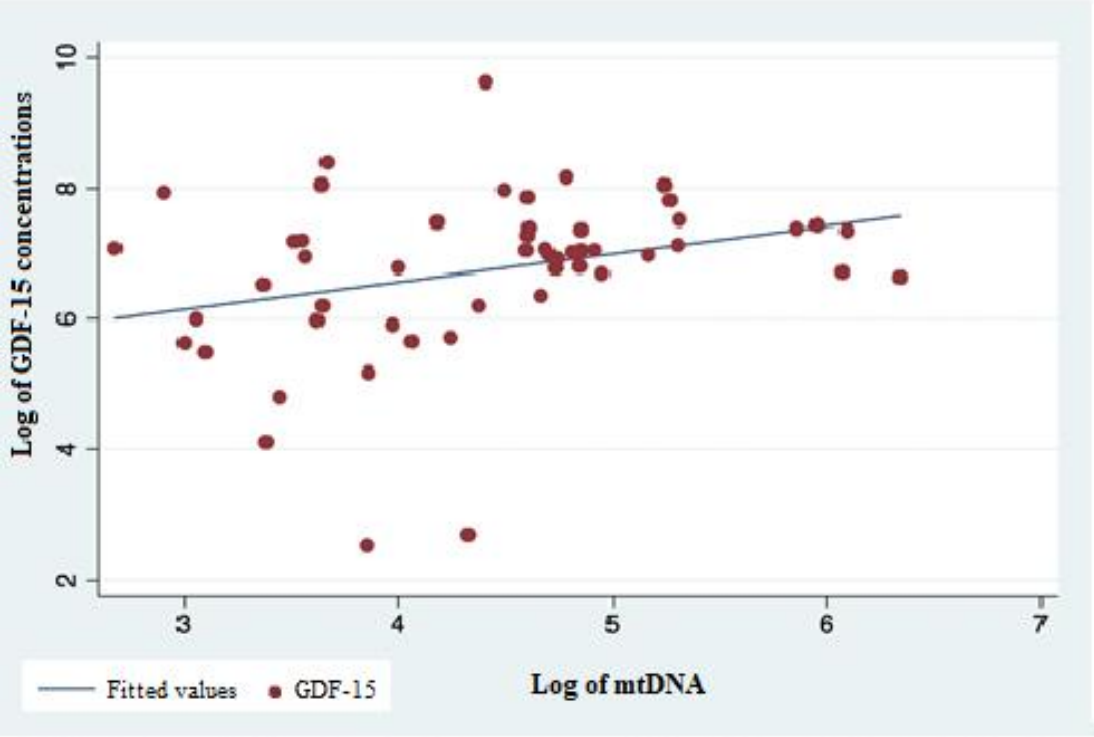

Figure 5.1: Scatterplot showing the correlation between the Log of the mtDNA and the Log of the GDF-15 concentrations at baseline, in HIV-positive and HIV-negative participants. A positive correlation between the two variables was found, as shown by the regression line running across the data. (Pearson's r=0.296)

5.2.2 Linear Regression Analysis between the Transformed Growth and Differentiation Factor 15 Concentrations, with the Transformed Mitochondrial Deoxyribonucleic Acid Levels from the Same Time Point

A linear regression was performed for the transformed GDF-15 concentrations and the transformed mtDNA levels, from the same time point for both the HIV-positive and HIV-negative participants, to determine whether there was a linear relationship between the two variables. These results for the HIV-positive and -negative participants are presented in Table 5.4 and for the HIV-positive participants alone in Tables 5.5 and 5.6.

Table 5.4: The linear regression analysis for the Log of GDF-15 concentrations and the Log of the mtDNA levels for both HIV-positive and HIV-negative participants measured at baseline.

Log GDF-15 baseline	Coeff.	Std. Err.	t	P > ltl	95% Conf. Interval)		*F* (1, 51)	Prob > F	R-Squared
Log mtDNA	0.427	0.193	2.210	**0.031****	0.0340	0.814	4.900	0.031	0.088
Constant	4.859	0.865	5.620	**0.0001****	3.122	6.595			

* Based on the qPCR data and the corresponding GDF-15 concentrations obtained from 14 HIV-negative participants and 39 HIV-positive participants

** Values in bold indicate significance

Abbreviations: Coeff=Coefficient; **Std. Err**=Standard error of the regression; **t**=t-value; **95% Conf. Interval**=95% Confidence interval; ***F***=F-value

Table 5.5: The linear regression analysis for the Log of GDF-15 concentrations and the Log of the mtDNA levels for the HIV-positive participants measured at baseline.

Log GDF-15 baseline	Coeff.	Std. Err.	t	P > ltl	95% Conf. Interval)		*F* (1, 39)	Prob > F	R-Squared
Log mtDNA	-0.174	0.170	-1.020	0.312	-0.519	0.170	1.050	0.312	0.028
Constant	8.094	0.793	10.210	**0.0001****	6.488	9.701			

* Based on the qPCR data and the corresponding GDF-15 concentrations obtained from 14 HIV-negative participants and 39 HIV-positive participants

** Values in bold indicate significance

Abbreviations: Coeff=Coefficient; **Std. Err**=Standard error of the regression; **t**=t-value; **95% Conf. Interval**=95% Confidence interval; ***F***=F-value

Table 5.6: The linear regression analysis for the Log of GDF-15 concentrations and the Log of the mtDNA levels of the HIV-positive participants both measured 12-months after treatment.

Log GDF-15 at 12-months post-cART	Coeff.	Std. Err.	t	P > ltl	95% Conf. Interval)		*F* (1, 39)	Prob > F	R-Squared
Log mtDNA	0.0110	0.1280	0.0900	0.9320	-0.2490	0.2710	0.0100	0.9320	0.0002
Constant	7.4140	0.5980	12.4000	**0.0001****	6.2020	8.6250			

* Based on the qPCR data and the corresponding GDF-15 concentrations obtained from 14 HIV-negative participants and39 HIV-positive participants

** Values in bold indicate significance

Abbreviations: Coeff=Coefficient; **Std. Err**=Standard error of the regression; **t**=t-value; **95% Conf. Interval**=95% Confidence interval; ***F***=F-value

The linear regression showed that the transformed baseline GDF-15 concentrations could statistically predict the Log of the mtDNA levels, from the same time point when the HIV-negative and HIV-positive participants were evaluated together, but not when the HIV-positive participants were assessed on their own, either at baseline or 12 months.

5.2.3 The Association between the Systemic Fibroblast and Growth Factor 21 and Growth and Differentiation Factor 15 Concentrations and the Two Defined Mitochondrial Deoxyribonucleic Acid Fold Change Subgroups at each Time Point

The measured concentrations of the plasma biomarkers, FGF-21 and GDF-15, at baseline and after 12 months of cART, as well as the difference between these two time points, were compared with two categories of mtDNA fold changes (depletion [< 1] or recovery [≥ 1]) following 12-months of cART in only the HIV-positive participants (n=39). These results are shown in Table 5.7.

Table 5.7: Fibroblast growth factor 21 and GDF-15 concentrations over time and two mtDNA fold change categories following 12-months of treatment.

Category	**Statistical measure**	**HIV-positive participants (n=39)**		***p*-value**
		mtDNA depletion: < 1 n=22	**mtDNA recovery: ≥ 1 n=17**	
FGF-21 concentrations at baseline (pg/mL)	Median (IQR)	8.64* (8.64 - 8.64)	8.64* (8.64 - 8.64)	0.878
FGF-21 concentrations at 12-months post-cART (pg/mL)	Median (IQR)	8.64* (8.64 - 8.64)	8.64* (8.64 - 8.64)	0.679
GDF-15 concentrations at baseline (pg/mL)	Median (IQR)	1,558.00 (1,072.85 – 1,835.48)	1,155.36 (885.29 – 1,344.35)	0.322
GDF-15 concentrations at 12-months post-cART (pg/mL)	Median (IQR)	1,623.90 (1,225.03 – 3,169.44)	1,757.45 (1,360.11 – 1,992.95)	0.843

* Values remain unchanged for the 25th, 50th and 75th percentiles

Abbreviations: **pg**=Picogram; **mL**=Millilitre

The current study found no associations between the measured GDF-15 concentrations, at baseline and 12-months following cART, with the mtDNA fold change following 12-months of treatment (p=0.322 and 0.843, respectively). Interestingly, participants who experienced a reduction in mtDNA (n=22) had slightly higher concentrations of GDF-15 at baseline, which subsequently decreased over the 12-months on treatment. In contrast, the participants who displayed a recovery in mtDNA (n=17) showed lower GDF-15

concentrations at baseline with a greater increase in concentration of the biomarker 12-months post-cART.

There was also no association found between the two defined mtDNA fold change categories and the measured concentrations of FGF-21 at baseline and 12-months post-cART for participants who presented with mtDNA depletion or recovery, as the median FGF-21 concentration for all subgroups remained unchanged.

5.2.4 The Association between two Biomarker Categories and the Mitochondrial Deoxyribonucleic Acid Fold Change over Time

The association between the systemic biomarkers, FGF-21 and GDF-15, dichotomised according to their respective medians at baseline and 12-months post-cART, with the mtDNA fold change over time for the HIV-positive participants, is shown in Tables 5.8 and 5.9, respectively.

As was noted previously, the participants were grouped according to whether they had a reduction or recovery in mtDNA following 12-months of treatment. This was followed by grouping the participants into two categories for each biomarker based on their recorded median concentrations at each time point. For both the baseline and 12-months post-cART FGF-21 concentrations, the participants were grouped as either having a concentration of less than or equal to 8.64 picograms (pg)/millilitre (mL) or greater than 8.64 pg/mL. These results are shown in Table 5.8.

Table 5.8: The association between FGF-21 categories at baseline and 12-months post-cART and the mtDNA fold change over time.

Category	Statistical measure	HIV-positive participants (n=39)		*p*-value
		mtDNA depletion: < 1 n=22	mtDNA recovery: ≥ 1 n=17	
FGF-21 concentrations at baseline (pg/mL)				0.679
≤ 8.64	n	18	15	
> 8.64	n	4	2	
FGF-21 concentrations at 12-months post-cART (pg/mL)				0.598
≤ 8.64	n	20	16	
> 8.64	n	2	1	

For both the baseline and 12-months post-cART categories, most of the FGF-21 concentrations observed in participants who experienced depletion or recovery of mtDNA concentrations had concentrations that were less than or equal to 8.64 pg/mL (baseline; 18 out of 22 [81.82%] and 15 out of 17 [88.24%], and 12-months post-cART; 20 out of 22 [90.91%] and 16 out of 17 [94.12%]). No associations were found between the categories of the baseline or 12-months FGF-21 and the two defined mtDNA fold change categories (p=0.679 and 0.598 respectively). Similarly, no associations were found when this analysis was repeated with FGF-21 divided into quartiles (data not shown).

Again, participants were placed in two categories according to their median GDF-15 concentration for each time point. For the baseline GDF-15 concentration, the participants were grouped as either having a concentration of equal to or less than 1,248.94 pg/mL, and greater than 1,248.94 pg/mL. The 12-months post-cART subgroups allocated

participants into groups according to whether they had concentrations equal to or less than 1,639.93 pg/mL and greater than 1,639.93 pg/mL. These results are shown in Table 5.9.

Table 5.9: The association between GDF-15 categories at baseline and 12-months post-cART and the mtDNA fold change over time.

Category	Statistical measure	HIV-positive participants (n=39)		*p*-value
		mtDNA depletion: < 1 n=19	mtDNA recovery: ≥ 1 n=20	
GDF-15 concentrations at baseline (pg/mL)				0.079
≤ 1,248.94	n	8	14	
> 1,248.94	n	11	6	
GDF-15 concentrations at 12-months post-cART (pg/mL)				0.855
≤ 1,639.93	n	11	11	
> 1,639.93	n	8	9	

No significant differences were found between the GDF-15 categories and the two mtDNA groups at baseline or 12-months post-cART (p=0.079 and 0.855, respectively) although it should be noted that the baseline category just missed statistical significance. In this regard, one can see that more participants with mtDNA recovery (14 out of 20 [70%]) had GDF-15 levels in the lower category at baseline. This possible association was no longer evident after 12-months with fewer participants with mtDNA recovery (11 out of 20 [55%]) now falling into this category. Once again, no associations were found when this analysis was repeated with GDF-15 divided into quartiles (data not shown).

5.2.5 Relationship between Logarithmically Transformed Growth and Differentiation Factor 15 Concentrations and the Transformed Mitochondrial Deoxyribonucleic Acid Fold Change over Time

As was the case in Chapter 3, section 3.8.4, the FGF-21 and GDF-15 (baseline and 12-months post-cART) data were transformed before a Pearson's correlation test and linear regression analysis were performed. As mentioned above, these tests were only performed for the GDF-15 concentrations at baseline and 12-months post-cART. The data were used to determine the relationship between the variables with the overall mtDNA fold change over time.

5.2.5.1 Correlation between the Transformed Fibroblast Growth Factor 21 and Growth and Differentiation Factor 15 (Baseline and 12-Months Post-Combination Antiretroviral Treatment) with the Mitochondrial Deoxyribonucleic Acid Fold Change over Time

As described above, a Pearson's correlation test was performed to determine whether there was a significant correlation between the transformed mtDNA fold change and transformed GDF-15 concentrations at baseline and 12-months post-cART. As previously mentioned, the tests were only performed for the GDF-15 concentrations at both time points. The correlation coefficients (r) and *p*-values are shown as a matrix represented in Tables 5.10 and 5.11.

Table 5.10: Pearson's correlation between the Log of the mtDNA fold change over time and the Log of the GDF-15 concentrations at baseline.

Categories		Log mtDNA fold change	Log GDF-15 baseline
Log mtDNA fold change:	Pearson's correlation (r)	1.000	
	p-value	-	
	n	39	
Log GDF-15 at baseline:	Pearson's correlation (r)	0.080	1.000
	p-value	0.954	-
	n	39	39

* Based on the qPCR data and the corresponding GDF-15 concentrations obtained from 39 HIV-positive participants

Table 5.11: Pearson's correlation between the Log of the mtDNA fold change and the Log of the GDF-15 concentrations at 12-months post-cART.

Categories		Log mtDNA fold change	Log GDF-15 at 12-months post-cART
Log mtDNA fold change:	Pearson's correlation (r)	1.000	
	p-value	-	
	n	39	
Log GDF-15 at 12-months post-cART:	Pearson's correlation (r)	-0.090	1.000
	p-value	0.397	-
	n	39	39

* Based on the qPCR data and the corresponding GDF-15 concentrations obtained from 39 HIV-positive participants

The Pearson's correlation test found no relationship between the Log of the GDF-15 concentrations at baseline and 12-month post-cART with the Log of the mtDNA fold change over time (p=0.954 and 0.397 respectively).

5.2.5.2 Linear Regression Analysis between the Transformed Growth and Differentiation Factor 15 and the Mitochondrial Deoxyribonucleic Acid Fold Change over Time

As described above, a linear regression was performed for the transformed GDF-15 concentrations at either time point, in order to determine if there was a linear relationship between the transformed GDF-15 concentrations and the transformed changes in the mtDNA fold change over 12-months of cART. This was only done for the HIV-positive participants. These results are presented in Tables 5.12 and 5.13, respectively.

Table 5.12: The linear regression analysis for the Log of the GDF-15 concentrations at baseline and the Log of the mtDNA fold change.

Log mtDNA	Coeff.	Std. Err.	t	P > ltl	95% Conf. Interval)		*F* (1, 39)	Prob > F	R-Squared
Log GDF-15 at baseline	0.0121	0.2080	0.0600	0.9540	-0.4100	0.4343	0.0001	0.9539	0.0001
Constant	-0.1498	1.5243	-0.1000	0.9220	-3.2383	2.9388			

* Based on the qPCR data and the corresponding GDF-15 concentrations obtained from 39 HIV-positive participants

Abbreviations: Coeff=Coefficient; **Std. Err**=Standard error of the regression; **t**=t-value; **95% Conf. Interval**=95% Confidence interval; ***F***=F-value

From the linear regression, it was found that the transformed baseline GDF-15 concentrations could not statistically predict the Log mtDNA fold change.

Table 5.13: The linear regression analysis for the Log of GDF-15 concentrations following 12-months of cART and the Log of the mtDNA fold change.

Log mtDNA	Coeff.	Std. Err.	t	P > ltl	95% Conf. Interval)		*F* (1, 37)	Prob > F	R-Squared
Log GDF-15 at 12-months post-cART	-0.2378	0.2773	-0.8600	0.3970	-0.7998	0.3241	0.0001	0.9539	0.0001
Constant	1.7142	2.0745	0.8300	0.4140	-2.48992	5.9176			

* Based on the qPCR data and the corresponding GDF-15 concentrations obtained from 39 HIV-positive participants

Abbreviations: Coeff=Coefficient; **Std. Err**=Standard error of the regression; **t**=t-value; **95% Conf. Interval**=95% Confidence interval; ***F***=F-value

Similarly, the linear regression analysis also found that the transformed GDF-15 concentrations following 12-months of cART could not statistically predict the Log of the mtDNA fold change.

5.2.6 Multivariate Linear Regression Analysis of Logarithmically Transformed Baseline Growth and Differentiation Factor 15, Mitochondrial Deoxyribonucleic Acid/ Nuclear Deoxyribonucleic Acid Ratio and the Age for Both of the Human Immunodeficiency Virus-Positive and -Negative Participants

Given the statistically significant associations observed between age and both mtDNA/nRNA and GDF-15 at baseline, multivariable regression was performed and the results are presented in Table 5.14.

Table 5.14: Multivariate Linear regression analysis using the Log of the GDF-15 concentrations, Log of age and the Log of the mtDNA/nDNA ratio as dependent variables.

Log GDF-15 at baseline	Coeff.	Std. Err.	t	P > ltl	95% Conf. Interval)		*F* (2, 50)	Prob > F	R-Squared
Log mtDNA/nDNA ratio	0.414	0.195	2.120	**0.039**	0.022	0.806			
Log Age	0.385	0.629	0.610	0.543	-0.878	1.649	2.610	0.084	0.095
Constant	3.502	2.380	1.470	0.147	-1.278	8.282			

* Based on the qPCR data and the corresponding GDF-15 concentrations obtained from 39 HIV-positive participants and14 HIV-negative participants

Abbreviations: Coeff=Coefficient; **Std. Err**=Standard error of the regression; **t**=t-value; **95% Conf. Interval**=95% confidence interval; ***F***=F-value

From the analysis it was found that the age of the participants did not reach statistical significance in this particular subgroup. However, the baseline log of the GDF-15 value remained significantly associated with the mtDNA/nRNA ratio at baseline.

5.3 Discussion

In Chapters 3 and 4, the current study investigated whether the long-term use of cART and the severity of HIV-1 infection (as measured by CD4+ T-cell count and viral load [VL]) had an effect on the expression of the plasma biomarkers, FGF-21 and GDF-15, as well as the mtDNA content in PBMCs, over 12-months, as a measure of mitochondrial toxicity (MT). The present chapter investigated whether any associations between the plasma biomarkers and mtDNA content could be found, thereby assessing the potential usefulness of FGF-21 and GDF-15 as systemic biomarkers of MT.

Our findings show that, when comparing the concentrations of GDF-15 and levels of mtDNA at corresponding time points, no significant relationship at either of the two time points was found when assessing HIV-positive participants on their own. In contrast, it was found that the combined GDF-15 concentrations measured at baseline for both the HIV-infected and -uninfected participants were significantly associated and positively correlated with the mtDNA concentrations from the same time point.

Although this finding missed statistical significance, it is interesting to note that participants who experienced mtDNA depletion also presented with higher GDF-15 concentrations at baseline, when compared to those who had mtDNA recovery. The same was true when the baseline GDF-15 concentrations were dichotomised and compared with the mtDNA fold change over time. It is possible that the limited number of study participants being recruited for the study precluded the attainment of statistical significance. Regardless, as no association was found between the mtDNA fold change and GDF-15 at baseline and 12-months following cART, it would follow that the plasma markers may not be good alternatives to the standard mtDNA/nDNA ratio for diagnosing and monitoring MT in HIV-infected individuals on nucleoside reverse transcriptase inhibitor (NRTI)-based antiretroviral (ARV) regimens.

Although most participants presented with normal levels of FGF-21, there were some who showed abnormal levels whilst not showing any significant mtDNA depletion or recovery, therefore, suggesting that the concentration of FGF-21 was influenced by a non-mitochondrial source, as has been reported in other metabolic conditions such as type 2 diabetes mellitus and fatty non-alcoholic liver disease.[243-244] These findings coincide with those reported by Payne

et al., who investigated whether the concentrations of serum FGF-21 correlated with mitochondrial dysfunction in muscle biopsies from HIV-infected individuals on contemporary cART regimens. These authors found that the concentration of serum FGF-21, albeit elevated, did not correlate with the severity of muscle mitochondrial defect, hence being a poor predictor of mitochondrial dysfunction.[230] Furthermore, similar to the findings of the current study, the fact that some individuals did experience depletion of mtDNA, whilst simultaneously presenting with normal FGF-21 levels, further suggests that this biomarker may not be sensitive enough to detect less severe cases of mitochondrial defects. In previous studies, the association between elevated FGF-21 concentrations in HIV-infection, were more aligned with HIV-related conditions such as obesity, insulin resistance and dyslipidaemia.[245] However, in the current study, the effects of these conditions were minimised by recruiting participants prior to cART initiation (baseline), so as to allow the focus of the study to be on the effect of a NRTI-based HIV regimen on the biomarker concentrations.

Although GDF-15 has been linked to MT in several previous studies; such as the study conducted by Yatsuga *et al*., no evidence of elevated GDF-15 concentrations being associated with MT was found in the present study, when the HIV-positive participants were assessed alone, however, when the entire cohort (HIV-positive and -negative) was assessed as a whole it was found that a significant association did exist between GDF-15 and MT at both time points. Because significance was only found when the HIV-negative participants, who presented with much lower GDF-15 concentrations, were combined with the HIV-positive participants, it could be suggested that there is a stronger association related to lower concentrations of GDF-15 than higher values. Many other studies have associated increased GDF-15 expression with certain cancers such as breast, colon and pancreas.[173,234,246] Furthermore, high expression of GDF-15 has been found in cancer biopsies, suggesting that serum GDF-15 may be a useful indicator for the diagnosis and monitoring of cancer.[247] When assessing the relationship between GDF-15 and MT, many researchers; such as Montero *et al*., have found that when comparing the circulating serum levels of GDF-15 and FGF-21 in a cohort exclusively of children diagnosed with mitochondrial disease, that GDF-15 was a far more sensitive and specific biomarker than FGF-21 for the diagnosis of these diseases.[175] Furthermore, limited research has been done to evaluate whether these biomarkers correlate with the measured mtDNA/nDNA ratio in an HIV-infected cohort on an NRTI-based ARV regimen.

A multivariable regression analysis of the results found that when age, GDF-15 concentrations and the mtDNA/nDNA ratio were compared to each other, a significant relationship was observed between the GDF-15 concentrations and the mtDNA fold change, with no significance being associated with the age of the participants. This could be due to the small number of elderly HIV-infected participants being recruited for this study. However, when assessing the relationship between the GDF-15 concentrations and age, a significant relationship was observed, particularly in the concentrations measured prior to receiving treatment. The findings show that at either of the two-time points, older participants (HIV-positive and -negative) displayed higher concentrations of GDF-15, with the highest being recorded at 12-months post-treatment. Several studies have described the process of aging as a progressive accumulation of somatic mutations on mtDNA over a lifetime, which result in a decline in electron transport chain (ETC) activity, increased production of reactive species and additional mtDNA mutations.

Furthermore, increased oxidative damage is commonly associated with aging and manifests as cellular and tissue dysfunctions probably brought about by insufficient energy production and apoptosis.[248-249] As previously mentioned, increased concentrations of GDF-15 have been found in individuals with mitochondrial disease, hence, many studies recommend the use of GDF-15 as a potential diagnostic marker of mitochondrial dysfunction. In addition, a study by Tanaka *et al.* that investigated the role of GDF-15 in mitochondrial disorders, found that this biomarker was also induced in response to declines in the production of energy.[250] Therefore, from the above-mentioned studies it can be postulated that as age increases, there is a proportional decrease in the function of the mitochondria which may result in a decline in energy production and induce an increase in GDF-15 concentrations.

5.4 Conclusion

Our findings conclude that plasma FGF-21 and GDF-15 concentrations do not correlate with the standard measure of mtDNA/nDNA ratio. We have therefore demonstrated that, in this setting, these biomarkers are a less sensitive and specific alternative method of MT detection in HIV-infected individuals placed on NRTI-based ARV regimens. Regardless of both biomarkers having been successfully associated with mitochondrial defects and

damage in other studies, in the present study the concentrations did not indicate the presence of mitochondrial recovery or depletion in the participants, as was found with the mtDNA/nDNA ratios. Unlike with FGF-21, the GDF-15 concentrations showed the greatest variation across the subgroups of participants, however, even these measurements showed no significant correlations with the mtDNA/nDNA ratios. Furthermore, there was a significant relationship between the baseline GDF-15 concentrations and aging, which could possibly be attributed to the decline in mitochondrial integrity associated with age inducing an increase in GDF-15. It remains unclear whether the elevated concentrations of GDF-15 in the HIV-infected individuals were due to the virus, an underlying inflammatory condition or the NRTIs themselves. Regardless, given the increased use of NRTI-based ARV regimens, the findings of the current study suggest that further research on this topic should be carried out to further investigate the relationship between HIV and HIV-associated conditions and the prolonged use of NRTIs coupled with decreases in mtDNA levels, with variations in GDF-15 concentrations over time.

CHAPTER 6

GENERAL DISCUSSION AND CONCLUSION

6.1 Discussion

Combination antiretroviral therapy (cART) consists of a cocktail of drugs that are taken life-long by human immunodeficiency virus (HIV)-infected individuals.[3,16] The antiretroviral (ARV) medication has been shown to increase the life expectancy of those infected; however, a number of non-acquired immunodeficiency syndrome (AIDS)-defined risks have been associated with the chronic, long-term use of these drugs. These include; individuals developing metabolic complications such as diabetes, dyslipidaemia and decreased bone density.[60,245] Nucleoside reverse transcriptase inhibitors (NRTIs) have been associated with adverse effects such as lactic acidosis, cardiovascular complications and most notably, mitochondrial toxicity (MT), which refers to mitochondrial damage resulting in depletion of mitochondrial deoxyribonucleic acid (mtDNA), which then disrupts the organelle's normal function. The depletion of mtDNA may arise prior to the symptoms of MT and may therefore be used as an indicator of early MT in HIV-infected individuals on NRTI-based ARV regimens.[118,230]

The gold standard of assessing MT requires muscle biopsies in which the mtDNA/nuclear (n) DNA ratio is determined; however, due to the invasiveness of the sample collection, easier sampling methods are required.[50,151] The current study investigated the possible associations between disease severity and cART and mitochondrial damage by determining the mtDNA/nDNA ratio in peripheral blood mononuclear cells (PBMCs), as well as assessing the systemic biomarkers, fibroblast growth factor 21 (FGF-21) and growth and differentiation factor 15 (GDF-15), as an alternative to the mtDNA/nDNA ratio as an early indicator of MT in HIV-1 infected individuals. The use of PBMCs to determine the mtDNA/nDNA ratio has been explored by several previous studies as a non-invasive alternative to the tissue biopsy samples and makes use of quantitative polymerase chain reaction (qPCR) to quantify and compare the genomic DNA and mtDNA as a means of monitoring mitochondrial health. The current study, therefore, compared two non-

invasive approaches of monitoring MT with each other, and assessed whether they were associated with one another and/or were influenced by factors associated with HIV-infection *per se* and/or chronic use of NRTIs.

When assessing the extent of MT using the PBMCs mtDNA/nDNA ratio, it was found that mtDNA depletion was observed, probably as a result of the effect of the chronic viral infection, coupled with the use of NRTIs in the HIV-positive participants. This is concluded based on the fact that, when compared to the HIV-negative individuals, the HIV-positive participants had lower mtDNA copy numbers at baseline (pre-treatment) and experienced a decrease in mtDNA over the 12-months on combined ART (cART). Furthermore, the present study demonstrated that the severity of disease, as measured by the HIV viral load (VL) in plasma, but not the cluster of differentiation 4 (CD4+) T-cell count, was associated with baseline mtDNA levels.

Concentrations of GDF-15 were higher in HV-infected participants than in uninfected participants at both baseline and 12 months. However, in the HIV-positive participants the differences in GDF-15 concentrations between the two-time points were minimal. These finding may suggest that perhaps the long-term use of cART may not be an influencing factor for the changes in GDF-15, but rather another factor such as an infection, inflammation or another underlying condition. Furthermore, when the GDF-15 concentrations of the HIV-positive participants were compared to the mtDNA levels at specific time points, no associations were found. However, when the combined GDF-15 concentrations from baseline for both the HIV-positive and –negative participants were compared with the mtDNA levels, a significant association was found which further indicate that the increase in GDF-15 levels may be due to other factors outside of NRTI-associated mitochondrial depletion. These possible factors may include chronic inflammation, with/without the presence of HIV, or conditions such as; diabetes or obesity which have also been shown to increase the expression of GDF-15.

In the entire group, GDF-15 levels increased between baseline and 12 months, although the difference was not statistically significant. Regarding the FGF-21 concentrations, it was found that most participants had concentrations which fell below the detection limit of the assay, with only a few showing elevated levels. Interestingly, all the participants with FGF-21 concentrations in the highest quartile were HIV-positive. Regardless, there

was no association between FGF-21 with either mtDNA depletion or recovery. These finding suggest that GDF-15 may be a more sensitive biomarker than FGF-21 in the detection of MT.

Importantly, a significant association was also found between the baseline GDF-15 concentration and aging, with older participants displaying higher concentrations of the biomarker. The increase in GDF-15 concentration with age may be attributed to age-related decreases in mtDNA triggering an increase in the expression GDF-15, which, as mentioned previously, has been associated with oxidative stress (OS) brought about by mitochondrial disorders or depletions in mtDNA. In contrast, no association was found between FGF-21 and aging at either of the two-time points. In addition, when the association between the mtDNA/nDNA ratio with aging was assessed, an association was also found with older participants presenting with decreased mtDNA content over time. However, similar to the GDF-15 concentrations, it can be speculated that these finding are more associated with age-related decreases in mtDNA, rather than the chronic use of NRTIs or HIV.

In the present study most of the participants from both HIV-positive and -negative groups presented as non-tobacco users. When the association between the use of tobacco with age, gender, CD4+ T-cell count (baseline and 12-months post treatment) and VL were assessed, no associations were found. Furthermore, albeit not significant, most of tobacco users in the study experienced mtDNA depletions, suggesting that the use of tobacco may have an effect on the levels of mtDNA. As previously mentioned, this may be attributed to tobacco smoke-induced electron transport chain (ETC) impairments which may result in OS, which subsequently leads to mitochondrial damage.

No associations were found between the levels of mtDNA and the CD4+ T-cell count in the HIV-infected individuals before and after treatment. However, it was found that participants who experienced a decrease in mtDNA levels also presented with the lowest CD4+ T-cell count, albeit that the association just missed statistical significance. In contrast, the GDF-15 biomarker showed a significant association with the CD4+ T-cell count at baseline and 12-months post-treatment. In fact, participants with lowest CD4+ T-cell counts had the highest levels of plasma GDF-15. From these finding it could be speculated that factors more associated with HIV such as; reactive oxygen species (ROS)

and inflammation may be responsible for the decrease in mtDNA and consequential increase in GDF-15 concentrations. In contrast, the FGF-21 concentrations remained similar between the HIV-infected individuals, even following 12-months of cART. However, when the FGF-21 concentrations were evaluated further, a significant association was found between the biomarker and the baseline CD4+ T-cell count. The findings showed that an inverse relationship existed between FGF-21 and baseline CD4 T-cell count, in that, participants who expressed higher FGF-21 concentrations, also had a lower CD4+ T-cell count, at baseline.

In addition, significance was just missed when the associations between the baseline PBMC levels of mtDNA and the viral load (VL) were evaluated. However, when the VLs were further dichotomised into three subgroups a significant difference was found, with participants with the highest VL having the highest baseline delta (Δ) Ct values. This translates to the participants with the severest HIV infection displaying the lowest mtDNA levels, which may suggest that the virus may be directly affecting the mitochondria, therefore, resulting in a more noticeable decrease in mtDNA.

When analysing the relationship between GDF-15 and FGF-21 concentrations with the VLs, no associations were found. However, when the association between the baseline GDF-15 concentrations and VL was evaluated, as association was found, only when the GDF-15 concentrations were dichotomised into three groups. The findings showed that individuals with the lowest VL also presented with highest baseline GDF-15 concentrations, when compared to individuals with less severe HIV. Furthermore, 12-months after treatment it was also found that a significant difference in the concentrations of GDF-15 between these groups existed. As speculated in Chapter 4, these changes may be a result of chronic inflammatory conditions associated HIV which may induce an increase in ROS, therefore, suggesting a stronger association possibly exists between inflammation and the VL.

As was found with the CD4+ T-cell count association with GDF-15, this association may result from other factors related to HIV and chronic NRTI-administration in addition to mtDNA damage. Growth and differentiation factor-15 proved to have a stronger association with the participants baseline CD4+ T-cell count and VL, when compared to

the FGF-21 concentrations or mtDNA/nDNA ratio. However, when comparing the two variables, the CD4+ T-cell count proved to have a greater relationship with GDF-15, than the VL.

6.2 Conclusion

In conclusion, when comparing, FGF-21 and GDF-15 concentrations with changes in mtDNA/nDNA, it was found that there was no association between the biomarkers and mtDNA/nDNA. From the mtDNA/nDNA ratios alone, it was evident that the use of NRTIs coupled with an HIV infection had an effect on the mtDNA content over time in the HIV-positive participants. Notably, participants with higher VLs displayed lower mtDNA contents pre-treatment, and better recovery post-treatment, suggesting that the virus may play a greater role in the depletion of mtDNA than the use of NRTIs. Furthermore, when assessing if there was an association between the extent of MT with disease severity and immune suppression, it was found that neither of these variables affected the mtDNA content measured in the PBMCs of HIV-infected over time.

In contrast, when observing the biomarker concentrations alone, it was found that the levels of FGF-21 were not affected by either HIV infection or its treatment, as most HIV-positive and –negative participants had FGF-21 concentrations below the limits of detection, irrespective of CD4+ T-cell count, baseline VL or the participant being placed on a NRTI-based ARV regimen, making it a poor candidate for detecting mitochondrial disorders in this setting. Interestingly, there were a few participants who did display high FGF-21 concentrations at both time points, with all of them being HIV-positive. Furthermore, when these individuals were further evaluated, a significant association was found between with their FGF-21 levels and the baseline CD4+ T-cell count. Unlike the FGF-21 concentrations, GDF-15 has shown potential as a marker of disease progression in individuals infected with HIV as increased levels were found following 12-months of cART. Furthermore, associations were found between GDF-15 concentrations with both the baseline CD4+ T-cell count and VL (when dichotomised), albeit failing to show an association with the PBMC mtDNA fold change observed. In addition, age has also been shown to be a contributing factor to the increase in levels of the biomarker, however, this may be associated more with age rather than an effect of HIV or NRTIs.

6.3 Recommendations for Future Research

It would be of value to investigate the effect that different ARV regimens have on the mtDNA/nDNA ratio in PBMCs, as well as the GDF-15 and FGF-21 concentrations. In 2019 the recommendation for first-line and second-line ARV regimens was amended to include the use of the integrase strand transfer inhibitor (INSTI), dolutegravir (DTG) (TLD regimen: tenofovir disoproxil fumarate-lamivudine-dolutegravir), as opposed to the previous regimen which included efavirenz (EFV) for the treatment of HIV in all populations.[43] Several studies have associated the use of DTG with conditions of the central nervous system such as neuropsychiatric disorders (*i.e.* depression and suicidal actions) and neural tube defects in pregnant women.[251-252] It would be interesting to explore whether these adverse effects involve mitochondrial toxicity of the tissues in question. Further investigation into the effect this drug has on the mtDNA content with the added element of exploring its impact on the concentrations of FGF-21 and GDF-15 may give valuable insight into the mitochondrial toxicity profile that each regimen has.

Furthermore, studies have yet to evaluate the effect that a month-long post-exposure prophylaxis regimen has on the mitochondria and concentrations of FGF-21 and GDF-15 of HIV-uninfected participants. A study conducted by Baño *et al.* investigated the toxicity of the treatment without viral interference in the PBMCs of HIV-uninfected participants and found there to be subclinical mitochondrial damage.[253] Therefore, exploring the effects that the short-term treatment has on the concentrations of systemic biomarkers associated with mtDNA damage (particularly GDF-15) in uninfected participants could give insight as to whether the increase in GDF-15 that was observed in the present study was indeed due to viral interference as opposed to an effect of the use of cART.

REFERENCES

1. Gallo RC, Montagnier L. The discovery of HIV as the cause of AIDS. New England Journal of Medicine. 2003; 349(24):2283-5. doi:https://doi.org/10.1056/nejmp038194

2. Sidibé M. UNAIDS Data 2018. Antiretrovirals for Prevention: Realizing the Potential. Closing Commentary by the Executive Director of UNAIDS. 2018; doi:https://doi.org/10.2174/157016211798038579

3. Weston R, Marett B. HIV infection: Pathology and disease progression. Clinical Pharmacist. 2009; 1:387-92.

4. Statistics South Africa. Mid-year population estimates. 2019.

5. Keele BF, Van Heuverswyn F, Li Y, Bailes E, Takehisa J, Santiago ML, Bibollet-Ruche F, Chen Y, Wain LV, Liegeois F. Chimpanzee reservoirs of pandemic and nonpandemic HIV-1. Science. 2006; 313(5786):523-6. doi:https://doi.org/10.1126/science.1126531

6. Campbell-Yesufu OT, Gandhi RT. Update on human immunodeficiency virus (HIV)-2 infection. Clinical Infectious Diseases. 2011; 52(6):780-7. doi:https://doi.org/10.1093/cid/ciq248

7. De Cock KM, Adjorlolo G, Ekpini E, Sibailly T, Kouadio J, Maran M, Brattegaard K, Vetter KM, Doorly R, Gayle HD. Epidemiology and transmission of HIV-2: Why there is no HIV-2 pandemic. Journal of the American Medical Association. 1993; 270(17):2083-6. doi:https://doi.org/10.1001/jama.1993.03510170073033

8. de Mendoza C, Cabezas T, Caballero E, Requena S, Amengual MJ, Peñaranda M, Sáez A, Tellez R, Lozano AB, Treviño A. HIV type 2 epidemic in Spain: Challenges and missing opportunities. AIDS. 2017; 31(10):1353-64. doi:https://doi.org/10.1097/qad.0000000000001485

9. Soriano V, Gomes P, Heneine W, Holguín A, Doruana M, Antunes R, Mansinho K, Switzer WM, Araujo C, Shanmugam V. Human immunodeficiency virus type 2 (HIV-2) in Portugal: Clinical spectrum, circulating subtypes, virus isolation, and plasma viral load. Journal of Medical Virology. 2000; 61(1):111-6. doi:https://doi.org/10.1002/(sici)1096-9071(200005)61:1%3C111::aid-jmv18%3E3.0.co;2-w

10. Marlink R, Kanki P, Thior I, Travers K, Eisen G, Siby T, Traore I, Hsieh C-C, Dia MC, Gueye E-H. Reduced rate of disease development after HIV-2 infection as compared to HIV-1. Science. 1994; 265(5178):1587-90. doi:https://doi.org/10.1126/science.7915856

11. MacNeil A, Sarr AD, Sankalé J-L, Meloni ST, Mboup S, Kanki P. Direct evidence of lower viral replication rates in vivo in human immunodeficiency virus type 2 (HIV-2) infection than in HIV-1 infection. Journal of Virology. 2007; 81(10):5325-30. doi:https://doi.org/10.1128/jvi.02625-06

12. Stuver S. Human immunodeficiency viruses and human T-cell lymphotropic viruses: IARC monographs on the evaluation of carcinogenic risks to humans, Vol. 67. Cancer Causes and Control. 1997; 8(6):930. doi:https://www.ncbi.nlm.nih.gov/books/NBK419321/

13. IARC WGotE. Human Immunodeficiency Virus-1. Biological Agents: International Agency for Research on Cancer; 2012.

14. Shan L, Yang H-C, Rabi SA, Bravo HC, Shroff NS, Irizarry RA, Zhang H, Margolick JB, Siliciano JD, Siliciano RF. Influence of host gene transcription level and orientation on HIV-1 latency in a primary-cell model. Journal of Virology. 2011; 85(11):5384-93. doi:https://doi.org/10.1128/jvi.02536-10

15. Desai M, Iyer G, Dikshit R. Antiretroviral drugs: Critical issues and recent advances. Indian Journal of Pharmacology. 2012; 44(3):288. doi:https://doi.org/10.4103/0253-7613.96296

16. Shete A, Paranjape R. Is cure of HIV infection in sight? The Indian Journal of Medical Research. 2013; 138(6):824.

17. Shaw GM, Hunter E. HIV transmission. Cold Spring Harbor Perspectives in Medicine. 2012:a006965.

18. Evans D. Ten years on ART-where to now? SAMJ: South African Medical Journal. 2013; 103(4):229-31.

19. Lederman MM, Connick E, Landay A, Kuritzkes DR, Spritzler J, St. Clair M, Kotzin BL, Fox L, Heath Chiozzi M, Leonard JM. Immunologic responses associated with 12 weeks of combination antiretroviral therapy consisting of zidovudine, lamivudine, and ritonavir: Results of aids clinical trials group protocol Journal of Infectious Diseases. 1998; 178(1):70-9. doi:https://doi.org/10.1086/515591

20. Arts EJ, Hazuda DJ. HIV-1 antiretroviral drug therapy. Cold Spring Harbor Perspectives in Medicine. 2012:a007161.

21. Deeks SG. Treatment of antiretroviral-drug-resistant HIV-1 infection. The Lancet. 2003; 362(9400):2002-11.

22. Carr A, Cooper DA. Adverse effects of antiretroviral therapy. Lancet. 2000; 356(9239):1423-30. doi:https://doi.org/10.1016/s0140-6736(00)02854-3

23. Palmer C. HIV treatments and highly active antiretroviral therapy. Australian Prescriber. 2003; 26(3):59-61. doi:https://doi.org/10.18773/austprescr.2003.042

24. Hladik F, McElrath MJ. Setting the stage: Host invasion by HIV. Nature Reviews Immunology. 2008; 8(6):447-57. doi:https://doi.org/10.1038/nri2302

25. Levy JA. HIV pathogenesis: 25 years of progress and persistent challenges. AIDS. 2009; 23(2):147-60. doi:https://doi.org/10.1097/qad.0b013e3283217f9f

26. Luckheeram RV, Zhou R, Verma AD, Xia B. CD4. Clinical and Developmental Immunology. 2012; 2012

27. Parkin J, Cohen B. An overview of the immune system. The Lancet. 2001; 357(9270):1777-89.

28. Nisole S, Saïb A. Early steps of retrovirus replicative cycle. Retrovirology. 2004; 1(1):9. doi: https://doi.org/10.1186/1742-4690-1-9

29. Fauci AS. The human immunodeficiency virus: Infectivity and mechanisms of pathogenesis. Science. 1988; 239(4840):617-22. doi: doi: 10.1126/science.3277274

30. Levy JA. Pathogenesis of human immunodeficiency virus infection. Microbiological Reviews. 1993; 57(1):183-289. doi:doi.org/10.1111/j.1749-6632.1989.tb16459.x

31. Nie Z, Phenix B, Lum J, Alam A, Lynch D, Beckett B, Krammer P, Sekaly R, Badley A. HIV-1 protease processes procaspase 8 to cause mitochondrial release of cytochrome c, caspase cleavage and nuclear fragmentation. Cell Death and Differentiation. 2002; 9(11):1172-84. doi:doi: 10.1038/sj.cdd.4401094

32. Haas RH, Parikh S, Falk MJ, Saneto RP, Wolf NI, Darin N, Wong L-J, Cohen BH, Naviaux RK. The in-depth evaluation of suspected mitochondrial disease. Molecular Genetics and Metabolism. 2008; 94(1):16-37. doi:https://10.1016/j.ymgme.2007.11.018.

33. Grulich AE, Van Leeuwen MT, Falster MO, Vajdic CM. Incidence of cancers in people with HIV/AIDS compared with immunosuppressed transplant recipients: a meta-analysis. The Lancet. 2007; 370(9581):59-67.

34. Naif HM. Pathogenesis of HIV infection. Infectious Disease Reports. 2013; 5(11):26-30. doi:https://doi.org/10.4081/idr.2013.s1.e6

35. Kirchhoff F. HIV life cycle: Overview. Encyclopedia of AIDS. 2013:1-9. doi:https://doi.org/10.1007/978-1-4939-7101-5_60

36. Fanales-Belasio E, Raimondo M, Suligoi B, Buttò S. HIV virology and pathogenetic mechanisms of infection: A brief overview. Annali Dell'Istituto Superiore di Sanita. 2010; 46:5-14. doi:https://doi.org/10.1590/s0021-25712010000100002

37. Cihlar T, Fordyce M. Current status and prospects of HIV treatment. Current Opinion in Virology. 2016; 18:50-6. doi:https://doi.org/10.1016/j.coviro.2016.03.004

38. FDA UFaDA [Internet]. Antiretroviral drugs used in the treatment of HIV infection. Maryland2018 [cited 2019 22/03/2019].

39. Romashov LV, Ananikov VP. Synthesis of HIV-1 capsid protein assembly inhibitor (CAP-1) and its analogues based on a biomass approach. Organic & Biomolecular Chemistry. 2016; 14(45):10593-8.

40. Schuurman R, Nijhuis M, van Leeuwen R, Schipper P, de Jong D, Collis P, Danner SA, Mulder J, Loveday C, Christopherson C. Rapid changes in human immunodeficiency virus type 1 RNA load and appearance of drug-resistant virus populations in persons treated with lamivudine (3TC). Journal of Infectious Diseases. 1995; 171(6):1411-9. doi:https://doi.org/10.1093/infdis/171.6.1411

41. Romashov LV, Ananikov VP. Synthesis of HIV-1 capsid protein assembly inhibitor (CAP-1) and its analogues based on a biomass approach. Organic and Biomolecular Chemistry. 2016; 14(45):10593-8. doi:https://doi.org/10.1039/c6ob01731b

42. WHO, Geneva: World health organization [Internet]. Consolidated guidline on the use of antiretroviral drugs for treating and preventing HIV infection: Recommendations for public health approach Geneva: World Health Organization (WHO); 2016 [cited 2019 3 Febuary 2019]. Available from: www.who.int/hiv/pub/arv/arv-2016/en.accessed 3 Febuary 2019.

43. Health NDo, Africa S. ART Clinical guidelines for the management of HIV in adults, pregnancy, adolescents, children, infants and neonates. NDoH Pretoria; 2019.

44. Engelman A, Cherepanov P. The structural biology of HIV-1: Mechanistic and therapeutic insights. Nature. 2012; 10(4):279-90. doi:https://doi.org/10.1038/nrmicro2747

45. Reeves JD, Piefer AJ. Emerging drug targets for antiretroviral therapy. Drugs. 2005; 65(13):1747-66. doi:https://doi.org/10.2165/00003495-200565130-00002

46. Perez-Matute P, Perez-Martinez L, Blanco J, Oteo J. Role of mitochondria in HIV infection and associated metabolic disorders: Focus on nonalcoholic fatty liver disease and lipodystrophy syndrome. Oxidative Medicine and Cellular Longevity. 2013; 2013 doi:https://doi.org/10.1155/2013/493413

47. Miller V. Resistance to protease inhibitors. Journal of Acquired Immune Deficiency Syndromes 2001; 26:S34-50. doi:https://doi.org/10.1097/00042560-200103011-00005

48. Tadesse WT, Mekonnen AB, Tesfaye WH, Tadesse YT. Self-reported adverse drug reactions and their influence on highly active antiretroviral therapy in HIV infected patients: A cross sectional study. BioMed Central Pharmacology and Toxicology. 2014; 15(1):1-9. doi:https://doi.org/10.1186/2050-6511-15-32

49. Back DJ, Burger DM, Flexner CW, Gerber JG. The pharmacology of antiretroviral nucleoside and nucleotide reverse transcriptase inhibitors: Implications for once-daily dosing. Journal of Acquired Immune Deficiency Syndromes. 2005; 39:S1-S23. doi:https://doi.org/10.1097/01.qai.0000168882.67942.3f

50. Lewis W, Dalakas MC. Mitochondrial toxicity of antiviral drugs. Nature Medicine. 1995; 1(5):417-22. doi:https://doi.org/10.1038/nm0595-417

51. Lewis W, Day BJ, Copeland WC. Mitochondrial toxicity of NRTI antiviral drugs: An integrated cellular perspective. Nature 2003; 2(10):812-22. doi:https://doi.org/10.1038/nrd1201

52. Kakuda TN. Pharmacology of nucleoside and nucleotide reverse transcriptase inhibitor-induced mitochondrial toxicity. Clinical Therapeutics. 2000; 22(6):685-708. doi:https://doi.org/10.1016/s0149-2918(00)90004-3

53. Chinnery PF, Turnbull DM. Clinical features, investigation, and management of patients with defects of mitochondrial DNA. Journal of Neurology, Neurosurgery and Psychiatry. 1997; 63(5):559-63. doi:https://doi.org/10.1136/jnnp.63.5.559

54. Shoffner JM. Maternal inheritance and the evaluation of oxidative phosphorylation diseases. Lancet. 1996; 348(9037):1283-8. doi:https://doi.org/10.1016/s0140-6736(96)09138-6

55. Weber K, Wilson J, Taylor L, Brierley E, Johnson M, Turnbull D, Bindoff L. A new mtDNA mutation showing accumulation with time and restriction to skeletal muscle. American Journal of Human Genetics. 1997; 60(2):373.

56. Broder S. The development of antiretroviral therapy and its impact on the HIV-1/AIDS pandemic. Antiviral Research. 2010; 85(1):1-18. doi:https://doi.org/10.1016/j.antiviral.2009.10.002

57. Lee WA, Martin JC. Perspectives on the development of acyclic nucleotide analogs as antiviral drugs. Antiviral Research. 2006; 71(2-3):254-9. doi:https://doi.org/10.1016/j.antiviral.2006.05.020

58. Pau AK, George JM. Antiretroviral therapy: Current drugs. Infectious Disease Clinics. 2014; 28(3):371-402.

59. Hall AM, Hendry BM, Nitsch D, Connolly JO. Tenofovir-associated kidney toxicity in HIV-infected patients: A review of the evidence. American Journal of Kidney Diseases. 2011; 57(5):773-80. doi:https://doi.org/10.1053/j.ajkd.2011.01.022

60. Huang JS, Hughes MD, Riddler SA, Haubrich RH, Team ACTGAS. Bone mineral density effects of randomized regimen and nucleoside reverse transcriptase inhibitor selection from ACTG A5142. HIV Clinical Trials. 2013; 14(5):224-34. doi:https://doi.org/10.1310/hct1405-224

61. Cihlar T, Birkus G, Greenwalt DE, Hitchcock MJ. Tenofovir exhibits low cytotoxicity in various human cell types: Comparison with other nucleoside reverse transcriptase inhibitors. Antiviral Research. 2002; 54(1):37-45. doi:https://doi.org/10.1016/s0166-3542(01)00210-8

62. Apostolova N, Blas-García A, Esplugues JV. Mitochondrial interference by anti-HIV drugs: Mechanisms beyond Pol-γ inhibition. Trends in Pharmacological Sciences. 2011; 32(12):715-25. doi:https://doi.org/10.1016/j.tips.2011.07.007

63. de la Concepcion MR, Yubero P, Domingo JC, Iglesias R, Domingo P, Villarroya F, Giralt M. Reverse transcriptase inhibitors alter uncoupling protein-1 and mitochondrial biogenesis in brown adipocytes. Antiviral Therapy. 2005; 10(4):515-26. doi:https://doi.org/10.1097/00002030-200404090-00018

64. Falkenberg M, Larsson N-G, Gustafsson CM. DNA replication and transcription in mammalian mitochondria. Annual Review of Biochemistry. 2007; 76:679-99. doi:https://doi.org/10.1146/annurev.biochem.76.060305.152028

65. Mitchell P. 1961 nature publishing group. Nature. 1961; 191:144-8.

66. White AJ. Mitochondrial toxicity and HIV therapy. Sexually Transmitted Infections. 2001; 77(3):158-73. doi:https://doi.org/10.1136/sti.77.3.158

67. Hahn A, Zuryn S. Mitochondrial genome (mtDNA) mutations that generate reactive oxygen species. Antioxidants. 2019; 8(9):392. doi:https://doi.org/10.3390/antiox8090392

68. Ho PW, Ho JW, Liu H-F, So DH, Zero H, Chan K-H, Ramsden DB, Ho S-L. Mitochondrial neuronal uncoupling proteins: A target for potential disease-modification in Parkinson's disease. Translational Neurodegeneration. 2012; 1(1):1-9. doi:https://doi.org/10.1186/2047-9158-1-3

69. Balaban RS, Nemoto S, Finkel T. Mitochondria, oxidants, and aging. Cell. 2005; 120(4):483-95. doi:https://doi.org/10.1016/j.cell.2005.02.001

70. Turrens JF. Mitochondrial formation of reactive oxygen species. The Journal of Physiology. 2003; 552(2):335-44. doi:https://doi.org/10.1113/jphysiol.2003.049478

71. Ighodaro O, Akinloye O. First line defence antioxidants-superoxide dismutase (SOD), catalase (CAT) and glutathione peroxidase (GPX): Their fundamental role in the entire antioxidant defence grid. Alexandria Journal of Medicine. 2018; 54(4):287-93. doi:https://doi.org/10.1016/j.ajme.2017.09.001

72. Halliwell B, Cross CE, Borish ET, Pryor WA, Ames BN, Saul RL, Mccord JM, Harman D. Oxygen radicals and human disease. Annals of Internal Medicine. 1987; 107(4):526-45. doi:https://doi.org/10.1016/0076-6879(90)86093-b

73. Lam GY, Huang J, Brumell JH, editors. The many roles of NOX2 NADPH oxidase-derived ROS in immunity. Seminars in Immunopathology; 2010: Springer.

74. Snezhkina AV, Kudryavtseva AV, Kardymon OL, Savvateeva MV, Melnikova NV, Krasnov GS, Dmitriev AA. ROS Generation and Antioxidant Defense Systems in Normal and Malignant Cells. Oxidative medicine and cellular longevity. 2019; 2019

75. Saccani A, Saccani S, Orlando S, Sironi M, Bernasconi S, Ghezzi P, Mantovani A, Sica A. Redox regulation of chemokine receptor expression. Proceedings of the National Academy of Sciences. 2000; 97(6):2761-6. doi:https://doi.org/10.1073/pnas.97.6.2761

76. Okechukwu IB. Oxidative stress, redox regulation and elite controllers of HIV infection: Towards a functional cure. Trends in Basic and Therapeutic Options in HIV Infection–Towards a Functional Cure. 2015; doi:https://doi.org/10.5772/60806

77. Sena LA, Chandel NS. Physiological roles of mitochondrial reactive oxygen species. Molecular Cell. 2012; 48(2):158-67. doi:https://doi.org/10.1016/j.molcel.2012.09.025

78. Wei Y-H, Lu C-Y, Wei C-Y, Ma Y-S, Lee H-C. Oxidative stress in human aging and mitochondrial disease-consequences of defective mitochondrial respiration and impaired antioxidant enzyme system. Chinese Journal of Physiology. 2001; 44(1):1-12.

79. Girotti AW. Mechanisms of lipid peroxidation. Journal of free radicals in biology & medicine. 1985; 1(2):87-95.

80. Dröge W. Free radicals in the physiological control of cell function. Physiological Reviews. 2002; 82(1):47-95. doi:https://doi.org/10.1152/physrev.00018.2001

81. Moussa Z, Judeh ZM, Ahmed SA. Nonenzymatic Exogenous and Endogenous Antioxidants. In: Das K, Das S, Biradar MS, Bobbaralla V, Tata SS, editors. Free Radical Medicine and Biology. Rijeka: IntechOpen; 2020.

82. Halliwell B, Gutteridge JM. [1] Role of free radicals and catalytic metal ions in human disease: an overview. Methods in enzymology: Elsevier; 1990. p. 1-85.

83. Bunker V. Free radicals, antioxidants and ageing. Medical Laboratory Sciences. 1992; 49(4):299-312.

84. Birben E, Sahiner UM, Sackesen C, Erzurum S, Kalayci O. Oxidative stress and antioxidant defense. World Allergy Organization Journal. 2012; 5(1):9-19. doi:https://doi.org/10.1097/wox.0b013e3182439613

85. Habib LK, Lee MT, Yang J. Inhibitors of catalase-amyloid interactions protect cells from β-amyloid-induced oxidative stress and toxicity. Journal of Biological Chemistry. 2010; 285(50):38933-43. doi:https://doi.org/10.1074/jbc.m110.132860

86. Masella R, Di Benedetto R, Varì R, Filesi C, Giovannini C. Novel mechanisms of natural antioxidant compounds in biological systems: Involvement of glutathione and glutathione-related enzymes. The Journal of Nutritional Biochemistry. 2005; 16(10):577-86. doi:https://doi.org/10.1016/j.jnutbio.2005.05.013

87. Yasukawa T, Kang D. An overview of mammalian mitochondrial DNA replication mechanisms. The Journal of Biochemistry. 2018; 164(3):183-93. doi:https://doi.org/10.1093/jb/mvy058

88. Anderson S, Bankier AT, Barrell BG, de Bruijn MH, Coulson AR, Drouin J, Eperon IC, Nierlich DP, Roe BA, Sanger F. Sequence and organization of the human mitochondrial genome. Nature. 1981; 290(5806):457-65. doi:https://doi.org/10.1038/290457a0

89. García-Lepe UO, Bermúdez-Cruz RM. Mitochondrial genome maintenance: Damage and repair pathways. In: Mognato M, editor. DNA Repair. Rijeka: IntechOpen; 2019.

90. Quan Y, Xin Y, Tian G, Zhou J, Liu X. Mitochondrial ROS-Modulated mtDNA: A Potential Target for Cardiac Aging. Oxidative Medicine and Cellular Longevity. 2020; 2020

91. Ivanov AV, Valuev-Elliston VT, Ivanova ON, Kochetkov SN, Starodubova ES, Bartosch B, Isaguliants MG. Oxidative stress during HIV infection: Mechanisms and consequences. Oxidative Medicine and Cellular Longevity. 2016; doi:https://doi.org/10.1155/2016/8910396

92. Holt IJ, Reyes A. Human mitochondrial DNA replication. Cold Spring Harbor Perspectives in Biology. 2012; 4(12):a012971. doi:https://doi.org/10.1016/j.tibs.2009.03.007

93. Graziewicz MA, Day BJ, Copeland WC. The mitochondrial DNA polymerase as a target of oxidative damage. Nucleic Acids Research. 2002; 30(13):2817-24. doi:https://doi.org/10.1093/nar/gkf392

94. Wisnovsky S, Jean SR, Liyanage S, Schimmer A, Kelley SO. Mitochondrial DNA repair and replication proteins revealed by targeted chemical probes. Nature Chemical Biology. 2016; 12(7):567-73. doi:https://doi.org/10.1038/s41589-018-0040-5

95. Gray H, Wong TW. Purification and identification of subunit structure of the human mitochondrial DNA polymerase. Journal of Biological Chemistry. 1992; 267(9):5835-41. doi:https://doi.org/10.1016/s0021-9258(18)42629-4

96. Longley MJ, Ropp PA, Lim SE, Copeland WC. Characterization of the native and recombinant catalytic subunit of human DNA polymerase γ: Identification of residues critical for exonuclease activity and dideoxynucleotide sensitivity. Biochemistry. 1998; 37(29):10529-39. doi:https://doi.org/10.1021/bi980772w

97. Wernette CM, Kaguni LS. A mitochondrial DNA polymerase from embryos of drosophila melanogaster, purification, subunit structure, and partial characterization. Journal of Biological Chemistry. 1986; 261(31):14764-70. doi:https://doi.org/10.1016/s0021-9258(18)66938-8

98. Copeland WC, Longley MJ. DNA polymerase gamma in mitochondrial DNA replication and repair. The Scientific World Journal. 2003; 3:34-44. doi:https://doi.org/10.1100/tsw.2003.09

99. Okoye AA, Picker LJ. CD 4+ T-cell depletion in HIV infection: Mechanisms of immunological failure. Immunological Reviews. 2013; 254(1):54-64. doi:https://doi.org/10.1111/imr.12066

100. Dröge W, Eck H-P, Mihm S. Oxidant-antioxidant status in human immunodeficiency virus infection. Methods in Enzymology: Elsevier; 1994. p. 594-601.

101. Martin JA, Sastre J, de la Asunción JG, Pallardó FV, Viña J. Hepatic γ-cystathionase deficiency in patients with AIDS. Jama. 2001; 285(11):1444-5.

102. Elbim C, Pillet S, Prevost M, Preira A, Girard P, Rogine N, Matusani H, Hakim J, Israel N, Gougerot-Pocidalo M. Redox and activation status of monocytes from human immunodeficiency virus-infected patients: Relationship with viral load. Journal Of Virology. 1999; 73(6):4561-6. doi:https://doi.org/10.1128/jvi.73.6.4561-4566.1999

103. Salmen S, Montes H, Soyano A, Hernández D, Berrueta L. Mechanisms of neutrophil death in human immunodeficiency virus-infected patients: role of reactive oxygen species, caspases and map kinase pathways. Clinical & Experimental Immunology. 2007; 150(3):539-45.

104. Parikh S, Goldstein A, Koenig MK, Scaglia F, Enns GM, Saneto R, Anselm I, Cohen BH, Falk MJ, Greene C. Diagnosis and management of mitochondrial disease: A consensus statement from the Mitochondrial Medicine Society. Genetics in Medicine. 2015; 17(9):689-701. doi:https://doi.org/10.1038/gim.2014.177

105. Casula M, Weverling GJ, Wit FW, Timmermans EC, Stek Jr M, Lange JM, Reiss P. Mitochondrial DNA and RNA increase in peripheral blood mononuclear cells from HIV-1–infected patients randomized to receive stavudine-containing or stavudine-sparing combination therapy. The Journal of Infectious Diseases. 2005; 192(10):1794-800. doi:https://doi.org/10.1086/497140

106. Halestrap AP, Brenner C. The adenine nucleotide translocase: A central component of the mitochondrial permeability transition pore and key player in cell death. Current Medicinal Chemistry. 2003; 10(16):1507-25. doi:https://doi.org/10.2174/0929867033457278

107. Gazdag Z, Stromájer-Rácz T, Belagyi J, Zhao RY, Elder RT, Virág E, Pesti M. Regulation of unbalanced redox homeostasis induced by the expression of wild-type HIV-1 viral protein R (NL4-3Vpr) in fission yeast. Acta Biologica Hungarica. 2015; 66(3):326-38. doi:https://doi.org/10.1556/018.66.2015.3.8

108. Kruman II, Nath A, Mattson MP. HIV-1 protein Tat induces apoptosis of hippocampal neurons by a mechanism involving caspase activation, calcium overload, and oxidative stress. Experimental Neurology. 1998; 154(2):276-88. doi:https://doi.org/10.1006/exnr.1998.6958

109. Perry SW, Norman JP, Litzburg A, Zhang D, Dewhurst S, Gelbard HA. HIV-1 transactivator of transcription protein induces mitochondrial hyperpolarization and synaptic stress leading to apoptosis. The Journal of Immunology. 2005; 174(7):4333-44. doi:https://doi.org/10.4049/jimmunol.174.7.4333

110. Miura T, Goto M, Hosoya N, Odawara T, Kitamura Y, Nakamura T, Iwamoto A. Depletion of mitochondrial DNA in HIV-1-infected patients and its amelioration by antiretroviral therapy. Journal of Medical Virology. 2003; 70(4):497-505. doi:https://doi.org/10.1002/jmv.10423

111. Morse CG, Voss JG, Rakocevic G, McLaughlin M, Vinton CL, Huber C, Hu X, Yang J, Huang DW, Logun C. HIV infection and antiretroviral therapy have divergent effects on mitochondria in adipose tissue. Journal of Infectious Diseases. 2012; 205(12):1778-87. doi:https://doi.org/10.1093/infdis/jis101

112. Banki K, Hutter E, Gonchoroff NJ, Perl A. Molecular ordering in HIV-induced apoptosis oxidative stress, activation of caspases, and cell survival are regulated by transaldolase. Journal of Biological Chemistry. 1998; 273(19):11944-53. doi:https://10.1074/jbc.273.19.11944.

113. Mattman A, Sirrs S, Mezei MM, Salvarinova-Zivkovic R, Alfadhel M, Lillquist Y. Mitochondrial disease clinical manifestations: An overview. British Columbia Medical Journal. 2011; 53(4):183-7.

114. Yu F, Hao Y, Zhao H, Xiao J, Han N, Zhang Y, Dai G, Chong X, Zeng H, Zhang F. Distinct mitochondrial disturbance in CD4+ T and CD8+ T cells from HIV-infected patients. Journal of Acquired Immune Deficiency Syndromes. 2017; 74(2):206-12. doi:https://doi.org/10.1097/qai.0000000000001175

115. Schank M, Zhao J, Moorman JP, Yao ZQ. The impact of HIV-and ART-induced mitochondrial dysfunction in cellular senescence and aging. Cells. 2021; 10(1):174. doi:https://doi.org/10.3390/cells10010174

116. Kohler JJ, Lewis W. A brief overview of mechanisms of mitochondrial toxicity from NRTIs. Environmental and Molecular Mutagenesis. 2007; 48(3-4):166-72. doi:https://doi.org/10.1002/em.20223

117. Payne BA, Wilson IJ, Hateley CA, Horvath R, Santibanez-Koref M, Samuels DC, Price DA, Chinnery PF. Mitochondrial aging is accelerated by anti-retroviral therapy through the clonal expansion of mtDNA mutations. Nature Genetics. 2011; 43(8):806-10. doi:https://doi.org/10.1038/ng.863

118. Wallace D. Mitochondria and cancer. Nature Reviews Cancer. 2012; 12(10):685-98. doi:https://doi.org/10.1038/nrc3365

119. Barouch DH. Challenges in the development of an HIV-1 vaccine. Nature. 2008; 455(7213):613-19. doi:https://doi.org/10.3389/fgene.2020.00497

120. Dalakas MC, Illa I, Pezeshkpour G, Laukaitis JP, Cohen B, Griffin JL. Mitochondrial myopathy caused by long-term zidovudine therapy. New England Journal of Medicine. 1990; 322(16):1098-105. doi:https://doi.org/10.1056/nejm199004193221602

121. Brinkman K, Smeitink JA, Romijn JA, Reiss P. Mitochondrial toxicity induced by nucleoside-analogue reverse transcriptase inhibitors is a key factor in the pathogenesis of antiretroviral therapy-related lipodystrophy. Lancet. 1999; 354(9184):1112-5. doi:https://doi.org/10.1016/s0140-6736(99)06102-4

122. Côté HCF, Brumme ZL, Craib KJP, Alexander CS, Wynhoven B, TIng L, Wong H, Harris M, Harrigan R, O'Shaughnessy MV, Montaner JSG. Changes in mitochondrial DNA as a marker of nucleoside toxicity in HIV-infected patients New England Journal of Medicine. 2002; 346(11):811-20. doi:https://doi.org/10.1056/nejmoa012035

123. Mallon PW, Unemori P, Sedwell R, Morey A, Rafferty M, William K, Chisholm D, Samaras K, Emery S, Kelleher A. In vivo, nucleoside reverse-transcriptase inhibitors alter expression of both mitochondrial and lipid metabolism genes in the absence of depletion of mitochondrial DNA. Journal of Infectious Diseases. 2005; 191(10):1686-96. doi:https://doi.org/10.1086/429697

124. Szewczyk A, Wojtczak L. Mitochondria as a pharmacological target. Pharmacological Reviews. 2002; 54(1):101-27. doi:https://doi.org/10.1124/pr.54.1.101

125. Moyle G. Mechanisms of HIV and nucleoside reverse transcriptase inhibitor injury to mitochondria. Antiviral Therapy. 2005; 10:M47-52.

126. Pinti M, Salomoni P, Cossarizza A. Anti-HIV drugs and the mitochondria. Biochimica et Biophysica Acta (BBA)-Bioenergetics. 2006; 1757(5-6):700-7. doi:https://doi.org/10.1016/j.bbabio.2006.05.001

127. Chandra S, Mondal D, Agrawal KC. HIV-1 protease inhibitor induced oxidative stress suppresses glucose stimulated insulin release: protection with thymoquinone. Experimental Biology and Medicine. 2009; 234(4):442-53. doi:https://doi.org/10.3181/0811-rm-317

128. Mukhopadhyay A, Wei B, Zullo SJ, Wood LV, Weiner H. In vitro evidence of inhibition of mitochondrial protease processing by HIV-1 protease inhibitors in yeast: A possible contribution to lipodystrophy syndrome. Mitochondrion. 2002; 1(6):511-8. doi:https://doi.org/10.1016/s1567-7249(02)00042-9

129. Pilon A, Lum J, Sanchez-Dardon J, Phenix B, Douglas R, Badley AD. Induction of apoptosis by a nonnucleoside human immunodeficiency virus type 1 reverse transcriptase inhibitor. Antimicrobial Agents and Chemotherapy. 2002; 46(8):2687-91. doi:https://doi.org/10.1128/aac.46.8.2687-2691.2002

130. Apostolova N, Gomez-Sucerquia LJ, Moran A, Alvarez A, Blas-Garcia A, Esplugues J. Enhanced oxidative stress and increased mitochondrial mass during efavirenz-induced apoptosis in human hepatic cells. British Journal of Pharmacology. 2010; 160(8):2069-84. doi:https://doi.org/10.1111/j.1476-5381.2010.00866.x

131. Jamaluddin MS, Lin PH, Yao Q, Chen C. Non-nucleoside reverse transcriptase inhibitor efavirenz increases monolayer permeability of human coronary artery endothelial cells. Atherosclerosis. 2010; 208(1):104-11.

132. Crane HM, Grunfeld C, Willig JH, Mugavero MJ, Van Rompaey S, Moore R, Rodriguez B, Feldman BJ, Lederman MM, Saag MS. Impact of NRTIs on lipid levels among a large HIV-infected cohort initiating antiretroviral therapy in clinical care. AIDS. 2011; 25(2):185-95. doi:https://doi.org/10.1097/qad.0b013e328341f925

133. Constantinides VC, Papahatzaki MM, Papadimas GK, Karandreas N, Zambelis T, Kokotis P, Manda P. Diagnostic accuracy of muscle biopsy and electromyography in 123 patients with neuromuscular disorders. In Vivo. 2018; 32(6):1647-52. doi:https://doi.org/10.21873/invivo.11427

134. Lehtonen J. New tools for mitochondrial disease diagnosis: FGF21, GDF15 and next-generation sequencing [Doctrate]. Helsinki: University of Helsinki; 2017.

135. Parkin J, Cohen B. An overview of the immune system. Lancet. 2001; 357(9270):1777-89. doi:https://doi.org/10.1016/s0140-6736(00)04904-7

136. Koenig MK. Presentation and diagnosis of mitochondrial disorders in children. Pediatric Neurology. 2008; 38(5):305-13. doi:https://doi.org/10.1016/j.pediatrneurol.2007.12.001

137. Debray F-G, Mitchell GA, Allard P, Robinson BH, Hanley JA, Lambert M. Diagnostic accuracy of blood lactate-to-pyruvate molar ratio in the differential diagnosis of congenital lactic acidosis. Clinical Chemistry. 2007; 53(5):916-21. doi:https://doi.org/10.1373/clinchem.2006.081166

138. Suomalainen A, Elo JM, Pietiläinen KH, Hakonen AH, Sevastianova K, Korpela M, Isohanni P, Marjavaara SK, Tyni T, Kiuru-Enari S. FGF-21 as a biomarker for muscle-manifesting mitochondrial respiratory chain deficiencies: A diagnostic study. Lancet Neurology. 2011; 10(9):806-18. doi:https://doi.org/10.1016/s1474-4422(11)70155-7

139. Zschocke J, Hoffmann F. Vademecum metabolicum. Padiatrische Praxis. 2000; 58(4):730-. doi:https://doi.org/10.1023/a:1005684802792

140. Barshop BA. Metabolomic approaches to mitochondrial disease: Correlation of urine organic acids. Mitochondrion. 2004; 4(5-6):521-7. doi:https://doi.org/10.1016/j.mito.2004.07.010

141. Munnich A, Rötig A, Chretien D, Cormier V, Bourgeron T, Bonnefont JP, Saudubray JM, Rustin P. Clinical presentation of mitochondrial disorders in childhood. Journal of Inherited Metabolic Disease. 1996; 19(4):521-7. doi:https://doi.org/10.1201/9780429443336-21

142. Dimmock DP, Lawlor MW. Presentation and diagnostic evaluation of mitochondrial disease. Pediatric Clinics. 2017; 64(1):161-71. doi:https://doi.org/10.1016/j.pcl.2016.08.011

143. Alston CL, Rocha MC, Lax NZ, Turnbull DM, Taylor RW. The genetics and pathology of mitochondrial disease. The Journal of Pathology. 2017; 241(2):236-50. doi:https://doi.org/10.1002/path.4809

144. Ahmed ST, Craven L, Russell OM, Turnbull DM, Vincent AE. Diagnosis and treatment of mitochondrial myopathies. Neurotherapeutics. 2018; 15(4):943-53. doi:https://doi.org/10.1007/s13311-018-00674-4

145. Moraes CT, Ricci E, Bonilla E, DiMauro S, Schon EA. The mitochondrial tRNA (Leu [UUR]) mutation in mitochondrial encephalomyopathy, lactic acidosis, and strokelike episodes (MELAS): Genetic, biochemical, and morphological correlations in skeletal muscle. American Journal of Human Genetics. 1992; 50(5):934.

146. Rifai Z, Welle S, Kamp C, Thornton CA. Ragged red fibers in normal aging and inflammatory myopathy. Annals of Neurology: Official Journal of the American Neurological Association and the Child Neurology Society. 1995; 37(1):24-9. doi:https://doi.org/10.1002/ana.410370107

147. Pfeffer G, Chinnery PF. Diagnosis and treatment of mitochondrial myopathies. Annals of Medicine. 2013; 45(1):4-16. doi:https://doi.org/10.3109/07853890.2011.605389

148. Shanske S, Wong L-JC. Molecular analysis for mitochondrial DNA disorders. Mitochondrion. 2004; 4(5-6):403-15. doi:https://doi.org/10.1016/j.mito.2004.07.026

149. Cossarizza A. Tests for mitochondrial function and DNA: Potentials and pitfalls. Current Opinion in Infectious Diseases. 2003; 16(1):5-10. doi:https://doi.org/10.1097/00001432-200302000-00002

150. Edwards JG. Quantification of mitochondrial DNA (mtDNA) damage and error rates by real-time QPCR. Mitochondrion. 2009; 9(1):31-5. doi:https://doi.org/10.1016/j.mito.2008.11.004

151. Malik AN, Czajka A. Is mitochondrial DNA content a potential biomarker of mitochondrial dysfunction? Mitochondrion. 2013; 13(5):481-92. doi:https://doi.org/10.1016/j.mito.2012.10.011

152. Hosgood III HD, Liu C-S, Rothman N, Weinstein SJ, Bonner MR, Shen M, Lim U, Virtamo J, Cheng W-l, Albanes D. Mitochondrial DNA copy number and lung cancer risk in a prospective cohort study. Carcinogenesis. 2010; 31(5):847-9. doi:https://doi.org/10.1093/carcin/bgq045

153. Mengel-From J, Thinggaard M, Dalgård C, Kyvik KO, Christensen K, Christiansen L. Mitochondrial DNA copy number in peripheral blood cells declines with age and is associated with general health among elderly. Human Genetics. 2014; 133(9):1149-59. doi:https://doi.org/10.1007/s00439-014-1458-9

154. Kilbaugh TJ, Lvova M, Karlsson M, Zhang Z, Leipzig J, Wallace DC, Margulies SS. Peripheral blood mitochondrial DNA as a biomarker of cerebral mitochondrial dysfunction following traumatic brain injury in a porcine model. PLOS One. 2015; 10(6):e0130927. doi:https://doi.org/10.1371/journal.pone.0130927

155. Andreu AL, Martinez R, Marti R, García-Arumí E. Quantification of mitochondrial DNA copy number: Pre-analytical factors. Mitochondrion. 2009; 9(4):242-6. doi:https://doi.org/10.1016/j.mito.2009.02.006

156. Long YC, Kharitonenkov A. Hormone-like fibroblast growth factors and metabolic regulation. Biochimica et Biophysica Acta (BBA)-Molecular Basis of Disease. 2011; 1812(7):791-5.

157. Long YC, Kharitonenkov A. Hormone-like fibroblast growth factors and metabolic regulation. Biochimica et Biophysica Acta-Molecular Basis of Disease. 2011; 1812(7):791-5. doi:https://doi.org/10.1016/j.bbadis.2011.04.002

158. Kharitonenkov A, Shiyanova TL, Koester A, Ford AM, Micanovic R, Galbreath EJ, Sandusky GE, Hammond LJ, Moyers JS, Owens RA. FGF-21 as a novel metabolic regulator. The Journal of Clinical Investigation. 2005; 115(6):1627-35. doi:https://doi.org/10.1002/9780470910016.ch14

159. Eckard AR, Hughes HY, Hagood NL, O'Riordan MA, Labbato D, Kosco JC, Scott SE, McComsey GA. Fibroblast growth factor 21 is elevated in HIV and associated with interleukin-6. Journal of Acquired Immune Deficiency Syndromes. 2020; 83(5):e30-e3. doi:https://doi.org/10.1097/qai.0000000000002285

160. Nishimura T, Nakatake Y, Konishi M, Itoh N. Identification of a novel FGF, FGF-21, preferentially expressed in the liver. Biochimica et Biophysica Acta-Gene Structure and Expression. 2000; 1492(1):203-6. doi:https://doi.org/10.1016/s0167-4781(00)00067-1

161. Fisher FM, Maratos-Flier E. Understanding the physiology of FGF-21. Annual Review of Physiology. 2016; 78:223-41. doi:https://doi.org/10.1146/annurev-physiol-021115-105339

162. Tyynismaa H, Carroll CJ, Raimundo N, Ahola-Erkkilä S, Wenz T, Ruhanen H, Guse K, Hemminki A, Peltola-Mjøsund KE, Tulkki V. Mitochondrial myopathy induces a starvation-like response. Human Molecular Genetics. 2010; 19(20):3948-58. doi:https://doi.org/10.1093/hmg/ddq310

163. Arner P, Pettersson A, Mitchell PJ, Dunbar JD, Kharitonenkov A, Rydén M. FGF-21 attenuates lipolysis in human adipocytes: A possible link to improved insulin sensitivity. Federation of European Biochemical Societies letters. 2008; 582(12):1725-30. doi:https://doi.org/10.1016/j.febslet.2008.04.038

164. Nies VJ, Sancar G, Liu W, van Zutphen T, Struik D, Yu RT, Atkins AR, Evans RM, Jonker JW, Downes MR. Fibroblast growth factor signaling in metabolic regulation. Frontiers in Endocrinology. 2016; 6:193. doi:https://doi.org/10.3389/fendo.2015.00193

165. Davis RL, Liang C, Edema-Hildebrand F, Riley C, Needham M, SueCarolyn M. Fibroblast growth factor 21 is a sensitive biomarker of mitochondrial disease. Neurology. 2013; 81(21):1819-26. doi:https://doi.org/10.1212/01.wnl.0000436068.43384.ef

166. Lawton LN, de Fatima Bonaldo M, Jelenc PC, Qiu L, Baumes SA, Marcelino RA, de Jesus GM, Wellington S, Knowles JA, Warburton D. Identification of a novel member of the TGF-beta superfamily highly expressed in human placenta. Gene. 1997; 203(1):17-26. doi:https://doi.org/10.1016/s0378-1119(97)00485-x

167. Li P-X, Wong J, Ayed A, Ngo D, Brade AM, Arrowsmith C, Austin RC, Klamut HJ. Placental transforming growth factor-β is a downstream mediator of the growth arrest and apoptotic response of tumor cells to DNA damage and p53 overexpression. Journal of Biological Chemistry. 2000; 275(26):20127-35. doi:https://doi.org/10.1074/jbc.m909580199

168. Kalko SG, Paco S, Jou C, Rodríguez MA, Meznaric M, Rogac M, Jekovec-Vrhovsek M, Sciacco M, Moggio M, Fagiolari G. Transcriptomic profiling of TK2 deficient human skeletal muscle suggests a role for the p53 signalling pathway and identifies growth and differentiation factor-15 as a potential novel biomarker for mitochondrial myopathies. BioMed Central Genomics. 2014; 15(1):1-22. doi:https://doi.org/10.1186/1471-2164-15-91

169. Adela R, Banerjee SK. GDF-15 as a target and biomarker for diabetes and cardiovascular diseases: A translational prospective. Journal of Diabetes Research. 2015; doi:https://doi.org/10.1155/2015/490842

170. Tsai V, Lin S, Brown D, Salis A, Breit S. Anorexia–cachexia and obesity treatment may be two sides of the same coin: Role of the TGF-b superfamily cytokine MIC-1/GDF15. International Journal of Obesity. 2016; 40(2):193-7. doi:https://doi.org/10.1038/ijo.2015.242

171. Hagström E, Held C, Stewart RA, Aylward PE, Budaj A, Cannon CP, Koenig W, Krug-Gourley S, Mohler ER, Steg PG. Growth differentiation factor 15 predicts all-cause morbidity and mortality in stable coronary heart disease. Clinical Chemistry. 2017; 63(1):325-33. doi:https://doi.org/10.1373/clinchem.2016.260570

172. Lane RK, Hilsabeck T, Rea SL. The role of mitochondrial dysfunction in age-related diseases. Biochimica et Biophysica Acta-Bioenergetics. 2015; 1847(11):1387-400. doi:https://doi.org/10.1016/j.bbabio.2015.05.021

173. Yatsuga S, Fujita Y, Ishii A, Fukumoto Y, Arahata H, Kakuma T, Kojima T, Ito M, Tanaka M, Saiki R. Growth differentiation factor 15 as a useful biomarker for mitochondrial disorders. Annals of Neurology. 2015; 78(5):814-23. doi:https://doi.org/10.1002/ana.24506

174. Zimmers TA, Jin X, Hsiao EC, McGrath SA, Esquela AF, Koniaris LG. Growth differentiation factor-15/macrophage inhibitory cytokine-1 induction after kidney and lung injury. Shock. 2005; 23(6):543-8. doi:https://doi.org/10.1016/j.cytogfr.2013.05.003

175. Montero R, Yubero D, Villarroya J, Henares D, Jou C, Rodríguez MA, Ramos F, Nascimento A, Ortez CI, Campistol J. GDF-15 is elevated in children with mitochondrial diseases and is induced by mitochondrial dysfunction. PLOS One. 2016; 11(2):e0148709. doi:https://doi.org/10.1371/journal.pone.0155172

176. Gahan ME, Miller F, Sharon RL, Cherry CL, Jennifer F. Hoy a, Anne Mijch a, Rosenfeldt F, Wesselingh SL. Quantification of mitochondrial DNA in peripheral blood mononuclear cells and subcutaneous fat using real-time polymerase chain reaction. Journal of Clinical Virology. 2001; 3(22):241–7. doi:https://doi.org/10.1016/s1386-6532(01)00195-0

177. Brinkman K, ter Hofstede HJ, Burger DM, Smeitink JA, Koopmans PP. Adverse effects of reverse transcriptase inhibitors: Mitochondrial toxicity as common pathway. AIDS. 1998; 12(14):1735-44. doi:https://doi.org/10.1097/00002030-199814000-00004

178. Davis RL, Liang C, Edema-Hildebrand F, Riley C, Needham M, SueCarolyn M. Fibroblast growth factor 21 is a sensitive biomarker of mitochondrial disease. Neurology. 2013; 81:1819-26.

179. Montaner JS, Côté HC, Harris M, Hogg RS, Yip B, Chan JW, Harrigan PR, O'Shaughnessy MV. Mitochondrial toxicity in the era of HAART: Evaluating venous lactate and peripheral blood mitochondrial DNA in HIV-infected patients taking antiretroviral therapy. Journal of Acquired Immune Deficiency Syndromes. 2003; 34:S85-S90. doi:https://doi.org/10.1097/00126334-200309011-00013

180. Côté HC, Raboud J, Bitnun A, Alimenti A, Money DM, Maan E, Costei A, Gadawski I, Diong C, Read S. Perinatal exposure to antiretroviral therapy is associated with increased blood mitochondrial DNA levels and decreased mitochondrial gene expression in infants. The Journal of Infectious Diseases. 2008; 198(6):851-9. doi:https://doi.org/10.1086/591253

181. Swinehart DF. The Beer-Lambert law. Journal of chemical education. 1962; 39(7):333. doi:https://doi.org/10.1021/ed039p333

182. Al-Kafaji G, Aljadaan A, Kamal A, Bakhiet M. Peripheral blood mitochondrial DNA copy number as a novel potential biomarker for diabetic nephropathy in type 2 diabetes patients. Experimental and Therapeutic Medicine. 2018; 16(2):1483-92. doi:https://doi.org/10.3892/etm.2018.6319

183. Desai HD, Seabolt J, Jann MW. Smoking in patients receiving psychotropic medications. CNS Drugs. 2001; 15(6):469-94. doi:https://doi.org/10.2165/00023210-200115060-00005

184. Jiang W, Lederman MM, Hunt P, Sieg SF, Haley K, Rodriguez B, Landay A, Martin J, Sinclair E, Asher AI. Plasma levels of bacterial DNA correlate with immune activation and the magnitude of immune restoration in persons with antiretroviral-treated HIV infection. The Journal of Infectious Diseases. 2009; 199(8):1177-85. doi:https://doi.org/10.1086/597476

185. Chang CM, Edwards SH, Arab A, Del Valle-Pinero AY, Yang L, Hatsukami DK. Biomarkers of tobacco exposure: Summary of an FDA-sponsored public workshop. Cancer Epidemiology and Prevention Biomarkers. 2017; 26(3):291-302. doi:https://doi.org/10.1158/1055-9965.epi-16-0675

186. Benowitz N, Bernert J, Foulds J. Biochemical verification of tobacco use and abstinence. Nicotine and Tobacco Research. 2019; doi:https://doi.org/10.1093/ntr/ntz132

187. Bustin S, Benes V, Garson J, Hellemans J, Huggett J. The MIQE Guidelines: Minimum Information for Publication of Quantitative Real-Time PCR Experiments. Clinical Chemistry. 2009; 55(4):611-22. doi:https://doi.org/10.1373/clinchem.2008.112797

188. Shipley G. The MIQE guidelines uncloaked. PCR Troubleshooting and Optimization: The Esential Guide. 2011:151-65.

189. Gibson UE, Heid CA, Williams PM. A novel method for real time quantitative RT-PCR. Genome Research. 1996; 6(10):995-1001. doi:https://doi.org/10.1101/gr.6.10.995

190. Livak KJ, Schmittgen TD. Analysis of relative gene expression data using real-time quantitative PCR and the 2− ΔΔCT method. Methods. 2001; 25(4):402-8. doi:https://doi.org/10.1006/meth.2001.1262

191. Hellemans J, Mortier G, De Paepe A, Speleman F, Vandesompele J. qBase relative quantification framework and software for management and automated analysis of real-time quantitative PCR data. Genome Biology. 2007; 8(2):1-14. doi:https://doi.org/10.1186/gb-2007-8-2-r19

192. Milhem C, Ingelaere C, Moralès O, Delhem N. Beta-2 microglobulin a robust reference housekeeping genes for RNA expression normalization in real time PCR on human leukocytes. Biomedical Journal of Scientific and Technical Research. 2019; 31(4):24425-29. doi:doi:10.26717/BJSTR.2020.31.005146

193. Cuzin L, Delpierre C, Gerard S, Massip P, Marchou B. Immunologic and clinical responses to highly active antiretroviral therapy in patients with HIV infection aged > 50 years. Clinical Infectious Diseases. 2007; 45(5):654-7. doi:https://doi.org/10.1086/520652

194. Gunda DW, Kilonzo SB, Kamugisha E, Rauya EZ, Mpondo BC. Prevalence and risk factors of poor immune recovery among adult HIV patients attending care and treatment centre in northwestern Tanzania following the use of highly active antiretroviral therapy: A retrospective study. Biomedical Central Research Notes. 2017; 10(1):1-6. doi:https://doi.org/10.1186/s13104-017-2521-0

195. Montaner JS, Côté HC, Harris M, Hogg RS, Yip B, Harrigan PR, O'Shaughnessy MV. Nucleoside-related mitochondrial toxicity among HIV-infected patients receiving antiretroviral therapy: Insights from the evaluation of venous lactic acid and peripheral blood mitochondrial DNA. Clinical Infectious Diseases. 2004; 38(Supplement_2):S73-S9. doi:https://doi.org/10.1086/381449

196. Integrated DNA Technologies [Internet]. How to design primers and probes for PCR and qPCR. 2020 [cited 2020 3 Novemeber 2020]. Available from: How to design primers and probes for PCR and qPCR.

197. (UNAIDS) JUNPoHA [Internet]. People aged 50 years and older. UNAIDS; 2014 [cited 2021 9 June]. Available from: https://www.unaids.org/sites/default/files/media_asset/12_Peopleaged50yearsandolder.pdf.

198. Maagaard A, Holberg-Petersen M, Kvittingen E, Sandvik L, Bruun J. Depletion of mitochondrial DNA copies/cell in peripheral blood mononuclear cells in HIV-1-infected treatment-naïve patients. HIV Medicine. 2006; 7(1):53-8. doi:https://doi.org/10.1111/j.1468-1293.2005.00336.x

199. Shikuma CM, Hu N, Milne C, Yost F, Waslien C, Shimizu S, Shiramizu B. Mitochondrial DNA decrease in subcutaneous adipose tissue of HIV-infected individuals with peripheral lipoatrophy. AIDS. 2001; 15(14):1801-9. doi:https://doi.org/10.1097/00002030-200109280-00009

200. Gingelmaier A, Grubert TA, Kost BP, Setzer B, Lebrecht D, Mylonas I, Mueller-Hoecker J, Jeschke U, Hiedl S, Friese K. Mitochondrial toxicity in HIV type-1-exposed pregnancies in the era of highly active antiretroviral therapy. Antiviral Therapy. 2009; 14(3):331-8.

201. Hernández S, Catalán-García M, Morén C, García-Otero L, López M, Guitart-Mampel M, Milisenda J, Coll O, Cardellach F, Gratacós E. Placental mitochondrial toxicity, oxidative stress, apoptosis, and adverse perinatal outcomes in HIV pregnancies under antiretroviral treatment containing zidovudine. Journal of Acquired Immune Deficiency Syndromes. 2017; 75(4):e113-e9. doi:https://doi.org/10.1097/qai.0000000000001334

202. Kohler JJ, Hosseini SH, Hoying-Brandt A, Green E, Johnson DM, Russ R, Tran D, Raper CM, Santoianni R, Lewis W. Tenofovir renal toxicity targets mitochondria of renal proximal tubules. Laboratory Investigation. 2009; 89(5):513-9. doi:https://doi.org/10.1038/labinvest.2009.14

203. Selvaraj S, Ghebremichael M, Li M, Foli Y, Langs-Barlow A, Ogbuagu A, Barakat L, Tubridy E, Edifor R, Lam W. Antiretroviral therapy–induced mitochondrial toxicity: Potential mechanisms beyond polymerase-γ inhibition. Clinical Pharmacology and Therapeutics. 2014; 96(1):110-20. doi:https://doi.org/10.1038/clpt.2014.64

204. Li M, Sopeyin A, Paintsil E. Combination of tenofovir and emtricitabine with efavirenz does not moderate inhibitory effect of efavirenz on mitochondrial function and cholesterol biosynthesis in human T-lymphoblastoid cell line. Antimicrobial Agents and Chemotherapy. 2018; 62(9) doi:https://doi.org/10.1101/297044

205. Phenix BN, Lum JJ, Nie Z, Sanchez-Dardon J, Badley AD. Antiapoptotic mechanism of HIV protease inhibitors: Preventing mitochondrial transmembrane potential loss. Blood. 2001; 98(4):1078-85. doi:https://doi.org/10.1182/blood.v98.4.1078

206. Chen QM, Bartholomew JC, Campisi J, Acosta M, Reagan JD, Ames BN. Molecular analysis of H2O2-induced senescent-like growth arrest in normal human fibroblasts: p53 and Rb control G1 arrest but not cell replication. Biochemical Journal. 1998; 332(1):43-50. doi:https://doi.org/10.1042/bj3320043

207. Lee H-C, Yin P-H, Lu C-Y, Chi C-W, Wei Y-H. Increase of mitochondria and mitochondrial DNA in response to oxidative stress in human cells. Biochemical Journal. 2000; 348(2):425-32. doi:https://doi.org/10.1042/0264-6021:3480425

208. Suzuki H, Kumagai T, Goto A, Sugiura T. Increase in intracellular hydrogen peroxide and upregulation of a nuclear respiratory gene evoked by impairment of mitochondrial electron transfer in human cells. Biochemical and Biophysical Research Communications. 1998; 249(2):542-5. doi:https://doi.org/10.1006/bbrc.1998.9181

209. Li M, Schröder R, Ni S, Madea B, Stoneking M. Extensive tissue-related and allele-related mtDNA heteroplasmy suggests positive selection for somatic mutations. Proceedings of the National Academy of Sciences. 2015; 112(8):2491-6. doi:https://doi.org/10.1073/pnas.1419651112

210. Li M, Rothwell R, Vermaat M, Wachsmuth M, Schröder R, Laros JF, Van Oven M, De Bakker PI, Bovenberg JA, Van Duijn CM. Transmission of human mtDNA heteroplasmy in the genome of the Netherlands families: Support for a variable-size bottleneck. Genome Research. 2016; 26(4):417-26. doi:https://doi.org/10.1101/gr.203216.115

211. López-Otín C, Blasco MA, Partridge L, Serrano M, Kroemer G. The hallmarks of aging. Cell. 2013; 153(6):1194-217. doi:https://doi.org/10.1016/j.cell.2013.05.039

212. Ballard J, Whitlock M. The incomplete natural history of mitochondria. Molecular Ecology. 2004; 13(4):729-44. doi:https://doi.org/10.1046/j.1365-294x.2003.02063.x

213. Ding J, Sidore C, Butler TJ, Wing MK, Qian Y, Meirelles O, Busonero F, Tsoi LC, Maschio A, Angius A. Assessing mitochondrial DNA variation and copy number in lymphocytes of~ 2,000 Sardinians using tailored sequencing analysis tools. PLOS Genetics. 2015; 11(7):e1005306. doi:https://doi.org/10.1371/journal.pgen.1005549

214. Zhang R, Wang Y, Ye K, Picard M, Gu Z. Independent impacts of aging on mitochondrial DNA quantity and quality in humans. Biomed Central genomics. 2017; 18(1):1-14. doi:https://doi.org/10.1186/s12864-017-4287-0

215. Bouhours-Nouet N, May-Panloup P, Coutant R, De Casson FB, Descamps P, Douay O, Reynier P, Ritz P, Malthièry Y, Simard G. Maternal smoking is associated with mitochondrial DNA depletion and respiratory chain complex III deficiency in placenta. American Journal of Physiology-Endocrinology and Metabolism. 2005; 288(1):E171-E7. doi:https://doi.org/10.1152/ajpendo.00260.2003

216. Meyer JN, Leung MC, Rooney JP, Sendoel A, Hengartner MO, Kisby GE, Bess AS. Mitochondria as a target of environmental toxicants. Toxicological Sciences. 2013; 134(1):1-17. doi:https://doi.org/10.1093/toxsci/kft102

217. Miró O, Alonso JR, Jarreta D, Casademont J, Urbano-Márquez A, Cardellach F. Smoking disturbs mitochondrial respiratory chain function and enhances lipid peroxidation on human circulating lymphocytes. Carcinogenesis. 1999; 20(7):1331-6. doi:https://doi.org/10.1093/carcin/20.7.1331

218. Dikalov S, Itani H, Richmond B, Arslanbaeva L, Vergeade A, Rahman SJ, Boutaud O, Blackwell T, Massion PP, Harrison DG. Tobacco smoking induces cardiovascular mitochondrial oxidative stress, promotes endothelial dysfunction, and enhances hypertension. American Journal of Physiology-Heart and Circulatory Physiology. 2019; 316(3):H639-H46. doi:https://doi.org/10.1152/ajpheart.00595.2018

219. Smith P, Cooper J, Govan G, Harding A, Schapira A. Smoking and mitochondrial function: A model for environmental toxins. Quarterly Journal of Medicine. 1993; 86(10):657-60. doi:https://doi.org/10.1093/qjmed/86.10.657

220. Bandy B, Davison AJ. Mitochondrial mutations may increase oxidative stress: Implications for carcinogenesis and aging? Free Radical Biology and Medicine. 1990; 8(6):523-39. doi:https://doi.org/10.1016/0891-5849(90)90152-9

221. Muthumani K, Choo AY, Hwang DS, Chattergoon MA, Dayes NN, Zhang D, Lee MD, Duvvuri U, Weiner DB. Mechanism of HIV-1 viral protein R-induced apoptosis. Biochemical and Biophysical Research Communications. 2003; 304(3):583-92. doi:https://doi.org/10.1016/s0006-291x(03)00631-4

222. Shikuma CM, Gerschenson M, Chow D, Libutti DE, Willis JH, Murray J, Capaldi RA, Marusich M. Mitochondrial oxidative phosphorylation protein levels in peripheral blood mononuclear cells correlate with levels in subcutaneous adipose tissue within samples differing by HIV and lipoatrophy status. AIDS Research and Human Retroviruses. 2008; 24(10):1255-62. doi:https://doi.org/10.1089/aid.2007.0262

223. Larsen S, Hey-Mogensen M, Rabøl R, Stride N, Helge J, Dela F. The influence of age and aerobic fitness: Effects on mitochondrial respiration in skeletal muscle. Acta Physiologica. 2012; 205(3):423-32. doi:https://doi.org/10.1111/j.1748-1716.2012.02408.x

224. Hunter SE, Jung D, Di Giulio RT, Meyer JN. The qPCR assay for analysis of mitochondrial DNA damage, repair, and relative copy number. Methods. 2010; 51(4):444-51. doi:https://doi.org/10.1016/j.ymeth.2010.01.033

225. Subashini D, Dinesha TR, Srirama RB, Boobalan J, Poongulali S, Chitra DA, Mothi SN, Solomon SS, Saravanan S, Solomon S. Mitochondrial DNA content of peripheral blood mononuclear cells in ART untreated & stavudine/zidovudine treated HIV-1-infected patients. The Indian journal of medical research. 2018; 148(2):207. doi:https://doi.org/10.4103/ijmr.ijmr_1144_16

226. Urata M, Koga-Wada Y, Kayamori Y, Kang D. Platelet contamination causes large variation as well as overestimation of mitochondrial DNA content of peripheral blood mononuclear cells. Annals of Clinical Biochemistry. 2008; 45(5):513-4. doi:https://doi.org/10.1258/acb.2008.008008

227. Gellerich FN, Mayr JA, Reuter S, Sperl W, Zierz S. The problem of interlab variation in methods for mitochondrial disease diagnosis: Enzymatic measurement of respiratory chain complexes. Mitochondrion. 2004; 4(5-6):427-39. doi:https://doi.org/10.1016/j.mito.2004.07.007

228. Arts EJ, Hazuda DJ. HIV-1 antiretroviral drug therapy. Cold Spring Harbor Perspectives in Medicine. 2012; 2(4):a007161. doi:https://10.1101/cshperspect.a007161

229. Suomalainen A. Fibroblast growth factor 21: A novel biomarker for human muscle-manifesting mitochondrial disorders. Expert Opinion on Medical Diagnostics. 2013; 7(4):313-7. doi:https://doi.org/10.1517/17530059.2013.812070

230. Payne BA, Price DA, Chinnery PF. Elevated serum fibroblast growth factor 21 levels correlate with immune recovery but not mitochondrial dysfunction in HIV infection. AIDS Research and Therapy. 2013; 10(1):1-7. doi:https://doi.org/10.1186/1742-6405-10-27

231. Welsh JB, Sapinoso LM, Kern SG, Brown DA, Liu T, Bauskin AR, Ward RL, Hawkins NJ, Quinn DI, Russell PJ. Large-scale delineation of secreted protein biomarkers overexpressed in cancer tissue and serum. Proceedings of the National Academy of Sciences. 2003; 100(6):3410-5. doi:https://doi.org/10.1073/pnas.0530278100

232. Uhlen M, Zhang C, Lee S, Sjöstedt E, Fagerberg L, Bidkhori G, Benfeitas R, Arif M, Liu Z, Edfors F. A pathology atlas of the human cancer transcriptome. Science. 2017; 357(6352) doi:https://doi.org/10.1126/science.aan2507

233. Lagathu C, Eustace B, Prot M, Frantz D, Gu Y, Bastard J-P, Maachi M, Azoulay S, Briggs M, Caron M. Some HIV antiretrovirals increase oxidative stress and alter chemokine, cytokine or adiponectin production in human adipocytes and macrophages. Antiviral Therapy. 2007; 12(4):489.

234. Capel E, Auclair M, Caron-Debarle M, Capeau J. Short communication Effects of ritonavir-boosted darunavir, atazanavir and lopinavir on adipose functions and insulin sensitivity in murine and human adipocytes. Antiviral Therapy. 2012; 17:549-56. doi:https://doi.org/10.3851/imp1988

235. Moure R, Domingo P, Gallego-Escuredo JM, Villarroya J, del Mar Gutierrez M, Mateo MG, Domingo JC, Giralt M, Villarroya F. Impact of elvitegravir on human adipocytes: Alterations in differentiation, gene expression and release of adipokines and cytokines. Antiviral Research. 2016; 132:59-65. doi:https://doi.org/10.1016/j.antiviral.2016.05.013

236. Secemsky EA, Scherzer R, Nitta E, Wu AH, Lange DC, Deeks SG, Martin JN, Snider J, Ganz P, Hsue PY. Novel biomarkers of cardiac stress, cardiovascular dysfunction, and outcomes in HIV-infected individuals. The Journal of the American College of Cardiology: Heart Failure. 2015; 3(8):591-9. doi:https://doi.org/10.1016/j.jchf.2015.03.007

237. Moure R, Domingo P, Villarroya J, Gasa L, Gallego-Escuredo JM, Quesada-López T, Morón-Ros S, Maroto AF, Mateo GM, Domingo JC. Reciprocal effects of antiretroviral drugs used to treat HIV infection on the fibroblast growth factor 21/β-Klotho system. Antimicrobial Agents and Chemotherapy. 2018; 62(6):e00029-18. doi:https://doi.org/10.1128/aac.00029-18

238. Srinivasa S, Wong K, Fitch KV, Wei J, Petrow E, Cypess AM, Torriani M, Grinspoon SK. Effects of lifestyle modification and metformin on irisin and FGF 21 among HIV-infected subjects with the metabolic syndrome. Clinical Endocrinology. 2015; 82(5):678-85. doi:https://doi.org/10.1111/cen.12582

239. Elvstam O, Medstrand P, Jansson M, Isberg P, Gisslén M, Björkman P. Is low-level HIV-1 viraemia associated with elevated levels of markers of immune activation, coagulation and cardiovascular disease? HIV Medicine. 2019; 20(9):571-80. doi:https://doi.org/10.1111/hiv.12756

240. Cossarizza A, Pinti M, Nasi M, Gibellini L, Manzini S, Roat E, De Biasi S, Bertoncelli L, Montagna JP, Bisi L. Increased plasma levels of extracellular mitochondrial DNA during HIV infection: A new role for mitochondrial damage-associated molecular patterns during inflammation. Mitochondrion. 2011; 11(5):750-5. doi:https://doi.org/10.1016/j.mito.2011.06.005

241. Garrabou G, Lopez S, Morén C, Martínez E, Fontdevila J, Cardellach F, Gatell JM, Miro O. Mitochondrial damage in adipose tissue of untreated HIV-infected patients. AIDS. 2011; 25(2):165-70. doi:https://doi.org/10.1097/qad.0b013e3283423219

242. Garg H, Mohl J, Joshi A. HIV-1 induced bystander apoptosis. Viruses. 2012; 4(11):3020-43. doi:https://doi.org/10.3390/v4113020

243. Chen WW LL, Yang GY, Li K, Qi XY, Zhu W, Tang Y, Liu H, Boden G. Circulating FGF-21 levels in normal subjects and in newly diagnose patients with type 2 diabetes mellitus. Experimental and Clinical Endocrinology & Diabetes. 2008; 116:65-8. doi:https://doi.org/10.1055/s-2007-985148

244. Dushay J, Chui PC, Gopalakrishnan GS, Varela–Rey M, Crawley M, Fisher FM, Badman MK, Martinez–Chantar ML, Maratos–Flier E. Increased fibroblast growth factor 21 in obesity and nonalcoholic fatty liver disease. Gastroenterology. 2010; 139(2):456-63. doi:https://doi.org/10.1053/j.gastro.2010.04.054

245. Domingo P, Gallego-Escuredo JM, Domingo JC, del Mar Gutiérrez M, Mateo MG, Fernández I, Vidal F, Giralt M, Villarroya F. Serum FGF21 levels are elevated in association with lipodystrophy, insulin resistance and biomarkers of liver injury in HIV-1-infected patients. AIDS. 2010; 24(17):2629-37. doi:https://doi.org/10.1097/qad.0b013e3283400088

246. Hindricks J, Ebert T, Bachmann A, Kralisch S, Lössner U, Kratzsch J, Stolzenburg JU, Dietel A, Beige J, Anders M. Serum levels of fibroblast growth factor-21 are increased in chronic and acute renal dysfunction. Clinical Endocrinology. 2014; 80(6):918-24. doi:https://doi.org/10.1111/cen.12380

247. Roth P, Junker M, Tritschler I, Mittelbronn M, Dombrowski Y, Breit SN, Tabatabai G, Wick W, Weller M, Wischhusen J. GDF-15 contributes to proliferation and immune escape of malignant gliomas. Clinical Cancer Research. 2010; 16(15):3851-9. doi:https://doi.org/10.1158/1078-0432.ccr-10-0705

248. Bratic A, Larsson N-G. The role of mitochondria in aging. The Journal of Clinical Investigation. 2013; 123(3):951-7. doi:https://doi.org/10.1172/jci64125

249. Lee H-C, Wei Y-H. Mitochondria and aging. Advances in Mitochondrial Medicine. 2012:311-27. doi:https://doi.org/10.1093/geroni/igy023.1218

250. Tanaka M, Nishigaki Y, Fuku N, Ibi T, Sahashi K, Koga Y. Therapeutic potential of pyruvate therapy for mitochondrial diseases. Mitochondrion. 2007; 7(6):399-401. doi:https://doi.org/10.1016/j.mito.2007.07.002

251. AIDS I [Internet]. Dolutegravir integrase inhibitors pediatric ARV. n.d. [cited 2020 22 April]. Available from: https://aidsinfo.nih.gov/guidelines/html/2/pediatric-arv/435/dolutegravir.

252. Chui A. Effect of antiretroviral drug dolutegravir on mitochondrial function. Public Health Theses. 2020:1-23. doi:https://elischolar.library.yale.edu/ysphtdl/1928

253. Bañó M, Morén C, Barroso S, Juárez DL, Guitart-Mampel M, González-Casacuberta I, Canto-Santos J, Lozano E, León A, Pedrol E. Mitochondrial toxicogenomics for antiretroviral management: HIV post-exposure prophylaxis in uninfected patients. Frontiers in Genetics. 2020; 11:497. doi:https://doi.org/10.3389/fgene.2020.00497

APPENDICES

Appendix A: Demographic information for the HIV-positive participants of this study at baseline and 12-months cART initiation.

HIV-positive participants#	Age (Years)	Gender (F/M)	Baseline viral load (VL) (copies/mL)	12-months post-cART viral load (copies/mL)	Baseline CD4+ T-cell count (cell/µL)	12-months post-cART CD4+ T-cell count (cell/µL)	Baseline CD4+ T-cell percentage (%)	12-months post-cART CD4+ T-cell percentage (%)
006	22.73	F	5,000.00	50.00	141.00	390.00	10.88	32.32
012	30.82	F	720,000.00	50.00	191.00	222.00	13.56	21.12
021	44.87	F	12,800.00	50.00	47.00	517.00	4.41	34.44
044	39.19	M	560,000.00	50.00	369.00	520.00	29.22	15.91
052	44.00	F	11,400.00	50.00	223.00	538.00	24.18	39.52
054	33.00	F	7,600.00	50.00	570.00	583.00	40.48	36.55
058	34.45	F	3,800,000.00	50.00	139.00	138.00	8.81	4.8
060	35.00	F	26,000.00	50.00	538.00	511.00	39.52	26.78
064	33.00	F	122,000.00	50.00	412.00	581.00	11.02	31.45
067	21.52	F	28,000.00	50.00	248.00	23.00	16.31	2.41
072	51.72	F	340.00	50.00	435.00	831.00	1.7	45.20
075	35.45	M	1,900,00.00	50.00	182.00	323.00	14.04	22.84
076	37.52	M	56,000.00	50.00	121.00	223.00	9.94	16.62
085	43.82	M	8,200.00	50.00	173.00	483.00	11.85	21.96
103	38.35	M	320,000.00	50.00	2.00	308.00	0.38	17.54
105	43.29	F	440,000.00	50.00	.	424.00	.	26.78
106	38.03	F	108,000.00	50.00	86.00	231.00	6.47	10.80
109	53,86	F	240,000.00	50.00	213.00	749.00	12.83	42.26
112	28.97	F	162,000.00	50.00	18.00	149.00	3.36	17.36
115	37.85	M	920,000.00	50.00	117.00	346.00	12.05	19.31
133	32.13	M	5,000.00	50.00	273.00	1,024.00	23.9.0	24.47
135	31.40	M	220.00	50.00	626.00	686.00	27.88	31.87
138	58.78	M	96,000.00	50.00	48.00	452.00	13.35	27.81
148	66.68	F	860,000.00	50.00	164.00	271.00	12	23.72
160	27.65	M	360,000.00	50.00	251.00	274.00	7.39	13.14
165	31.59	F	50.00	50.00	306.00	370.00	17.30	34.35

167	39.14	M	260,000.00	50.00	309.00	205.00	14.07	20.72
189	37.43	F	240,000.00	50.00	128.00	496.00	8.54	22.56
190	36.96	M	480,000.00	50.00	122.00	439.00	9.89	16.00
191	40.22	M	180,000.00	50.00	7.008	114.00	5.33	8.40
197	38.02	F	10,000,000.00	50.00	.	.	.	.
201	31.48	F	1,300,000.00	50.00	153.00	463.00	9.46	36.22
203	35.28	M	560,000.00	50.00	216.00	450.00	14.74	25
207	66.1	F	2,200,000.00	50.00	86.00	427.00	3.68	18.53
208	48.22	F	120,000.00	50.00	183.00	1,471.00	14.09	39.2
210	38.27	F	22,000.00	50.00	251.00	375.00	20.06	28.14
211	51.70	M	220,000.00	50.00	17.00	160.00	2.13	9.83
221	46.08	M	86,000.00	50.00	576.00	1,046.00	25.43	31.86
230	53.50	M	136,000.00	50.00	347.00	492.00	24.56	28.58
239	31.04	F	300,000.00	50.00	554.00	460.00	31.75	8.97
243	58.75	M	340,000.00	50.00	184.00	536.00	10.04	17.33
245	29.38	F	50.00	50.00	363.00	659.00	14.68	28.86
246	25.03	F	14,400.00	50.00	225.00	904.00	10.70	26.10
249	35.52	F	50.00	50.00	339.00	907.00	7.03	30.45
258	40.12	M	58,000.00	50.00	74.00	52.00	6.94	5.2
268	31.1	F	50.00	50.00	317.00	737.00	30.97	38.01
269	49.02	F	178,00.000	50.00	306.00	1136.00	13.25	26.51
272	38.92	F	1,900,000.00	50.00	20.00	423.00	1.51	18.96
279	30.39	M	2,000,000.00	50.00	123.00	727.00	16.57	30.59
293	38.18	F	96,000.00	50.00	103.00	461.00	11.07	32.24
294	30.21	M	60,000.00	50.00	314.00	1399.00	27.97	30.67
303	30.24	F	72,000.00	50.00	182.00	609.00	19.71	45.44
305	35.91	F	540,000.00	50.00	35.00	433.00	11.93	20.79
312	42.37	M	16,000.00	50.00	152.00	606.00	14.59	10.97
317	44.96	F	42,000.00	50.00	350.00	550.00	20.31	37.31
318	38.47	M	40,000.00	50.00	79.00	448.00	7.99	15.29

Abbreviations: cART=Combination antiretroviral therapy; **CD4+**=Cluster of differentiation 4 positive; **F**=Female; **HIV**=Human immunodeficiency virus; **M** =Male; **mL**=Millilitre; **µL**=Microlitre; **VL**=Viral load

Appendix B: Demographic information for the healthy, HIV-negative participants.

HIV-negative participants #	Age (Years)	Gender (F/M)
1	25.00	M
2	35.00	F
3	36.00	F
4	44.00	F
5	50.00	M
6	70.00	M
7	24.00	F
8	55.00	F
9	42.00	F
10	45.00	F
11	61.00	F
12	41.00	F
13	26.00	M
14	29.00	M
15	28.00	M

Abbreviations: F=Female; **HIV**=Human immunodeficiency virus; **M** =Male

Appendix C: Concentration of the extracted DNA from the PBMCs of HIV-positive participants at baseline and 12-months after treatment.

HIV-positive participants #	DNA collected at baseline			DNA collected at 12-months post-cART		
	Concentration (ng/µL)	260/280	260/230	Concentration (ng/µL)	260/280	260/230
006	52.47	1.85	2.69	52.47	1.85	2.69
012	52.29	1.88	2.51	16.53	1.85	2.97
044	31.27	1.81	2.81	100.88	1.88	2.39
052	21.82	1.80	2.43	39.79	1.86	2.54
054	34.71	1.90	2.54	450	1.80	2.43
060	47.11	1.81	2.57	42.98	1.85	2.68
064	95.70	1.86	2.40	82.85	1.88	2.37
067	103.64	1.88	2.37	210.91	1.87	2.37
072	38.64	1.85	2.82	97.32	1.86	2.39
075	125.79	1.87	2.40	127.89	1.87	2.44
076	33.23	1.87	2.54	25.93	1.88	2.73
085	77.86	1.86	2.29	57.00	1.91	2.37
105	25.02	1.87	2.52	59.91	1.90	2.49
106	20.10	1.84	2.49	56.20	1.90	2.41
109	25.01	1.81	2.53	53.23	1.89	2.35
115	62.39	1.87	2.45	64.54	1.88	2.46
133	47.53	1.90	2.64	122.12	1.89	2.49
138	35.38	1.90	2.16	76.74	1.89	2.46
148	52.16	1.90	2.49	54.63	1.93	2.56
165	61.79	1.91	2.54	9.94	2.07	3.82
189	77.52	1.92	2.31	34.20	1.97	2.57
197	49.46	1.90	2.40	79.12	1.90	2.40
201	47.08	1.90	2.50	39.21	1.90	2.50

203	89.25	1.90	2.63	77.56	1.90	2.63
207	35.83	1.90	2.43	168.69	1.90	2.43
208	81.21	1.94	2.62	65.75	1.94	2.62
211	84.34	2.04	6.82	38.87	2.04	6.82
230	59.19	1.87	2.48	60.97	1.88	2.47
239	55.14	1.90	2.47	22.92	1.84	2.75
245	97.15	1.88	2.48	71.56	1.88	2.25
249	35.75	1.93	2.39	35.75	1.93	2.39
258	24.68	1.76	2.44	64.09	1.86	2.2
268	60.12	1.85	2.26	31.94	1.85	2.57
269	57.73	1.85	2.26	45.49	1.84	2.26
279	36.48	1.89	2.28	29.7	1.89	2.28
293	52.86	1.86	2.43	107.88	1.89	2.29
305	71.04	1.87	2.29	62.66	1.89	2.41
317	53.62	1.85	2.28	51.58	1.89	2.17
318	36.09	1.92	2.33	61.41	1.88	2.37

Abbreviations: cART=Combination antiretroviral therapy; **DNA**=Deoxyribonucleic acid; **HIV**=Human immunodeficiency virus; **ng**=Nanogram; **PBMC**=Peripheral blood mononuclear cell; **µL**=Microlitre

Appendix D: Concentration of the extracted DNA from the PBMCs of healthy, HIV-negative participants, at a single time point.

HIV-negative participants #	DNA concentration (ng/uL)	260/280	260/230
1	102.35	1.83	1.65
2	105.79	1.88	1.75
3	76.76	1.91	2.22
4	56.67	1.91	2.08
5	89.11	1.88	2.42
6	98.91	1.90	2.50
7	80.15	1.89	2.45
8	116.14	1.88	2.40
9	135.18	1.90	2.43
10	168.74	1.91	2.45
11	98.28	1.92	2.56
12	94.90	1.92	2.51
13	155.28	1.95	2.45
14	145.59	1.93	2.45
15	186.20	1.92	2.42

Abbreviations: DNA=Deoxyribonucleic acid; **HIV**=Human immunodeficiency virus; **ng**=Nanogram; **µL**=Microlitre; **PBMC**=Peripheral blood mononuclear cell

Appendix E: Mitochondrial *MT-CYB* and nuclear *B2M* gene standard curves.

Figure E1: Standard curve for the amplification of the *MT-CYB* gene.

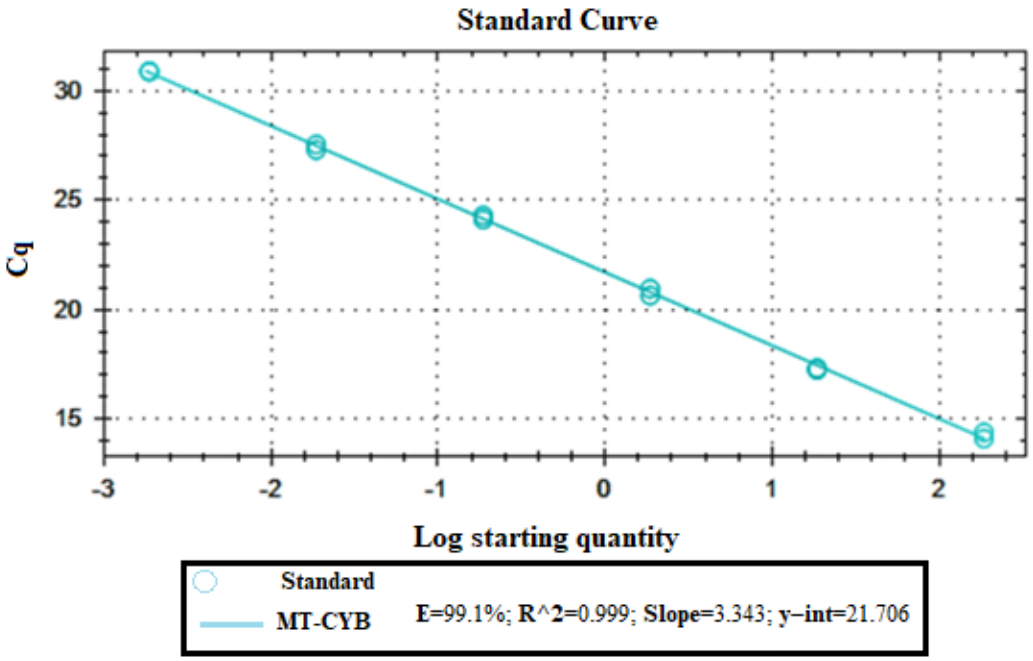

Figure E2: Standard curve for the amplification of the *B2M* gene.

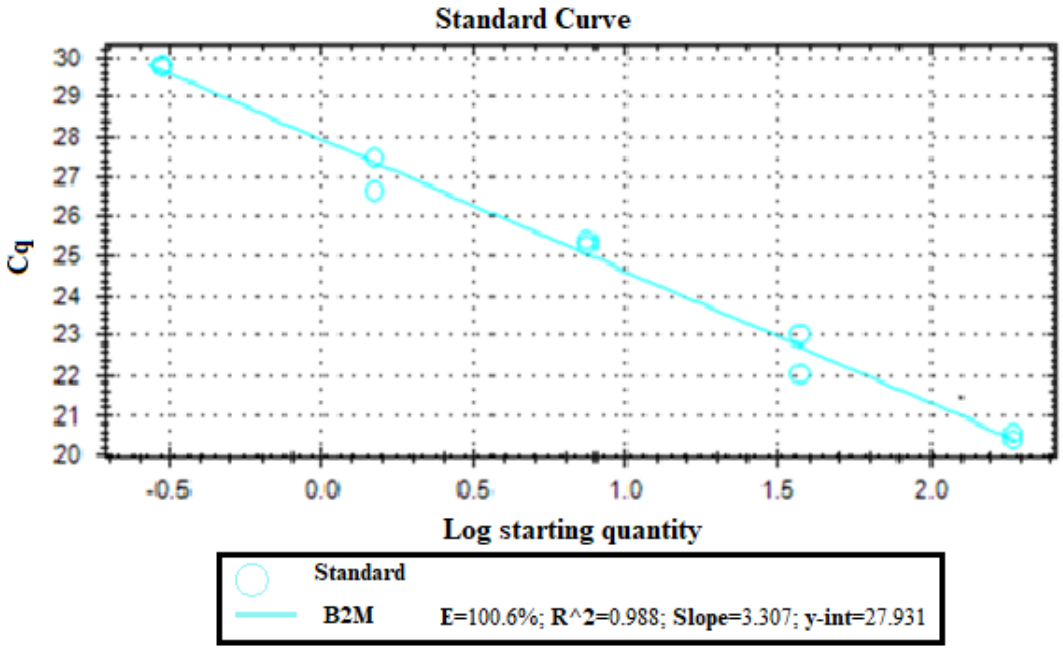

Abbreviations: B2M=Beta-2-microglobulin gene; **Cq**=PCR cycle number; **E**=Efficiency; **Log**=Logarithm; **MT-CYB**=Mitochondrial cytochrome b gene; **R^2**=Coefficient of correlation; **y-int**=y-intercept

Appendix F: Mitochondrial cytochrome b and *B2M* gene Ct values for the HIV-positive participants at baseline and 12-months post treatment.

HIV-positive participants #	Ct-Baseline for *MT-CYB*	Ct 12-Months post-cART for *MT-CYB*	Ct-Baseline for *B2M*	Ct 12-months post-cART for *B2M*
006	15.84	14.44	21.61	21.55
012	15.05	16.13	21.41	23.20
044	14.93	11.93	22.02	19.04
052	16.48	16.08	23.24	21.94
054	15.25	16.13	22.09	21.39
060	14.91	14.85	21.74	21.78
064	15.09	15.52	18.95	21.08
067	15.13	15.04	20.42	19.24
072	15.61	14.78	21.64	20.49
075	15.00	12.02	19.86	19.00
076	15.18	16.12	22.17	22.41
085	15.53	15.05	20.65	21.08
105	15.49	14.62	22.45	20.97
106	15.87	14.66	20.06	21.06
109	15.80	15.13	22.80	21.29
115	16.07	14.69	21.14	20.97
133	15.07	14.45	21.80	20.43
138	15.89	14.68	22.37	20.89
148	15.02	15.14	21.66	21.40
165	12.31	16.74	21.46	24.82
189	14.75	15.32	21.53	22.52
197	14.78	14.17	21.68	21.43

201	14.59	15.17	22.04	21.69
203	14.58	14.82	21.23	21.24
207	14.82	14.14	22.42	20.30
208	14.33	14.19	21.27	21.47
211	12.49	15.03	20.94	22.36
230	14.16	14.62	21.72	21.76
239	14.79	15.12	21.93	23.26
245	14.04	11.78	21.04	19.91
249	14.00	14.73	22.59	22.43
258	15.43	15.79	23.09	21.48
268	15.45	15.53	21.76	22.42
269	11.95	14.74	20.71	22.04
279	15.81	15.81	22.44	22.89
293	15.11	15.37	21.75	20.62
305	15.55	12.20	20.80	20.25
317	14.49	15.26	22.14	22.23
318	14.14	14.19	22.63	21.74

Abbreviations: B2M=Beta-2-microglobulin gene; **cART=**Combination antiretroviral therapy; **Ct**=Cycle threshold; **HIV=**Human immunodeficiency virus; **MT-CYB**=Mitochondrial cytochrome b gene

Appendix G: Mitochondrial cytochrome b and *B2M* gene Ct values for the healthy, HIV-negative participants.

HIV-negative participants#	Ct values for *MT-CYB*	Ct values for *B2M*
1	15.18	20.15
2	14.86	20.43
3	14.70	20.94
4	15.16	21.02
5	15.81	20.14
6	15.07	19.48
7	13.28	28.46
8	15.24	20.46
9	14.43	20.08
10	15.10	20.24
11	15.19	20.45
12	14.75	20.48
13	14.91	19.79
14	14.92	19.39
15	13.89	20.01

Abbreviations: B2M=Beta-2-microglobulin; **Ct**=Cycle threshold; **HIV=**Human immunodeficiency virus; **MT-CYB**=Mitochondrial cytochrome b gene

Appendix H: The qPCR MIQE guidelines for authors and other researchers.

Table 1. MIQE checklist for authors, reviewers, and editors.[a]

Item to check	Importance	Item to check	Importance
Experimental design		qPCR oligonucleotides	
Definition of experimental and control groups	E	Primer sequences	E
Number within each group	E	RTPrimerDB identification number	D
Assay carried out by the core or investigator's laboratory?	D	Probe sequences	D[d]
Acknowledgment of authors' contributions	D	Location and identity of any modifications	E
Sample		Manufacturer of oligonucleotides	D
Description	E	Purification method	D
Volume/mass of sample processed	D	qPCR protocol	
Microdissection or macrodissection	E	Complete reaction conditions	E
Processing procedure	E	Reaction volume and amount of cDNA/DNA	E
If frozen, how and how quickly?	E	Primer, (probe), Mg^{2+}, and dNTP concentrations	E
If fixed, with what and how quickly?	E	Polymerase identity and concentration	E
Sample storage conditions and duration (especially for FFPE[b] samples)	E	Buffer/kit identity and manufacturer	E
Nucleic acid extraction		Exact chemical composition of the buffer	D
Procedure and/or instrumentation	E	Additives (SYBR Green I, DMSO, and so forth)	E
Name of kit and details of any modifications	E	Manufacturer of plates/tubes and catalog number	D
Source of additional reagents used	D	Complete thermocycling parameters	E
Details of DNase or RNase treatment	E	Reaction setup (manual/robotic)	D
Contamination assessment (DNA or RNA)	E	Manufacturer of qPCR instrument	E
Nucleic acid quantification	E	qPCR validation	
Instrument and method	E	Evidence of optimization (from gradients)	D
Purity (A_{260}/A_{280})	D	Specificity (gel, sequence, melt, or digest)	E
Yield	D	For SYBR Green I, C_q of the NTC	E
RNA integrity: method/instrument	E	Calibration curves with slope and *y* intercept	E
RIN/RQI or C_q of 3′ and 5′ transcripts	E	PCR efficiency calculated from slope	E
Electrophoresis traces	D	CIs for PCR efficiency or SE	D
Inhibition testing (C_q dilutions, spike, or other)	E	r^2 of calibration curve	E
Reverse transcription		Linear dynamic range	E
Complete reaction conditions	E	C_q variation at LOD	E
Amount of RNA and reaction volume	E	CIs throughout range	D
Priming oligonucleotide (if using GSP) and concentration	E	Evidence for LOD	E
Reverse transcriptase and concentration	E	If multiplex, efficiency and LOD of each assay	E
Temperature and time	E	Data analysis	
Manufacturer of reagents and catalogue numbers	D	qPCR analysis program (source, version)	E
C_qs with and without reverse transcription	D[c]	Method of C_q determination	E
Storage conditions of cDNA	D	Outlier identification and disposition	E
qPCR target information		Results for NTCs	E
Gene symbol	E	Justification of number and choice of reference genes	E
Sequence accession number	E	Description of normalization method	E
Location of amplicon	D	Number and concordance of biological replicates	D
Amplicon length	E	Number and stage (reverse transcription or qPCR) of technical replicates	E
In silico specificity screen (BLAST, and so on)	E	Repeatability (intraassay variation)	E
Pseudogenes, retropseudogenes, or other homologs?	D	Reproducibility (interassay variation, CV)	D
Sequence alignment	D	Power analysis	D
Secondary structure analysis of amplicon	D	Statistical methods for results significance	E
Location of each primer by exon or intron (if applicable)	E	Software (source, version)	E
What splice variants are targeted?	E	C_q or raw data submission with RDML	D

[a] All essential information (E) must be submitted with the manuscript. Desirable information (D) should be submitted if available. If primers are from RTPrimerDB, information on qPCR target, oligonucleotides, protocols, and validation is available from that source.
[b] FFPE, formalin-fixed, paraffin-embedded; RIN, RNA integrity number; RQI, RNA quality indicator; GSP, gene-specific priming; dNTP, deoxynucleoside triphosphate.
[c] Assessing the absence of DNA with a no–reverse transcription assay is essential when first extracting RNA. Once the sample has been validated as rDNA free, inclusion of a no–reverse transcription control is desirable but no longer essential.
[d] Disclosure of the probe sequence is highly desirable and strongly encouraged; however, because not all vendors of commercial predesigned assays provide this information, it cannot be an essential requirement. Use of such assays is discouraged.

Abbreviations: qPCR=Quantitative polymerase chain reaction; **MIQE**=Minimum Information for the Publication of Quantitative Real-Time PCR experiments

Appendix I: The association between categorical variables (*i.e.* age and gender) and the concentrations of FGF-21 and GDF-15 at baseline and 12-months post-cART.

Table I1: The association between the two age subgroups created from the entire study population and the Fibroblast and growth factor 21 (FGF-21) concentration, at each time point.

Category	Statistical measure	FGF-21 concentrations at baseline (pg/mL) (n=71)	*p*-value	FGF-21 concentrations at 12-months post-cART (pg/mL) (n=71)	*p*-value
Age (Years)					
≤ 38 (n=35)	Mean	17.04	0.322	9.73	0.697
> 38 (n=36)	Mean	38.09		16.80	

Abbreviations: FGF-21=Fibroblast and growth factor 21; **cART**=Combination antiretroviral therapy; **pg**=Picograms; **mL**=Millilitres

Table I2: The association between the gender of the entire study population and the FGF-21 concentrations at each time point.

Category	Statistical measure	FGF-21 concentrations at baseline (n=71)	*p*-value	FGF-21 concentrations at 12-months post-cART (n=71)	*p*-value
Gender					
Female	n	42	0.898	42	0.226
Male	n	29		29	

Abbreviations: FGF-21=Fibroblast and growth factor 21; **cART**=Combination antiretroviral therapy

Table I3: The association between the gender of the entire study population and the GDF-15 concentrations at each time point.

Category	Statistical measure	GDF-15 concentrations at baseline (n=71)	*p*-value	GDF-15 concentrations at 12-months post-cART (n=71)	*p*-value
Gender					
Female	n	42	0.953	42	0.717
Male	n	29		29	

Abbreviations: GDF-15=Growth and differentiation factor 15; **cART**=Combination antiretroviral therapy

Fibroblast growth factor 21 and Growth and differentiation factor 15 as potential systemic biomarkers of mitochondrial toxicity and associations with disease severity and immune suppression in HIV-1 infected patients in Tshwane, South Africa

Senku Ramabula[1], Theresa M Rossouw[1], Helen C. Steel[1].

Key word: Mitochondrial toxicity, Growth and differentiation factor 15, Antiretroviral therapy, Fibroblast growth factor 21, Nucleotide-reverse transcriptase inhibitors

[1]Department of Immunology, School of Medicine, Faculty of Health Sciences, University of Pretoria, Pretoria, South Africa

Correspondence to: Senku Ramabula

Department of Dermatology,

Faculty of Health Sciences,

University of Pretoria

PO BOX 667

Pretoria, 0001

South Africa.

E-mail: senkuramabula@gmail.com

SUMMARY

INTRODUCION

Nucleoside reverse-transcriptase inhibitors provide the backbone of first-line HIV regimens, however, chronic use of this class of drug has been associated with several deleterious side-effects which manifest as conditions such as mitochondrial toxicity (MT). The measurement of MT is complex. Currently accepted methods, which rely on measuring the mtDNA relative to nuclear (n) DNA (mtDNA/nDNA) ratio, require costly specimens that are difficult to obtain, such as muscle biopsies. Several studies have, however, suggested that peripheral blood mononuclear cells (PBMCs) should reflect what is found in muscle biopsies. In addition, two biomarkers; serum fibroblast growth factor 21 (FGF-21) and serum growth and differentiation factor 15 (GDF-15), have been identified as possible alternatives to the current method of MT detection. To the best of our knowledge, these biomarkers have, however, not been assessed in the study of MT in HIV-infected individuals.

METHOD

The extent of MT was determined by detecting changes in mtDNA content, measured as the mtDNA/nDNA ratio by utilizing a quantitative polymerase chain reaction (qPCR) assay. The systemic levels of FGF-21 and GDF-15 were assessed by measuring the concentrations of these biomarkers present in plasma samples using suspension bead array technology.

RESULT

From the results obtained, it was found that there was a depletion in mtDNA copy number in the HIV-infected individuals following a 12-month NRTI-based cART regimen. In addition, when compared to the HIV-negative controls, the HIV-positive participants displayed lower expression of mtDNA.

It was also observed that GDF-15 was a more sensitive biomarker than FGF-21, which showed negligible differences in concentration in either the HIV-positive (baseline [p=0380] and 12-months post-cART [p=0.9150]) or the healthy, HIV-negative participants, whilst the levels of GDF-15 were higher in the HIV-infected participants, at both baseline (p=0.0001) and 12-months following cART (p= 0.0001), when compared to

the HIV-uninfected participants. However, no correlation between the biomarkers FGF-21 and GDF-15 and the standard measure of MT, the mtDNA/nDNA ratio, was found.

CONCLUSION

The study indicated that the biomarkers may not be a suitable alternative for determining changes in mtDNA in HIV-infected individuals placed on NRTI-based ART regimens. Growth and differentiation factor 15 levels may, however, be indicative of disease progression, particularly in relation to the CD4+ T-cell count and baseline VL. Furthermore, there was a significant relationship between the baseline GDF-15 concentrations and aging, which could possibly be attributed to the decline in mitochondrial integrity associated with age inducing an increase in GDF-15.

UNIVERSITEIT VAN PRETORIA
UNIVERSITY OF PRETORIA
YUNIBESITHI YA PRETORIA

Faculty of Health Sciences

Institution: The Research Ethics Committee, Faculty Health Sciences, University of Pretoria complies with ICH-GCP guidelines and has US Federal wide Assurance.

- FWA 00002567, Approved dd 22 May 2002 and Expires 03/20/2022.
- IORG #: IORG0001762 OMB No. 0990-0279 Approved for use through February 28, 2022 and Expires: 03/04/2023.

Faculty of Health Sciences **Research Ethics Committee**

21 June 2021

Approval Certificate
Annual Renewal

Dear Miss S Ramabula

Ethics Reference No.: 485/2019
Title: Fibroblast growth factor 21 and growth differentiation factor 15 as potential systemic biomarkers of mitochondrial toxicity and associations with disease severity and immune suppression in HIV-1 infected patients in Tshwane, South Africa

The **Annual Renewal** as supported by documents received between 2021-05-11 and 2021-06-17 for your research, was approved by the Faculty of Health Sciences Research Ethics Committee on 2021-06-17 as resolved by its quorate meeting.

Please note the following about your ethics approval:

- Renewal of ethics approval is valid for 1 year, subsequent annual renewal will become due on 2022-06-21.
- Please remember to use your protocol number (485/2019) on any documents or correspondence with the Research Ethics Committee regarding your research.
- Please note that the Research Ethics Committee may ask further questions, seek additional information, require further modification, monitor the conduct of your research, or suspend or withdraw ethics approval.

Ethics approval is subject to the following:

- The ethics approval is conditional on the research being conducted as stipulated by the details of all documents submitted to the Committee. In the event that a further need arises to change who the investigators are, the methods or any other aspect, such changes must be submitted as an Amendment for approval by the Committee.

We wish you the best with your research.

Yours sincerely

On behalf of the FHS REC, Dr R Sommers
MBChB, MMed (Int), MPharmMed, PhD
Deputy Chairperson *of the Faculty of Health Sciences Research Ethics Committee, University of Pretoria*

The Faculty of Health Sciences Research Ethics Committee complies with the SA National Act 61 of 2003 as it pertains to health research and the United States Code of Federal Regulations Title 45 and 46. This committee abides by the ethical norms and principles for research, established by the Declaration of Helsinki, the South African Medical Research Council Guidelines as well as the Guidelines for Ethical Research: Principles Structures and Processes, Second Edition 2015 (Department of Health)